

MECHANISMS OF THE 3- HYDROXYL-3- METHYLGLUTARYL-COENZYME A REDUCTASE INHIBITOR- INDUCED MYOTOXICITY IN HUMAN SKELETAL MUSCLE CELL CULTURES

Vom Fachbereich Chemie
der Technischen Universität Kaiserslautern
zur Verleihung des akademischen Grades
„Doktor der Naturwissenschaften“
genehmigte Dissertation

Betreuer: Prof. Dr. Wolfgang E. Trommer
Prof. Dr. Armin Wolf

Vorgelegt von
Léopold Ndountse Tchabda
Kaiserslautern 2005

Datum der wissenschaftlichen Aussprache: 26 Juli 2005

Promotionskommission:

Vorsitzender: Prof. Dr. Dr. Dieter Schrenk

1. Berichterstatter: Prof. Dr. Wolfgang E. Trommer

2. Berichterstatter: Prof. Dr. Armin Wolf

Die experimentellen Arbeiten zur vorliegenden Dissertation wurden unter der Betreuung von Prof. Dr. A. Wolf in der Abteilung „Biomarker Development“ der Novartis Pharma AG in Basel/ Schweiz in der Zeit von Juni 2002 bis Juni 2005 durchgeführt.

Herrn Prof. Dr. Armin Wolf danke ich für die Vergabe des Themas und die immerwährende Unterstützung bei der Durchführung der Arbeit. Seine konstruktiven Anregungen und Ratschläge sowie die stete Diskussionsbereitschaft haben maßgeblich zum Gelingen dieser Arbeit beigetragen.

Herrn Prof. Dr. W.E. Trommer danke ich für das Interesse an der vorliegenden Arbeit, Seine wohlwollende Unterstützung sowie für die Vertretung vor dem Fachbereich Chemie der Technischen Universität Kaiserslautern.

1	INTRODUCTION	1
1.1	3-Hydroxyl-3-methylglutaryl-coenzyme A reductase Inhibitors.....	1
1.1.1	Biochemical properties of the 3-hydroxyl-3-methylglutaryl-coenzyme A reductase.....	2
1.1.2	Chemical structures and pharmacokinetic properties of statins	4
1.1.3	Pleiotropic effects of statins	7
1.1.4	Anti- and pro-oxidative effect of statins	8
1.2	Myopathy/Rhabdomyolysis.....	9
1.2.1	Etiology of Rhabdomyolysis	9
1.2.2	Current view of cellular mechanisms of rhabdomyolysis.....	14
1.2.3	Statins and rhabdomyolysis	14
1.2.4	Oxidative stress and Rhabdomyolysis	18
1.3	Purpose of the study.....	20
2	MATERIAL AND METHODS.....	21
2.1	Cell culture	21
2.2	Microscopic methods	22
2.2.1	Light microscopy.....	22
2.2.2	Confocal laser scanning microscopy	22
2.2.2.1	Principle	22
2.2.2.2	Analysis of the mitochondrial membrane potential.....	23
2.3	Enzymatic methods.....	24
2.3.1	Determination of caspase-3 activity	24
2.3.2	Determination of lactate dehydrogenase activity	25
2.3.3	Determination of glutathione content	25
2.3.4	Determination of lactate	27
2.3.5	Determination of ATP content.....	27
2.4	Analytical methods	28
2.4.1	Determination of intracellular reactive oxygen species	28
2.4.2	TBARS assay	29
2.4.3	Determination of mitochondrial membrane potential	29

2.4.4	Determination of nuclear morphology by Hoechst 33342 staining...	30
2.4.5	Determination of protein concentration	30
2.4.5	Determination of total antioxidant capacity	31
2.5	Gene expression analysis	32
2.5.1	RNA extraction	32
2.5.2	cDNA synthesis	32
2.5.3	Real-time PCR.....	33
2.5.4	Calculation of results	34
2.6	Statistical evaluation.....	35
3	RESULTS AND DISCUSSION.....	37
3.1	Time and concentration dependent changes of statin-induced cellular events	37
3.1.1	Oxidative stress.....	37
3.1.1.1	Formation of reactive oxygen species	37
3.1.1.2	Cellular glutathione levels	39
3.1.1.3	TBARS assay	41
3.1.2	Apoptosis	43
3.1.2.1	Mitochondrial membrane potential	43
3.1.2.2	Caspase-3 activity	47
3.1.2.3	Nuclear morphology	49
3.1.3	Cytotoxicity.....	51
3.1.3.1	Intracellular ATP	51
3.1.3.2	Lactate dehydrogenase release.....	54
3.1.4	Discussion.....	57
3.2	Interaction between the cellular events-induced by statins	62
3.2.1	Role of caspase-3 inhibitors on statin-induced cellular events.....	62
3.2.1.1	Cytotoxicity	62
3.2.1.2	Nuclear morphology	64
3.2.1.3	Discussion	65

3.2.2	Role of pro- and anti-oxidants on statin-induced cellular events.....	66
3.2.2.1	Effect of BSO on statin-induced ROS formation, caspase-3 activity and LDH-leakage.....	66
3.2.2.2	Effect of NAC on statin-induced ROS formation, caspase-3 activity and LDH-leakage.....	67
3.2.2.3	Effect of DTT on statin-induced ROS formation, caspase-3 activity and LDH-leakage.....	68
3.2.2.4	Effect TPGS on statin-induced ROS formation, caspase-3 activity and LDH-leakage.....	69
3.2.2.5	Effect of 5-OH-FV on statin-induced ROS formation, caspase-3 activity and LDH-leakage.....	70
3.2.2.6	Effect of 6-OH-FV on statin-induced ROS formation, caspase-3 activity and LDH-leakage.....	72
3.2.2.7	Effect of M-2 and M-3 on statin-induced changes on nuclear morphology	74
3.2.2.8	Total antioxidative capacity of statins and FV metabolites	75
3.2.2.9	Discussion	78
3.2.3	Role of HMG-CoA reductase in statin-induced cellular events.....	81
3.2.3.1	Effect of MVA on statin-induced ROS formation, caspase-3 activity and LDH-leakage.....	81
3.2.3.2	Effect of F or FPP on statin-induced ROS formation, caspase-3 activity and LDH-leakage.....	83
3.2.3.3	Effect of GG or GGPP on statin-induced ROS formation, caspase-3 activity and LDH-leakage	85
3.2.3.4	Effects of MVA, F and GG on statin-induced changes on nuclear morphology	87
3.2.3.5	Effect of ubiquinone on statin-induced cytotoxicity	90
3.2.3.6	Cytotoxic effect of active and inactive HMG-CoA reductase inhibitors	91
3.2.3.7	Total antioxidative capacity of MVA and its derivatives F, FPP, GG, and GGPP.....	93
3.2.3.8	Discussion	94

3.2.4	Role of Calcium on statin-induced cellular events	97
3.2.4.1	ROS formation.....	97
3.2.4.2	Caspase-3 activity	98
3.2.4.3	Discussion	99
3.2.5	Gene expression analysis	101
3.2.5.1	Gene expression analysis in hSkMCs after treatment with statin	101
3.2.5.2	Confirmation of glycolytic activity by determination of lactate content in hSkMCs.....	103
3.2.5.3	Discussion	104
4	SUMMARY	106
5	ZUSAMMENFASSUNG	108
6	REFERENCES.....	110
5	APPENDIX.....	130

Abbreviations

[Ca ²⁺] _i	Intracellular calcium
AA	Ascorbic acid
ABTS [®]	2, 2'-Azino-di [3-ethylbenzthiazoline sulphonate]
Ac	Acetate
AMC	4-amino-4-methyl coumarin
ASAT	Aspartat amino transferase
ATP	Adenosine triphosphate
ATV	Atorvastatin
BAPTA-AM	1,2-Bis(O-aminophenoxy)ethane -N,N,N',N'-tetraaceticacid-acetoxymethyl ester
BSA	Bovine serum albumin
BSO	Buthionine-(S, R)-sulfoximine
CHD	Coronary heart disease
CHO	Aldehyde
CK	Creatine kinase
CLSM	Confocal laser scanning microscopy
CPK	Creatine phosphokinase
DCFH-DA	2', 7'-dichlorofluorescein diacetate
DEVD	Asp-Glu-Val-Asp
DMSO	Dimethyl sulfoxide
DTNB	5, 5'-dithiobis-2-nitrobenzoic acid
DTT	Dithiothreitol
eNOS	Endothelial nitric oxide synthase
ETC	Electron-transfer-chain
F	Farnesol
FPP	Farnesyl-PP
FV	Fluvastatin
GG	Geranylgeraniol
GGPP	Geranylgeranyl-PP
GSH	Reduced glutathione
GSSG	Oxidized glutathione
HDL-C	High-density lipoprotein cholesterol

HMG-CoA	3-Hydroxy-3-methylglutaryl-CoA
HMGCR1	3-Hydroxy-3-methylglutaryl-CoA reductase inhibitor
HskMC	Human skeletal muscle cells
LDH	Lactate dehydrogenase
LDL-C	Low-density lipoprotein cholesterol
LOV	Lovastatin
MI	Myocardial Infarctus
MVA	Mevalonate
NAC	N-acetylcysteine
NAD(P) ⁺	Nicotinamide adenosine dinucleotide (phosphate) oxidized form
NAD(P)	Nicotinamide adenosine dinucleotide (phosphate) reduced form
NKS	NKS-104 (pitavastatin)
PBS	Phosphate buffered saline
PRA	Pravastatin
ROS	Reactive oxygen species
SIM	Simvastatin
SREBPs	Sterol regulatory element binding proteins
TAC	Total antioxidant capacity
TBA	Thiobarbituric acid
TBARS	Thiobarbituric acid reactive substances
TG	Triglycerides
TNB	5-thio-2-nitrobenzoic acid
TPGS	DL- α -tocopherol-polyethylene-glycol-1000-succinate
Trolox-C	6-hydroxyl-2, 5, 7, 8-tetramethylchroman-2-carboxylic acid

Figures

Fig. 1: Inhibition of HMG CoA reductase by statins

Fig. 3: Vacuolation of Type IIB myofibers in an early stage of rhabdomyolysis

Fig. 4: Succinyl dehydrogenase stain of rat muscle with early necrosis of Type IIB fibers

Fig. 5: Statin-induced rhabdomyolysis in rat muscle

Fig. 6: Statin-induced chronic rhabdomyolysis in rat muscle

Fig. 7: Synthesis of bioactive signaling molecules from the isoprenoid/cholesterol biosynthetic pathway

Fig. 8: standard curve

Fig. 9: Effect of 10 μ M of statins on intracellular ROS formation

Fig. 10: Concentration-dependency of statin-induced formation of intracellular ROS

Fig. 11: Concentration-dependency of statin-induced changes of GSH on hSkMCs after 4 hours

Fig. 12: Concentration-dependency of statin-induced changes of GSH on hSkMCs after 24 hours

Fig. 13: Concentration dependency of statin-induced intracellular and extracellular TBARS formation on hSkMCs after 48 h

Fig. 14: Concentration dependency of statin-induced intracellular and extracellular TBARS formation on hSkMCs after 72 h

Fig. 15: Time course of statin-induced decrease of mitochondrial membrane potential in hSkMCs

Fig. 16: Concentration dependent effect of statins on hSkMCs mitochondrial membrane potential

Fig. 17: Representative micrographs of the distribution of the MitoTracker fluorescence

Fig. 18: Effect of statins on the mitochondrial membrane potential determined by MitoTracker Red and MitoTracker Green fluorescence intensities after 1 hour incubation

Fig. 19: Time course of statin-induced caspase-3 activity in hSkMCs cultures.

Fig. 20: Concentration-dependency of statin-induced caspase-3 activity on hSkMCs

Fig. 21: Effect of statins on hSkMCs nuclear morphology

Fig. 23: Time course of effect of statins on hSkMCs intracellular ATP

Fig. 24: Concentration-dependent effects of statins on hSkMCs intracellular ATP

Fig. 25: Effect of 10 μ M statins on intracellular ATP after 72 h incubation of hSkMCs

Fig. 26: Time course of statin-induced cytotoxicity in hSkMCs cultures

Fig. 27: Concentration-dependency of statin-induced cytotoxicity on hSkMCs

Fig. 28: Concentration-dependency of cytotoxicity after 72 hours incubation of hSkMCs with statins

- Fig. 29:** Postulated causal relation between ROS formation, apoptosis and necrosis and sequence of events
- Fig. 30:** Effect of caspase-3 inhibitors on SIM and LOV (A), NKS, FV and ATV (B)-induced LDH-leakage
- Fig. 31:** Effect of caspase-3 inhibitor on statin-induced nuclear morphology change
- Fig. 32:** Inhibitory effect M-2 on statin-induced ROS formation, caspase-3 activity and LDH-Leakage
- Fig. 33:** Inhibitory effect M-3 on statin-induced ROS formation, caspase-3 activity and LDH-Leakage.
- Fig. 34:** Effect of M-2 and M-3 on NKS-induced nuclear morphology change on hSkMCs.
- Fig. 35:** Radical cation scavenging capacity of M-2, M-3 and TPGS
- Fig. 36:** Radical cation scavenging capacity of statins
- Fig. 38:** Effect of F and GG on statin-induced nuclear change on hSkMCs
- Fig. 39:** Effect of MVA in statin-induced nuclear changes on hSkMCs
- Fig. 40:** Micrographs of Hoechst-stained hSkMCs after treatment with FV, ATV, SIM at the concentrations of 10 μ M for 72 hours supplemented with 400 μ M MVA.
- Fig. 41:** Effect of Q₁₀ in statin-induced cell membrane damage on hSkMCs
- Fig. 42:** Concentration-dependency cytotoxicity after 72 hours incubation of hSkMCs with FV and its enantiomers LBM830 (active), LBM912 (inactive)
- Fig. 43:** Concentration-dependency of cytotoxicity after 72 hours incubation of hSkMCs with LOV and deoxy-LOV (NVP VAG380)
- Fig. 44:** Radical cation scavenging capacity of MVA and its derivatives (F, FPP, GG, GGPP).
- Fig. 45:** Effect BAPTA-AM on statin-induced ROS formation
- Fig. 46:** Effect of BAPTA-AM on statins-induced caspase-3 activity
- Fig. 47:** Effect of statins on the lactate content in the hSkMCs lysates after 4 hours
- Fig. 48:** Molecular hypothesis of statin-induced myopathy

Tables

Tab. 1: Comparative efficacy of the different statins on various lipid fractions

Tab. 2: Lipophilicity and pharmacokinetic parameters of statins on the market

Tab. 3: Causes that increase the risk of rhabdomyolysis

Tab. 4: Clinical effects of rhabdomyolysis

Tab. 5: Factors that increase the risk of statin-induced myopathy

Tab. 7: TaqMan[®] Master Mix preparation

Tab. 8: ABI TaqMan[®] Gene Expression Assay

Tab. 9: Effect of BSO on statin-induced ROS formation, caspase-3 activity and LDH-Leakage

Tab. 10: Effect of NAC on statin-induced ROS formation, caspase-3 activity and LDH-Leakage

Tab. 11: Effect of DTT on statin-induced ROS formation, caspase-3 activity and LDH-Leakage

Tab. 12: Effect of TPGS on statin-induced ROS formation, caspase-3 activity and LDH-Leakage

Tab. 13: Effect of MVA on statin-induced ROS formation, caspase-3 activity and LDH-leakage

Tab. 14: Effect of F or FPP on statin-induced ROS formation, caspase-3 activity and LDH-leakage

Tab. 15: Effect of GG or GGPP on statin-induced ROS formation, caspase-3 activity and LDH-leakage

Tab.16: Regulated genes following hSkMCs after 48 hours treatment with statins

1 INTRODUCTION

1.1 3-Hydroxy-3-methylglutaryl-coenzyme A reductase Inhibitors

Coronary heart disease (CHD) is the principal cause of morbidity and mortality in the Western world and kills about 6.7 million people per year. The traditional risk factors for CHD are: tobacco smoking, high blood pressure, obesity, sedentary lifestyle and age. The role of serum cholesterol, particularly low-density lipoprotein cholesterol (LDL-C), in the development of atherosclerosis is well established (Knopp *et al.*, 1994; Fielding and Fielding, 1996; Coresh and Kwiterovich, 1996; Knopp, 1999). The use of statins, have demonstrated that LDL-C lowering retards the development of atherosclerotic lesions and reduces both cardiovascular morbidity and mortality. The beneficial effect of the statins on the incidence of CHD and myocardial infarction (MI) was clearly shown in several large-scale clinical trials. In 2003, statins were the first-choice drugs in the treatment of CHD, with an estimated 120 million people suitable for therapy (Downton and Clark 2003). Drugs in this class include simvastatin (Zocor[®]), lovastatin (Mevacor[®]), pravastatin (Pravachol[®]), atorvastatin (Lipitor[®]), fluvastatin (Lescol[®]), and cerivastatin (Baycol[®], Lipobay). Statins reduce not only cholesterol, but have a variety of other pleiotropic effects which might allow them to play a significant role in the prevention of cancer and chronic diseases like: neurological diseases (Alzheimer); osteoporosis; urologic diseases; and many other chronic diseases. Statins lower stroke incidence in high-risk patients (with CHD, mellitus of diabetes, or hypertension), including patients having the normal levels of serum cholesterol. The maximal doses administrated are 80 mg/day for lova-, simva- and atorva-statin, 40 mg/day for fluva- and prava-statin, 0.8 mg/day for cerivastatin. It was estimated from many trial tests that risk of CHD is reduced by 15% for each 10% of reduction of cholesterol plasma LDL-C, or of 25% for a reduction of 1 mmol/l of the total cholesterol of plasma. Lowering the LDL-C from 24 to 50%, the statins are less effective than the fibrates in the reduction of triglycerides (TG) and the increase in HDL-C (Tab. 1). In fact, the therapy of combination with the two agents of reduction of the cholesterol level induces another reduction in the levels of HDL-C compared with the monotherapy.

	ATV	Ceri ^a	FV	LOV	PRA	SIM	NKS	Gemfibrozil (Fibrate)
Serum LDL-C reduction (%) ^b	50	28	24	34	34	41	48	5-15
Serum HDL-C increase (%) ^b	6	10	8	9	12	12	— ^c	20
Serum triglyceride reduction (%) ^b	29	13	10	16	24	18	23	20-50

Tab. 1: Comparative efficacy of the different statins on various lipid fractions.

(% Serum LDL-C reduction, Serum HDL-C increase, Serum triglyceride reduction) (Schachter, 2005)

^aVoluntarily withdrawn from clinical use; ^bthis effect was elicited in patients with hypercholesterolaemia by a daily dose of 40 mg for atorvastatin (ATV), fluvastatin (FV), lovastatin (LOV), pravastatin (PRA) and simvastatin (SIM), 4 mg for pitavastatin (NKS) and 0.3 mg for cerivastatin (Ceri) ; ^cno significant effect reported. LDL-C, low-density lipoprotein cholesterol; HDL-C, high-density lipoprotein cholesterol.

1.1.1 Biochemical properties of the 3-hydroxyl-3-methylglutaryl-coenzyme A reductase

3-Hydroxyl-3-methylglutaryl-coenzyme A (HMG-CoA) reductase is the target of statins, which are very effectively in lowering the serum cholesterol levels. The HMG-CoA reductase consists of a single polypeptide chain of 888 amino acids with three functional portions: the amino terminal 339 residues are membrane bound and reside in the endoplasmic reticulum membrane, the residues 340-459 also call linker region, connect the membrane portion to the soluble C-terminal portion (residues 460-888) (Istvan *et al.*, 2000a; 2000b). The three dimensional structure of catalytic portion of the HMGR shows a close association of two monomers in a dimer and of two dimers in a tetramer. Statins contain different largely hydrophobic attachments and HMG-like moieties that may occupy the HMG-binding pocket, thereby blocking HMG-CoA's access to human HMG-CoA reductase. HMG-CoA reductase catalyzes the 4-electron reduction of HMG-CoA into CoA and mevalonate, a cholesterol precursor, with oxidation of two molecules NADPH (Fig. 1). Statins target hepatocytes and inhibit the conversion of HMG-CoA to mevalonate, thus inhibiting an early step of the cholesterol biosynthetic pathway. The induction of a conformation change of HMG-CoA

reductase in the active site makes the statins very specific and effective. The reduction of cholesterol biosynthesis in hepatocytes results in an upregulation of the hepatic LDL receptors. This has an influence on the reduction of circulating low-density lipoproteins and its precursors (intermediate density and very low density lipoproteins). As a consequence, low density lipoproteins and its precursors are cleared from the circulation (Goldstein and Brown, 1990). Furthermore, statins treatment lower triglyceride levels (5% to 10%) and raise the plasma concentration of anti-atherogenic high-density lipoproteins (HDL) (Ginsberg *et al.*, 1987; Vega *et al.*, 1998; Bakker-Arkema *et al.*, 1996; Grundy 1998; Brown *et al.*, 1998; Brown and Goldstein, 1986, 2004).

The inhibition of the HMG-CoA reductase results in the activation of a protease which slices the sterol regulatory element binding proteins (SREBPs) from the endoplasmic reticulum. SREBPs are translocated at the level of the nucleus, where they increase the gene expression for LDL receptor. All statins reduce LDL cholesterol non-linearly, dose-dependent, and after the administration of a single daily dose.

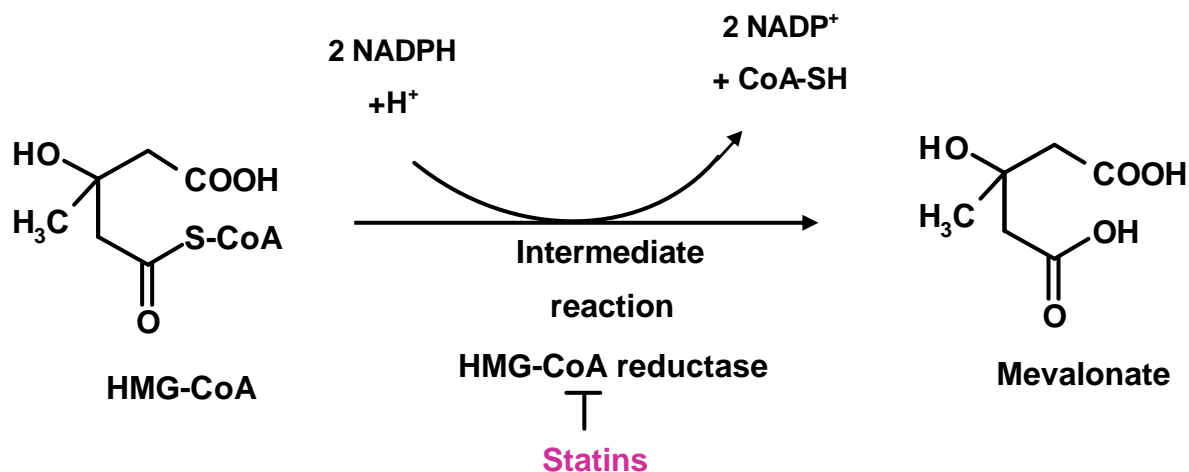
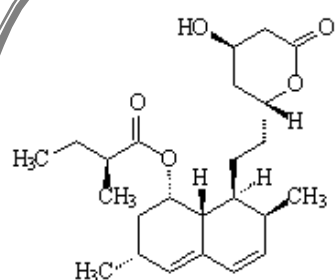


Fig. 1: Inhibition of HMG CoA reductase by statins

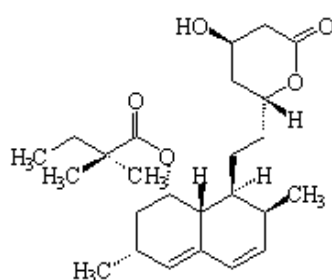
1.1.2 Chemical structures and pharmacokinetic properties of statins

The first statin structure identified was mevastatin, isolated in 1976 from the fungus *Penicillium citrinum* (Endo *et al.*, 1976, 1977; Endo and Kuroda, 1976). Lovastatin (LOV) was the first statin being approved by the United Food and drug Administration (Tobert 1987, 2003). LOV was isolated from *Aspergillus terreus*, chemical alteration of fungal products created drugs, such as simvastatin (SIM) and the microbial alteration led to drugs such as pravastatin (PRA). In 1988, SIM was approved for marketing, followed by PRA in 1991, fluvastatin (FV) in 1994, atorvastatin (ATV) in 1997, cerivastatin in 1998 and rosuvastatin in 2003 (Tobert 2003). FV, ATV, cerivastatin (Ceri), rosuvastatin and pitavastatin (NKS) are synthetic products with completely different chemical structure.

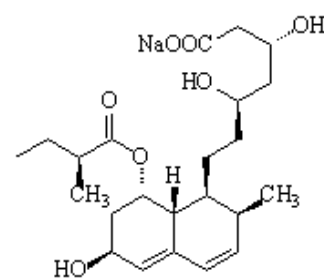
LOV and SIM occur in an inactive closed lactones ring form. They are converted in the liver into the open lactone form. The others statins are administered as active compound (acid form). The non synthetics statins posses a common main polyketide portion, a hydroxy-hexahydro naphthalene ring system, to which different side chains are linked at C8 and C6. The structures of the synthetic statins FV, NKS, Ceri and ATV are dissimilar and different from the natural statins. Only the HMG CoA-like moiety is common to both statins groups (Fig. 2). FV is derived from mevalolactone and was the first entirely synthetic statin available (Levy *et al.*, 1993), while ATV (Bakker-Arkema *et al.*, 1996) and NKS are a new generation of statins. Although chemically related, statins differ in their physicochemical and pharmacokinetic properties (Tab. 2). Among available HMG-CoA reductase inhibitors, there are pharmacokinetic differences in distribution, half-lives, systemic exposure, maximum concentrations, bioavailability, protein binding, metabolic pathways, the presence of active metabolites and excretion routes, strictly related to their physicochemical and biochemical properties, which in turn may translate into differences in long-term safety (Garcia *et al.*, 2003). In fact, the ability of a statin to penetrate into muscle tissue, and in particular in skeletal muscle cells (SkMCs), may be influenced by its hydrophilic/lipophilic character, circulating levels or by the presence of an active transport mechanism.



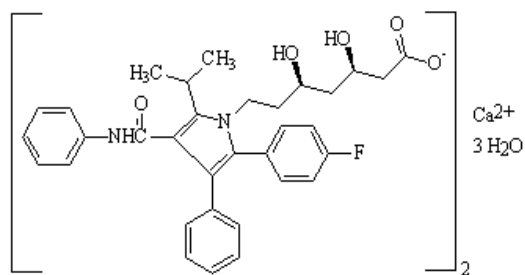
Lovastatin



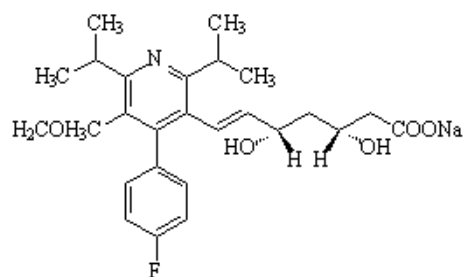
Simvastatin



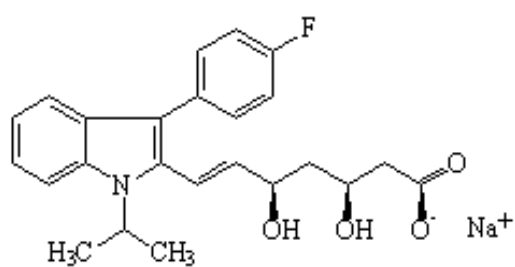
Pravastatin sodium



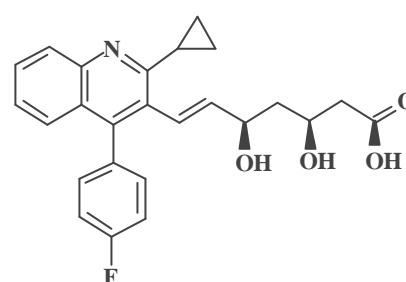
Atorvastatin calcium



Cerivastatin sodium



Fluvastatin sodium



Pitavastatin

Fig. 2: Chemical structures of statins drugs

Parameter	Atorvastatin	Cerivastatin	Fluvastatin	Lovastatin	Pravastatin	Simvastatin
Absorption						
Fraction absorbed (%)	30	98	98	30	34	60-80
T_{max} (hr)	2-3	2.5	0.5-1	2-4	0.9-1.6	1.3-2.4
C_{max} (ng/mL)	27-66	2	448	10-20	45-55	10-34
Bioavailability (%)	12	60	19-29	5	18	5
Effect of food	↓13%	0	↓15% to ↑25%	↑50%	↓30%	0
Distribution						
Fraction bound (%)	80-90	>99	>99	>95	43-55	94-98
Lipophilicity, (log P)	4.06	1.47	3.24	4.27	-0.22	4.68
Metabolism						
Hepatic metabolism	CYP3A4	CYP3A4/2C8	CYP2C9	CYP3A4	Sulfation	CYP3A4
Clearance (L/hr/kg)	0.25	0.20	0.97	0.26-1.1	0.81	0.45
Mainly cleared as	Metabolites	Metabolites	Metabolites	Metabolites	Unchanged	Metabolites
Hepatic extraction (%)	>70	NA*	>68	>70	46-66	78-87
Systemic metabolites	Active	Active	Inactive	Active	Inactive	Active
Excretion						
$t_{1/2}$ (hr)	15-30	2.1-3.1	0.5-2.3	2.9	1.3-2.8	2-3
Urinary excretion (%)	Negligible	30	6	10	20	13
Fecal excretion (%)	Major route	70	90	83	71	58
Other parameters						
Prodrug	no	no	no	yes	no	yes
Max. dose (mg/day)	80	0.8	40	80	40	80

NA* : non available (Blum, 1994; Schmitz *et al.* 2003; Corsini *et al.*, 1999)

Tab. 2: Lipophilicity and pharmacokinetic parameters of statins on the market

1.1.3 Pleiotropic effects of statins

The pleiotropic effects of a pharmacologic agent are actions other than those for which the agent was specifically developed. These effects may be undesirable, neutral or beneficial. The pleiotropic effects are either related or unrelated to the primary mechanism of action of the drug, and they are usually unanticipated. Many recent studies reported that the effects of statins extend beyond their cholesterol-lowering capacity (Takemoto *et al.*, 2001; Werner *et al.*, 2002) and most of their multiple activities are mediated by the ability to block the synthesis of isoprenoid products. Understanding the pleiotropic effects of statins is important to optimize their use in treatment and prevention of cardiovascular disease. Pleiotropic effects of statins include improvement of endothelial dysfunction, inhibition of inflammatory responses, stabilization of atherosclerotic plaques, and antioxidant properties.

Besides lowering blood cholesterol, statins prevent down regulation of endothelial nitric oxide synthase (eNOS) (Romano *et al.*, 2000; Martinez Gonzalez *et al.*, 2001). Other mechanisms include stabilization of eNOS messenger RNA by inhibiting the RhoA GTPase-dependent actin cytoskeleton (Laufs *et al.*, 1998). Statins, inhibit in a concentration dependent manner, arterial SMC migration induced by fibrinogen (Corsini *et al.*, 1999). Many studies reported the inhibition of SMC and the induction of apoptosis by statins (Muller *et al.*, 1999; Kaneider *et al.*, 2001).

Plaque instability is a major cause of acute coronary syndromes (Chesebro *et al.*, 1991; Fuster, 1995; Libby *et al.*, 1997). Statins prevents macrophage activation, the process that has been implicated in the pathophysiology of most acute coronary syndromes (Libby, 1995). Statins can decrease the level of metalloproteases released by macrophages, which might weaken the fibrous cap of plaque and make it susceptible for rupture. Statins also increase and stabilize the collagen content in plaque matrix. Many studies suggest that statins possess anti-inflammatory properties by their ability to reduce the inflammatory cells in atherosclerotic plaques (Vaughan *et al.*, 2000). Hypercholesterolemia is associated with hypercoagulability, as well as with platelet activation. Statins have been shown to inhibit platelet function. In addition, statins can affect thrombus formation by reducing platelet aggregation *in vitro*. Statins also increase the expression of bone morphogenetic protein-2, which is able to mediate osteoblast differentiation and bone formation. Hypercholesterolemia

increases the risk factor for Alzheimer's disease. The therapy with statins significantly reduces the risk for developing dementia, independently of their lipid status.

1.1.4 Anti- and pro-oxidative effect of statins

The important action of statins is their ability to scavenge oxygen free radicals in a concentration-dependent manner. Statins may reduce oxidative stress by reducing enhanced plasma levels of LDL, which are more susceptible to peroxidation in hypercholesterolemia (Lavy *et al.*, 1991; Cominacina *et al.*, 1994) and change the LDL structure, making them more resistant to peroxidation (Hussein *et al.*, 1997). Statins may also inhibit NAD (P) H oxidase, thus decreasing the generation of ROS. The antioxidative properties of statins also prevent the development of smooth muscle and cardiac hypertrophy via inhibition of Rac1-mediated oxidative stress (Takemoto *et al.*, 2001 and Wassmann *et al.*, 2001). Rac1 has been shown to be involved in the activation and assembly of NAD (P) H oxidase in vascular cells (Dusi *et al.*, 1995; Rinckel *et al.*, 1999). Statins decrease the cellular ROS production in macrophage (Pietsch *et al.*, 1996, Umetani *et al.*, 1996; Draude *et al.*, 1999). FV and its metabolites, particularly 5-OH-Fluvastatin (M-2) and 6-OH-Fluvastatin M-3, have the potential to protect against oxidative stress mediated by aqueous ROS such as $^1\text{O}_2$, O_2^- , $\cdot\text{OH}$, and OCL^- and primarily inhibit the initiation of lipid peroxidation (Nakashima *et al.*, 1999; 2001). Antioxidant effects of fluvastatin have been also reported in vivo in humans (Hussein *et al.*, 1997; Leonhardt *et al.*, 1997) and animals (Bandoh *et al.*, 1996; Mitani *et al.*, 1996).

Contrary to their antioxidants properties many studies reported the pro-oxidative effect of statins. The treatment of hypercholesterolemia patients with statins have shown a reduction of serum α -tocopherol and the susceptibility to significantly increased peroxidation (Caye-Vaugien *et al.*, 1990) and the depletion of plasma CoQ10 that result in impaired antioxidant protection, therefore leading to oxidative stress. Treatment with vitamin E within 5-12 days completely abolished muscle pains during statins treatment without CK-elevation (Sinzinger, 2000; Sinzinger *et al.*, 2000).

1.2 Myopathy/Rhabdomyolysis

The ACC/AHA/NHLBI (American College of Cardiology/American Heart Association/National Heart, Lung, and Blood Institute) task force considers myopathy to be a general term for disease of the muscles. The incidence of dose-dependent myotoxic effects, range from mild myalgia to rhabdomyolysis. It may be defined as a clinical and biochemical syndrome that results from injury which damages the integrity of the sarcolemma of skeletal muscle leading to the release of skeletal muscle contents including creatine kinase (CK), potassium, uric acid, myoglobin, calcium, phosphate, LDH, aldolase and ASAT, among others into systemic circulation (Poels and Gabreels, 1993; Dayer-Berenson, 1994), with abnormal elevations in CK levels (>10 times the upper limit of normal)

1.2.1 Etiology of Rhabdomyolysis

Rhabdomyolysis is a potential fatal consequence from a large variety of diseases, trauma, or toxic insults to skeletal muscle. The causes of rhabdomyolysis can be divided into hereditary, acquired and toxins (Tab. 3). The muscular signs and symptoms of the rhabdomyolysis are completely variable according to cases (Tab. 4). Tachycardia, fever, faintness, nausea, vomiting or red-coloured urine bed resulting from myoglobin excretion (Hamer, 1997) are the general internal disturbances. The complications of the rhabdomyolysis are due to the local effects of the muscle damage, and to the systemic effects of the substances released by the muscle (Tab. 4). Rhabdomyolysis, in its most severe form, leads to myoglobinuria with resulting acute renal failure and death (Sauret, 2002). Histological changes such as myofiber vacuolation (Fig. 3), necrosis of Type IIB fibers (Fig. 4) are associated with statin-induced skeletal myopathy. The diagnosis of rhabdomyolysis can be confirmed with a muscle biopsy. The muscle pathology is characterized by loss of cross striations and nuclei (Fig. 5 & 6). The main factors that increase the risk of statin-induced myopathy are patient characteristics and statins properties (Tab. 5). The treatment of rhabdomyolysis consists of the correction of hypotension, hypovolemia, and dehydration, as well as the prevention of the complications of acute renal failure. The therapy includes removal of the offending cause and careful monitoring of CK concentration. It also important to induce diuresis with large volume of fluid to prevent renal failure.

Causes of rhabdomyolysis

Medications and toxic substances

HMG-CoA reductase inhibitors
 Fibrates
 Niacin (nicotinic acid; Nicolar)
 Cyclosporine (Sandimmune)
 Itraconazole (Sporanox)
 Erythromycin
 Colchicines
 Zidovudine (Retrovir)
 Corticosteroids
 Alcohol
 Central nervous system depressants
 Cocaine
 Amphetamine
 Ecstasy (MDMA)
 Lysergic acid diethylamide LSD
 Neuromuscular blocking agents

Traumatic causes

Lightning strike
 Immobilization
 Extensive third-degree burn
 Crush injury

Heat-related causes

Heatstroke
 Malignant hyperthermia
 Neuroleptic malignant syndrome

Ischemic causes

Ischemic limb injury

Exertional causes

Marathon running
 Physical overexertion in untrained athletes
 Pathologic muscle exertion
 Heat dissipation impairment
 Physical overexertion in persons with sickle cell disease

Infectious causes

Viruses: influenza virus B, parainfluenza virus, adenovirus, coxsackievirus, echovirus, herpes simplex virus, cytomegalovirus, Epstein-Barr virus, human immunodeficiency virus
 Bacteria: Streptococcus, Salmonella, Legionella, Staphylococcus and Listeria species

Inflammatory causes

Polymyositis
 Dermatomyositis
 Capillary leak syndrome
 Snake bites (mostly in South America, Asia and Africa)

Metabolic and endocrinologic causes

Electrolyte imbalances: hyponatremia, hypernatremia, hypokalemia, hypophosphatemia, hypocalcemia
 Hypothyroidism, Thyrotoxicosis
 Diabetic ketoacidosis
 Nonketotic hyperosmolar syndrome

Hereditary Causes of Rhabdomyolysis

Lipid metabolism

Carnitine palmitoyltransferase deficiency
 Carnitine deficiency
 Short-chain and long-chain acyl-coenzyme A dehydrogenase deficiency

Carbohydrate metabolism

Myophosphorylase deficiency (McArdle's disease)
 Phosphorylase kinase deficiency
 Phosphofructokinase deficiency
 Phosphoglycerate mutase deficiency
 Lactate dehydrogenase deficiency (characteristic elevation of creatine kinase level with normal lactate dehydrogenase level)

Purine metabolism

Myoadenylate deaminase deficiency
 Duchenne's muscular dystrophy

Tab. 3: Causes that increase the risk of rhabdomyolysis

HMG-CoA = 3-hydroxy-3-methylglutaryl coenzyme A; LSD = lysergic acid diethylamide; MDMA = 3, 4-methylene dioxymethamphetamine.

Symptoms of rhabdomyolysis**Complications of rhabdomyolysis****Local effects**

Muscle pain
Tenderness
Swelling
Bruising
Weakness

Early complications

Hyperkalemia
Hypocalcemia
Hepatic inflammation
Cardiac arrhythmia
Cardiac arrest

Systemic effects

Tea-colored urine
Fever
Malaise
Nausea
Emesis
Confusion
Agitation
Delirium
Anuria

Late complications

Acute renal failure
Disseminated intravascular coagulation

Early or late complication

Compartment syndrome

Tab. 4: Clinical effects of rhabdomyolysis**Patient characteristics****Statin properties**

Increased age

Female sex

Renal insufficiency

Hepatic dysfunction

Hypothyroidism

Diet (grapefruit juice)

Polypharmacy

High systemic exposure

Lipophilicity

High bioavailability

Limited protein binding

Potential for drug-drug interactions metabolized by CYP pathways (particularly CYP3A4)

CYP = cytochrome P450.

Tab. 5: Factors that increase the risk of statin-induced myopathy

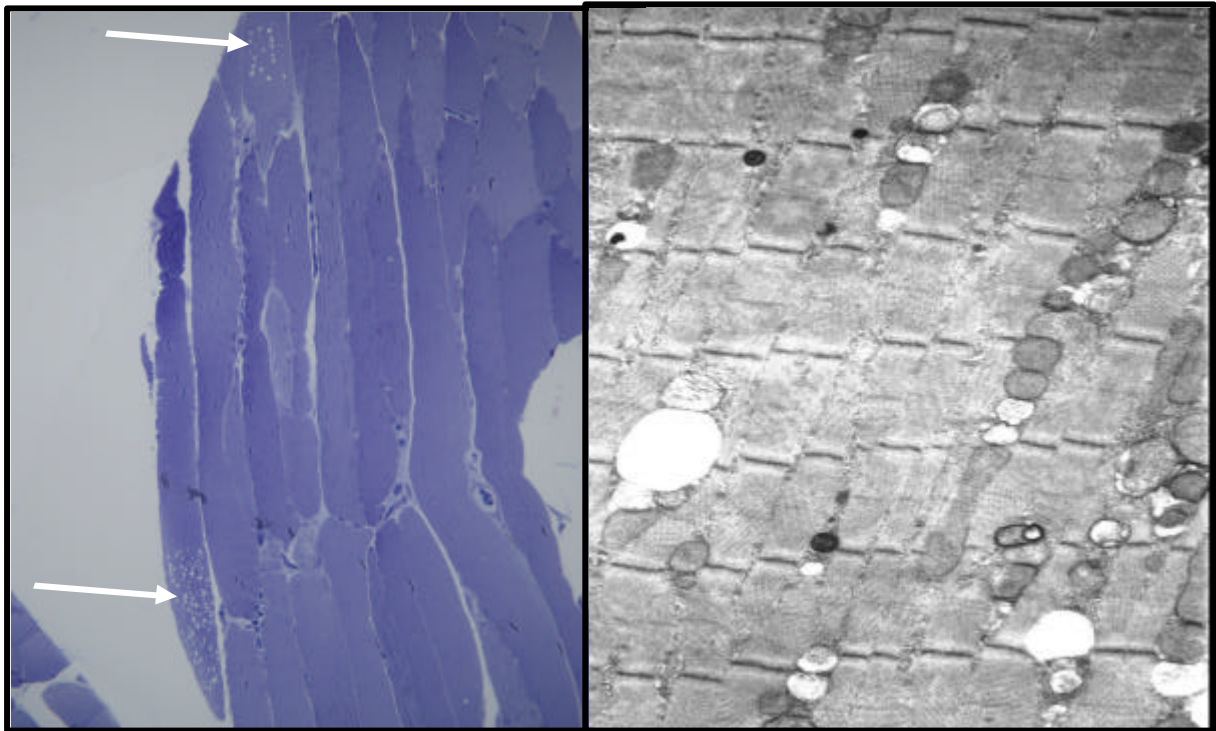


Fig. 3: Vacuolation of Type IIB myofibers in an early stage of rhabdomyolysis

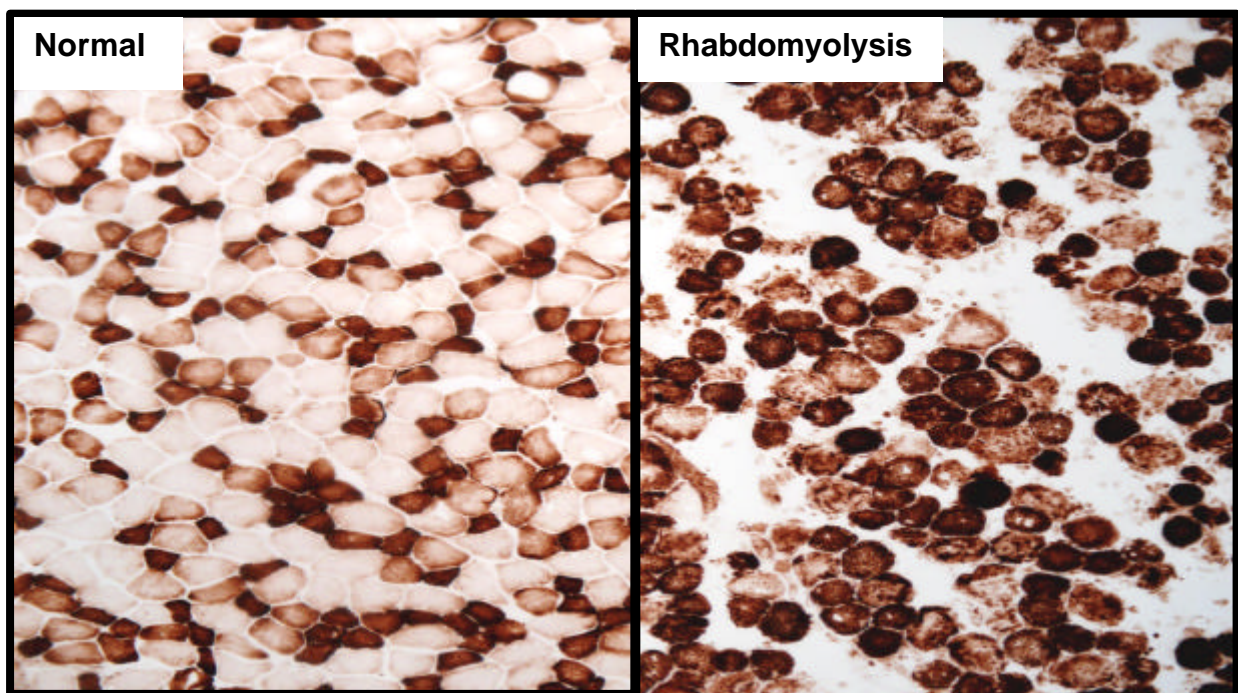


Fig. 4: Succinyl dehydrogenase stain of rat muscle with early necrosis of Type IIB fibers

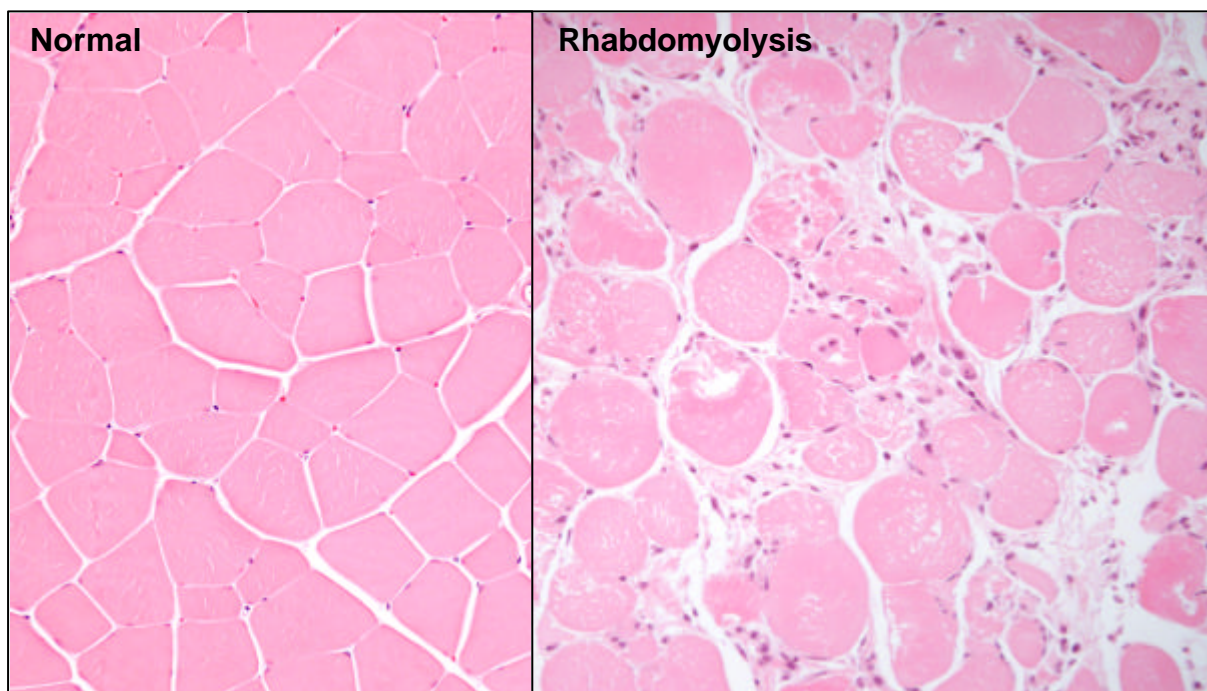


Fig. 5: Statin-induced rhabdomyolysis in rat muscle

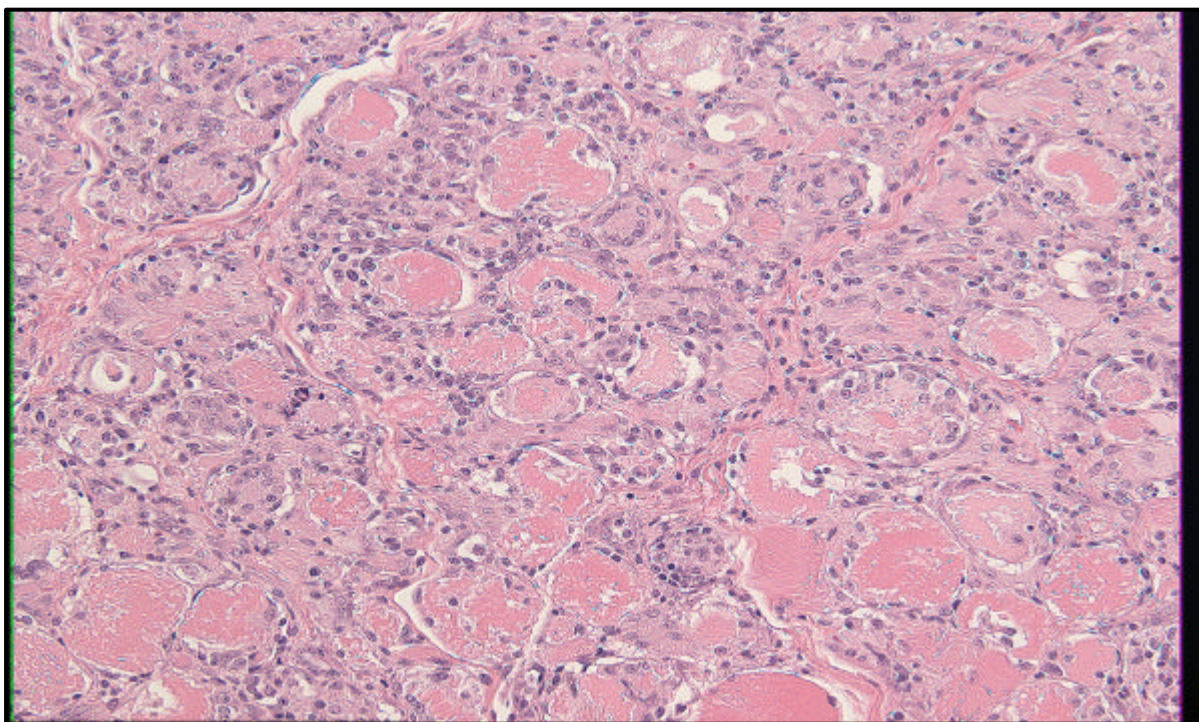


Fig. 6: Statin-induced chronic rhabdomyolysis in rat muscle

By Frank Voelker; Rhabdomyolysis in a two-week rat study with statins: A review of the pathology

1.2.2 Current view of cellular mechanisms of rhabdomyolysis

Rhabdomyolysis may occur through many conditions and various mechanisms, but the pathogenesis follows a final common pathway. The final events common to diverse causes of rhabdomyolysis are direct injury to the sarcolemma or an altered metabolic relationship between energy production and energy consumption in muscle cell, impairing the production or use of adenosine triphosphate (ATP) by skeletal muscle. Both lead to an increase of cellular permeability followed by the increase of intracellular sodium ion concentrations, the activation of Na^+ , K^+ , -ATPases and the increase of Na^+ - Ca^{2+} exchanger. Activation of these transport mechanisms enhances the accumulation of intracellular sodium and calcium, which activates neutral proteases within the cell, causing cell injury. The influx of calcium ions into the fiber leads to overcontraction of the contractile apparatus and to a disturbance of protein synthesis and mitochondrial metabolism, causing further cellular injury (Armstrong *et al.*, 1991). The elevated concentration of intracellular Ca^{2+} also induces increased interaction of actin and myosin filaments and release of phospholipids A2 resulting in a cascade of events leading to enhances the activity of the intracellular proteolytic enzymes, follow by the intracellular structures destruction.

The resultant myonecrosis is also characterized by the release of a variety of enzymes including CK and aldolase into the extracellular fluid and circulation. Additionally, potassium, myoglobin, creatinine and other predominantly intracellular constituents also enter the plasma compartment.

1.2.3 Statins and rhabdomyolysis

Most patients tolerate treatment with statins well. Around 0.5% to 2.0% of patients exhibit hepatic transaminase level elevations greater than three times the upper limit of normal, and this increase is dose-dependent (Bradford *et al.*, 1991; Hsu *et al.*, 1995). According to the published reviews of the foods and drugs administration (FDA) (Staffa *et al.*, 2002) and the Medicines Control Agency (Evans and Rees 2002a), fatal rhabdomyolysis was very rare (less than one death/million prescriptions). The rate of fatal rhabdomyolysis for cerivastatin was 16 to 80 times higher than that for other statins. The precise mechanism underlying statin-induced rhabdomyolysis is unclear (Evans and Rees, 2002b; Pasternak *et al.*, 2002; Thompson *et al.*, 2003). In the literature many hypotheses exist about the mechanism

of myotoxicity and rhabdomyolysis including, reduction of secondary metabolic intermediates, drug and drug interaction and the lipophilicity of the statins and the reduction of cholesterol content in skeletal muscle cell membranes.

The reduction of secondary metabolic intermediates

The inhibition of HMG-CoA reductase by the statins is approximately 14 steps and more than 9 enzymatic reactions before the terminal steps in cholesterologenesis. The inhibition of L-mevalonic acid (MVA) synthesis by statins also decreases the synthesis of important isoprenoid intermediates such as farnesylpyrophosphate (FPP) and geranylgeranylpyrophosphate (GGPP) (Goldstein and Brown, 1990), which mediate many of the cholesterol-independent effects of statins (Fig. 7). Johnson *et al.* (2004) suggest that statins induce apoptosis in rat myotubes by inhibiting the geranylgeranylation of proteins. Prenylation is a fundamental element of post transcriptional lipid modification of proteins and other compounds and affects their function. Protein isoprenylation permits the covalent attachment to membranes, subcellular localization, and intracellular trafficking of membrane-associated protein (van Aelst and D'Souza-Schorey, 1997). Some of the known isoprenoids include the following: isopentyladenosine, required for transfer RNA synthesis; heme A, a polyisoprenoid component of the electron transport chain; dolichols, required for glycoprotein synthesis; ubiquinone, a polyisoprenylated quinoid cofactor of the electron transport chain, which accepts electrons from complexes I and II (Beyer, 1992; Ernster and dallner, 1995; Do TQ *et al.*, 1996). Rho GTPases, including RhoA, Rac, and Cdc42, are major substrates for post-translational modification by isoprenylation. Other important prenylated proteins include the Ras family that requires attachment of a farnesyl group for its actions and plays a crucial role in cellular differentiation and proliferation, the Rab proteins which are necessary for vesicle transportation within the cell and the Rap family which is known to play a role in cell replication, platelet activation and the generation of oxygen radicals (Laufs *et al.*, 2000) (Tab.7). These suggest that the toxic effects could be related to the inhibitory effects of statins on cholesterol biosynthesis and not to the chemical toxicity of the compound.

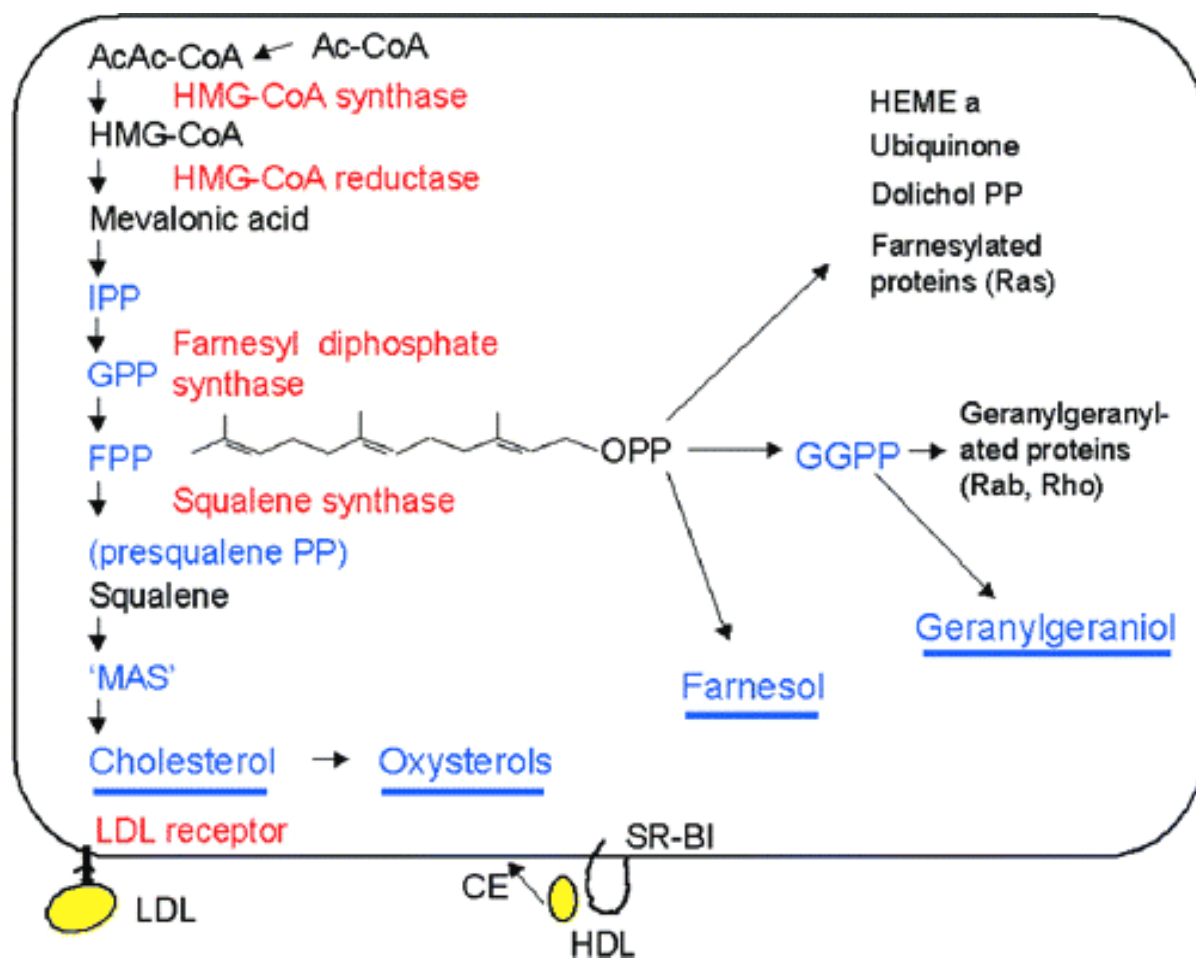


Fig. 7: Synthesis of bioactive signaling molecules from the isoprenoid/cholesterol biosynthetic pathway.

The synthesis of sterols and isoprenoids from acetyl-coenzyme A (CoA) is shown. Many intermediates and enzymes have been omitted for clarity. Genes that are transcriptionally regulated by SREBP are shown in red. Bioactive compounds discussed in the text are shown in the blue. Underlined compounds are discussed in more detail. HMG-CoA, 3-hydroxy-3-methylglutaryl-CoA; IPP, isopentenyl diphosphate; GPP, geranyl diphosphate; FPP, farnesyl diphosphate; GGPP, geranylgeranyl diphosphate; "MAS," meiosis-activating sterols; LDL, low-density lipoprotein; HDL, high-density lipoprotein; CE, cholesteryl esters; SR-BI, scavenger receptor class B type I. Synthesis begins with the transport of acetyl-CoA from the mitochondrion to the cytosol. The rate limiting step occurs at the 3-hydroxy-3-methylglutaryl-CoA (HMG-CoA) reductase, HMGR catalyzed step. The phosphorylation reactions are required to solubilize the isoprenoid intermediates in the pathway. Intermediates in the pathway are used for the synthesis of prenylated proteins, dolichol, coenzyme Q and the side chain of heme a.

Drug-drug interactions

Drug interactions commonly occur in patients taking multiple medications. Co-administration with drugs that inhibit the transport or the metabolism or that affect the activity of metabolizing enzymes and/or drug transporters at the intestinal, hepatic or renal level are potential sources of interaction for statins (Williams and Feely, 2002; Garnett, 1995). Some of the interactions of statins may not have clinical importance, but others may lead to decreased pharmacological effects or as it has been reported to cause serious adverse effects such as severe muscle toxicity, which can lead to rhabdomyolysis (Garnett, 1995).

In approximately 55% of the total number of cases, statin induced rhabdomyolysis was found to be related to drug-drug interactions (Bolego *et al.*, 2002). The risk of rhabdomyolysis increases when other drugs were administered concurrently to the statin that decreased the elimination of the statin. For instance, the incidence of myopathy has been reported to increase over 10-fold when some statins are co-administered with gemfibrozil, niacin, warfarin, digoxin, erythromycin, itraconazole, or cyclosporine (Marais and Larson, 1990; Maltz *et al.*, 1999; Bermingham *et al.*, 2000; Boger, 2001; Maxa *et al.*, 2002). Co-administration of propranolol decreased LOV plasma concentration slightly, while concomitant cyclosporine or itraconazole were associated with a greater potential to develop myopathy and rhabdomyolysis through an increase in systemic exposure to LOV. Food intake, age and gender may also modulate the systemic exposure of statins. As statins are usually prescribed over the long-term and patients at highest risk of coronary heart disease often receive more than one medication, the risk of potential drug interactions should be considered carefully during therapy.

The lipophilicity of HMG-CoA reductase inhibitor

Statin-induced rhabdomyolysis is a dose- and time-dependent phenomenon and the rate of myotoxicity for different statins may vary, possibly related to the lipophilicity of the statins (McTavish and Sorkin, 1991; Negre-aminou *et al.*, 1997; Farmer 2001; Thompson *et al.*, 2003). Lipophilic statins are more myotoxic because of the possible enhanced penetration of the cells. For instance, cerivastatin is associated with most muscle adverse effects (McTaggart *et al.*, 2001, Staffa *et al.*, 2002). The differences in myotoxicity between statins may be related to specific physicochemical properties.

The reduction of cholesterol content in skeletal muscle cell membranes

Membrane lipids are in dynamic equilibrium with plasma lipids, and low plasma cholesterol levels and decreased intracellular cholesterol may result in reduced membrane lipid content, making them unstable and leading to muscle toxicities. That may also affect the fluidity of the cell membrane and decrease cell proliferation (Levy *et al.*, 1992; Lijnen *et al.*, 1994; Morita *et al.*, 1997). However, *in vitro* neonatal rat skeletal muscle cells data demonstrated that the concurrently application of high dose cholesterol and HMG-CoA reductase inhibitor did not protect from rhabdomyolysis (Flint *et al.*, 1997). These results do not support the hypothesis that the cholesterol lowering effect is responsible for the statin-induced myotoxicity.

1.2.4 Oxidative stress and Rhabdomyolysis

Reactive oxygen species (ROS) are a normal by-product of several metabolic processes. The generation of ROS is considered to be a primary event under a variety of stress conditions (Noctor and Foyer 1998). Oxidative stress occurs when the generation of ROS in a system exceeds the system's ability to neutralize and eliminate them (Sies *et al.*, 1991). ROS may contribute to skeletal muscle degeneration in chronic heart failure (Tsutsui *et al.*, 2001), muscular dystrophies (Ragusa *et al.*, 1997), disuse atrophy (Kondo *et al.*, 1993), ischemia-reperfusion (Pattwell *et al.*, 2001), and exercise-induced muscle injuries (Zerba *et al.*, 1990). Although direct evidence of increased skeletal muscle ROS formation in these conditions is limited, all of these conditions have been associated with increased markers of oxidative stress including lipid and protein oxidation, glutathione oxidation and adaptive increases in antioxidants. The precise mechanism underlying of rhabdomyolysis is unknown. Many indirect evidences suggest the involvement of oxidative stress in the mechanism of rhabdomyolysis.

Exercise is one of the potential cofactor that may induce muscle injury (Evans and Cannon, 1991; Thompson *et al.*, 1991; Thompson *et al.*, 1997). Biochemical changes observed in fatigued muscle *in vivo*, such as increased production of thiobarbituric acid-reactive substances (Anzueto *et al.*, 1992) and GSH oxidation (Cooper *et al.*, 1980; Anzueto *et al.*, 1992) are indeed major markers of oxidative stress (Sen *et al.*, 1994a, 1994b, 1997; Sen, 1995).

Free iron and iron dextran are other factors inducing oxidative stress in skeletal muscle. It had been suggested that free iron within iron-dextran activated free radicals, initiating lipid peroxidation and leading to rhabdomyolysis, and myoglobulinuria (Foulkes, 1991). The hydroxyl radical as the most reactive of the formed radicals, is generated by the "Harber-Weiss reaction". This reaction is very fast if transition metal ions (iron, copper) are present in the reaction system (Halliwell and Gutteridge, 1986). Damage to muscle tissue released a large amount of the iron-containing protein, myoglobin, into the circulation. This protein and other heme proteins catalyze the production of ROS, which is a mechanism for possible secondary production of further oxidants after the initiation of cellular damage (Rice-Evans *et al.*, 1989, 1993, Rice-Evans and Burdon, 1993).

The lack of vitamin E and selenium (essentials antioxidants) in patients with myopathy constitute another indirect evidence of the involvement of oxidative stress in the mechanism of rhabdomyolysis. Selenium-deficient patient with myopathy usually have muscle pain that aggravated by physical activity, such as walking, crawling and muscle tenderness (Van Rij AM *et al.*, 1979). Vitamin E-deficient muscle seems to be more likely confronted with an intracellular calcium overload because of the membrane permeability, allowing the influx of calcium, which activates protease leading to muscle protein degradation (Dayton *et al.*, 1979). Plasma ubiquinone decrease might result in impaired antioxidant protection, therefore leading to oxidative stress. The oxidative stress is associated with programmed cell death or apoptosis. In the oxidative conditions, the different radicals led to the activation of distinct apoptotic pathways involving activation of specific cytoplasmic caspases, ROS can overwhelm the cell's natural defense mechanisms and activate pathways that lead to programmed cell death.

1.3 Purpose of the study

The mechanism of 3-hydroxyl-3-methylglutaryl-coenzyme-A reductase inhibitor-induced muscle side effects is not yet understood. A variety of statins have been shown to cause myopathy and rhabdomyolysis in animals and humans. A number of *in vitro* studies have investigated statin-induced myotoxicity, however there is currently no data about oxidative stress-induced by statins. To obtain a better understanding of the nature of the muscle side effects of statins, the present investigation examined NKS, SIM, LOV, ATV, PRA, and FV with regard to their ability to induced myotoxicity and also examined the underlying mechanism. The human skeletal muscle primary cell was used as *in vitro* model for the investigations. More specifically, the aims were to investigate and compare the cellular events induced by different statins by evaluating the involvement of oxidative stress and apoptosis in statins-induced myonecrosis and to establish the interaction between the cellular events induced by statins by evaluating the role of caspase-3 inhibitors, prooxidants, antioxidants and HMG-CoA downstream metabolites in statin-induced myonecrosis.

2 MATERIAL AND METHODS

2.1 Cell culture

Human skeletal muscle cells (hSkMCs) were purchased from BioWitthaker (Walkersville, NJ, USA). The cells were maintained in complete skeletal muscle cell growth medium (SkGM[®] Bulletkit[®]), which contains 500 ml of skeletal muscle cell basal medium (SkBM[®] Bulletkit[®], BioWitthaker) and SingleQuot[®] containing the following supplements: 0.5 ml of 10 µg/ml hEGF (human recombinant epidermal growth factor), 5 ml of 50 mg/ml fetuin, 5 ml of 10 mg/ml insulin, 0.5 ml of 0.39 mg/ml dexamethasone, 0.5 ml of 50 mg/ml gentamycin and 50 µg/ml amphotericin-B. Cells were seeded in 25 cm² tissue culture flasks (Nunc, Rockville, Denmark) and kept at 37°C in a 5% CO₂ incubator. The medium was renewed every 2 to 3 days. After reaching confluence, cells were released using the Reagentpack[™] (BioWitthaker) containing one 100 ml bottle of each of the following subculture reagents: HEPES buffered saline solution, trypsin/EDTA solution and trypsin neutralizing solution. The cells were then plated (8×10^4 cells/ml) in 6 Multiwell[™], (2×10^4 cells/ml) 24 Multiwell[™], PRIMARIA[™] well or (1.6×10^3 cells/ml) in Microtest[™] 96-well dishes (Becton Dickinson, NJ, USA) and were used for the different test at 70- 90% confluence.

The test compounds simvastatin (SIM), lovastatin (LOV), deoxylovastatin (NVP VAG380), atorvastatin (ATV), pravastatin (PRA) (LKT Laboratories), pitavastatin (NKS-104), fluvastatin (FV), fluvastatin enantiomers [LBM830 (active) and LBM912 (inactive)] (Novartis) were dissolved in DMSO, and aliquots of these solutions were added to the culture medium, resulting in a final concentration of 1% DMSO. Control plates received the DMSO-containing medium without statins.

Co-incubation experiments with statins were carried out with 50, 100 and 200 µM TPGS (Kodak), 1 mM DTT (Sigma), 2 mM NAC (Sigma), 2 mM BSO (Sigma), 10 and 100 µM geranylgeranyl-PP (GGPP), farnesol-PP (FPP), geranylgeraniol (GG) and farnesol (F) (Sigma), 400 µM mevalonic acid (Sigma), 5 µM and 20 µM BAPTA/AM (Sigma), 5-hydroxy-fluvastatin (M-2) and 6-hydroxy-fluvastatin (M-3) (Novartis). All HMG-CoA reductase downstream metabolites, anti- and pro-oxidant supplements were added to the cells 2 or 4 hours prior to addition of the different statins, and maintained during the incubation times indicated.

ROS formation was measured after 30 min of incubation, Caspase-3 activity was measured after 2 hours of incubation, and LDH-leakage was measured after 4, 24, 48 and 72 hours of incubation.

2.2 Microscopic methods

2.2.1 Light microscopy

Light microscopy was used to control cell viability, using the Leitz Diavert microscope. The cells were cultured in 25 mm dishes or in 6-well-plates. The pictures were taken with a digital camera (Leica Wild MPS 52).

2.2.2 Confocal laser scanning microscopy

2.2.2.1 Principle

Confocal laser scanning microscopy (CLSM) is fluorescence based imaging technique which has found wide applications in the biological sciences (Pawley and Erlandsen 1989; Boyde, 1994). By CLSM, it is possible to produce optical sections through a 3-dimensional (3-D) specimen. A series of optical sections can be recorded by moving the focal plane of the instrument step by step through the depth of the specimen.

To image the specimen point by point, a collimated, polarized laser beam is deflected stepwise in the x - and y -direction by a scanning unit before it is reflected by a dichroic mirror, so as to pass through the objective lens of the microscope, and focused onto the specimen. The emitted, longer-wavelength fluorescent light collected by the objective lens passes through the dichroic mirror and is focused into a small pinhole to eliminate all the out-of-focus light, which results in increases of contrast, clarity, and detection sensibility. Therefore, the CLSM does not only provide excellent resolution within the plane of section (0.25 μm in x - and y -direction), but also yields similarly good resolution between section planes (0.3 μm in z -direction). Confocal microscopes can also illuminate the specimen with different wavelengths of laser excitation as well as detect simultaneously several different wavelengths of emitted light.

The in-focus information of each specimen point is recorded by a photomultiplier through a detector pinhole positioned behind the confocal aperture, and the analog

output signal is digitized and fed into a computer. The obvious advantage of having a stack of serial optical sections through the specimen pixel by pixel in digital form is that either a composite projection image can be computed, or a volume-rendered 3-D representation of the specimen can be generated on a graphics computer.

The Leica TCS NT is not a no-compromise true point scanning system. It is equipped with an inverted microscope Leica DM IRBE and Argon/Krypton Laser. The Leica TCS NT uniquely uses a galvanometer-driven z-stage and a motorized xy-stage "Maerzhaeuser". The software version, Leica TCS NT 1.5.451, is used for image analysis.

2.2.2.2 Analysis of the mitochondrial membrane potential

MitoTracker green FM dye and Mito-tracker deep red 633 (Molecular Probes, Eugene, OR) were used to visualize mitochondria. These dyes bind through their chloromethyl moiety to free sulfhydryl groups in mitochondria. MitoTracker green becomes fluorescent once it accumulates in lipid environment of mitochondria regardless of membrane potential and Mito-tracker deep red 633 is an important tool for evaluating the distribution of active mitochondria. For our study 2×10^5 hSkMCs were seeded per well in 8-well culture slides and grown to sub-confluence. After 1h treatment with different statins, hSkMCs were incubated for 30 min at +37 °C, CO₂ with growth medium containing 370 nM MitoTracker green FM dye and 460 nM Mito-tracker deep red 633. Cells were washed twice with ice cold PBS and fixed for 5 min in methanol – at 20°C. After further washing with cold PBS, the slides were mounted in Gel Mount. The acquisition was done sequentially with a confocal microscope (Leica TCS SP2) and analyzed with Imaris 4.0 from Bitplane in standard size with a Gaussian filter. MitoTracker red was excited by a 633 nm laser line and emission from the dye was between 660 and 700 nm. MitoTracker green was excited by a 448 nm laser line and emission from the dye was between 510 and 533 nm, taking for each acquisition the same thickness. The Leica confocal software was used to generate images of individual fluorescent markers as well as overlay pictures demonstrating the relative distribution of the different fluorescent markers from the same portion of the slide. All experiments were performed on at least three different culture dates. For most experiments, data were converted to percent baseline or percent of untreated control.

2.3 Enzymatic methods

2.3.1 Determination of caspase-3 activity

Caspase-3 activity was determined according to the method of Rodriguez (Rodriguez *et al.*, 1996) using the fluorometric casPACE™ assay system kit (Promega, WI, USA). After treatment of about 2×10^6 cells in 6-well-plates, cells were washed once in ice-cold PBS and lysed in 500µl of buffer A [10 mM HEPES, pH 7.4, 42 mM KCL, 5 mM MgCl₂, 1 mM dithiothreitol (DTT), and protease inhibitors cocktail tablets (Roche, Mannheim, Germany)]. After three freeze-thaw cycles, the lysate was centrifuged for 20 min at 20,000g at 4°C. The supernatant (lysate) was removed and stored at -80°C until the assay was performed.

Lysates (70 µg proteins) were assayed in caspase assay buffer (312, 5 mM HEPES [pH 7.5]; 31.25% sucrose; 0.3125% CHAPS (3-[(3-cholamidopropyl) dimethylammonio]-1-propane sulfonate), 10 mM DTT with or without 100 µM protease inhibitors of caspase-3 [Ac-Asp-Glu-Val-Asp (DEVD)-CHO] were added in DMSO. The reaction was started with 20 µM the substrate for caspase-3 (Ac-DEVD-AMC), which was labeled with the fluorochrome AMC (7-amino-4-methyl coumarin) and the reaction was followed for 60 min. Fluorescence was measured at excitation 360 nm and emission 460 nm in a multi-well reader CytoFluor (PerSeptive Biosystems, MA, USA).

Fluorescence intensity was calibrated with standard concentrations of AMC. Protease activity was calculated from the slope of the recorder trace and expressed as pico moles per milligrams protein per min (pmol/mg protein/min). The difference between the substrate cleavage activity levels in the presence and absence of selective inhibitors reflected the contribution of the activity of caspase-3 activity.

2.3.2 Determination of lactate dehydrogenase activity

Extracellular and intracellular lactate dehydrogenase (LDH) activity was measured spectrophotometrically as an index of plasma membrane damage and loss of membrane integrity (Tyson *et al.*, 1987; Welder *et al.*, 1994).

LDH activity was determined measuring the reduction of pyruvic acid to lactic acid using the spectrophotometer Synchron CXS? (Beckman, CA, USA).



The NADH transformation in NAD⁺ was measured spectrophotometrically at the wavelength 340 nm and the decrease in NADH absorption is proportional to LDH activity. Enzyme activity was expressed as the percentage of the total LDH activity on the plates.

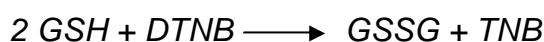
After incubation of the cells in 6 or 24 well plates, the supernatant was collected for the extracellular lactate dehydrogenase (LDH) activity measurement. The cells were washed with PBS and harvested in PBS. After ultrasonification, cell homogenates were used for the intracellular lactate dehydrogenase (LDH) activity assay. The results were expressed as the integral relative light units (RLUs).

2.3.3 Determination of glutathione content

For the determination of reduced glutathione (GSH) and oxidized glutathione (GSSG), a microtitre plate assay was used described by Vanderputte (1994). It is a modification of the microtitre plate technique reported by Baker *et al.* (1990), for the glutathione reductase-DTNB recycling assay of total glutathione and glutathione disulfide according to Tietze (1969). It has been shown that this approach is more sensitive for the determination of GSSG compared with the fluorimetric method of Hissin and Hilf, 1976 (Wolf *et al.*, 1997).

GSH is oxidized by 5, 5'-dithiobis-2-nitrobenzoic acid (DTNB) to give GSSG with stoichiometric formation of 5-thio-2-nitrobenzoic acid (TNB). GSSG is reduced to GSH by the action of the highly specific GSSG reductase and NADPH. The rate of TNB

formation is followed at 412 nm, and is proportional to the total GSH and GSSG present.



After incubation of the cells in 6-well plates, 300 μl of the medium was removed, acidified with 3 μl of HCl (1 M) and stored at -80°C until measurement of extracellular GSSG. The cells were washed with PBS and subsequently lysed by freezing and thawing in 300 μl HCl (10 mM). The homogenates (200 μl) were precipitated by 30 μl 6.5% (w/v) 5-sulfosalicylic acid (SSA) and centrifuged for 20 min at $2000 \times g$ at 4°C . Supernatants were stored at -80°C until used for analysis.

Standards of GSH and GSSG (10-300 nmol/ml as GSH equivalent) were prepared daily in 10 mM HCl, containing 1.3% of SSA. For the determination of GSH 20 μl of standard, 80 μl of sample, or blank were transferred to a micro titer plate (MaxiSorp TM; Nunc, Roskilde, Denmark) followed by addition of 40 μl stock buffer (NaH₂PO₄, 143 mM; EDTA, 6.3 mM: pH 7.4) to neutralize pH. The reaction mixture containing 40 μl DTNB, 40 μl NADPH in stock buffer was added and kept for 5 min at room temperature. The enzymatic reaction was started by adding 40 μl GSSG reductase. The plate was immediately placed in a Spectramax 250 microplate reader (Molecular devices Corp.) and the enzymatic reaction was followed kinetically for 2 min, at the wavelength 415 nm and with regular mixing of the plate. The final concentrations of reagents were 0.73 mM DTNB, 0.24 mM NADPH, and 1.2 IU/ml GSSG-reductase. Oxidized glutathione (GSSG) was measured after GSH derivatization by 2-vinylpyridine. 4 μl of 2-vinylpyridine were added to 80 μl of cell supernatant in the microtiter plate. For the determination of GSSG 40 μl standard, samples, or blanks were transferred to a microtiter plate. GSSG measurement was performed as described above. The results were expressed as GSH or GSSG in nmol/ml supernatant or mg protein, respectively.

2.3.4 Determination of lactate

The lactate concentration was determined spectrophotometrically according to Gutmann et al. (Gutmann *et al.* 1974). L-lactate is oxidized by nicotinamide-adenine dinucleotide (NAD⁺) in the presence of L-lactate dehydrogenase (L-LDH) to pyruvate (see page 25). The equilibrium of this reaction lies completely on the side of L-lactate. However, by trapping pyruvate in a subsequent reaction catalyzed by the enzyme glutamate-pyruvate transaminase (GPT) in the presence of L-glutamate, the equilibrium can be displaced in favor of pyruvate and NADH. The amount of NADH formed is stoichiometric to the amount of L-lactate. The NADH transformation in NAD⁺ was measured spectrophotometrically at the wavelength 340 nm and the decrease in NADH absorption is proportional to LDH activity. The increase in NADH is determined by means of its light absorbance at 340 nm.

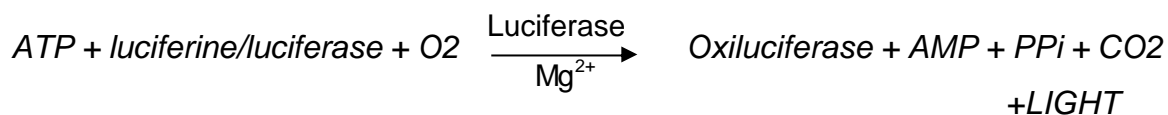


After incubation of the cells, the supernatant was collected. The cells were washed with PBS and harvested in PBS. After ultrasonification, cell homogenates were used for the assay. The results were expressed as the integral relative light units (RLUs).

2.3.5 Determination of ATP content

ATP was determined by bioluminescence using a commercially available ATP kit (Via Light TM HS, BioWhittaker) according to Crouch et al. (1993). Briefly, after the treatment of hSkMCs in 96 well-plates, Primaria (Becton Dickinson) in 100 μ l medium, 100 μ l of ATP releasing agent were added to each well, and incubated at room temperature for 5 min. Then 100 μ l of cell lysate were removed and added to wells of a 96 well assay plate, Optilux (Becton Dickinson). The plate was loaded into the luminometer (Luminoskan Ascent, Lab system) and 20 μ l of the luciferin/luciferase reagent were added to each well via the automated dispenser and the luminescence was immediately monitored over a 10 seconds period.

This method is based on the direct measurement ATP degradation by the luciferine/luciferase according to the following reaction:



Light intensity is measured at 560 nm in a spectroluminometer (Luminoskan Ascent, Lab system). This light intensity is direct proportional to ATP in the cells and was given as the integral relative light units (RLUs).

2.4 Analytical methods

2.4.1 Determination of intracellular reactive oxygen species

The formation of intracellular reactive oxygen species ROS was measured using the stable non polar 2',7'-dichlorofluorescein diacetate (DCFH-DA, Sigma-Aldrich). With this method, the amount of H₂O₂ generated by increased oxidative metabolism can be measured. Once in the viable cells DCFH-DA is deacetylated by intracellular esterases to the non fluorescent compound 2', 7'-dichlorofluorescein which reacts quantitatively with oxygen species within the cells in the presence of peroxidases to become highly fluorescent. Thus, the fluorescence intensity is proportional to the amount of peroxides produced by the cells. The hSkMCs seeded in 6-well plates and grown until 80% to 90%, were incubated 15 min with DCFH-DA (5 μM) at 37°C, 5%CO₂, then washed twice with PBS and treated with different concentrations of statins at different time points. Medium was removed; cells were washed with PBS and then ultrasonicated. Aliquots were taken for LDH determination before the cell homogenates were centrifuged, 5000 rpm, at 4°C for 20 minutes using GPR centrifuge (Beckman, UK). The supernatant was taken for fluorimetric determinations with an excitation wave length of 475 nm and an emission wave length of 525 nm using a luminescence spectrometer (PERKIN ELMER, LS 50, UK). The results were expressed as fluorescence intensity (DCF fluorescence per intracellular LDH).

2.4.2 TBARS assay

The thiobarbituric acid reactive substances (TBARS) are lipid peroxidation end products, which were determined in aliquots of cell culture medium and in cells. The measurement of TBARS formation was performed as described in Yagi (1994). Briefly, cells, grown in 6-well plates were scrapped off and resuspended in 1 ml PBS. 500 μ l of the supernatant or cells suspension were mixed with 1 ml of thiobarbituric acid (Fluka) (30 mM in water) and 3 ml of 1% H_3PO_4 (phosphoric acid). After 1 h incubation at 100 °C, the reactants were cooled to room temperature and acidified with 1% H_3PO_4 . TBARS were extracted 10 minutes with 4 ml of *n*-butanol and then centrifuged at 300 g for 10 min. The absorbance of the supernatant was measured at 553 nm emission wavelengths after an initial excitation at 515 nm using a fluorescence spectrometer (PERKIN ELMER, LS 50, UK). The concentrations were determined by using standards (1,1,3,3,-tetramethoxy propane or malonaldehyde bismethyl acetal) (Sigma-Aldrich), which were processed similarly.

2.4.3 Determination of mitochondrial membrane potential

Mitochondrial membrane potential was monitored by determination of the uptake of Rhodamine 123 according to the method of Wu (Wu *et al.*, 1990).

After 30 min incubation of hSkMCs with 1 μ M rhodamine 123 (Molecular Probes, Leiden, Netherlands) in a 96-well plate at 37°C, cells were washed with PBS and treated with statins for different incubation times. After the incubation, medium was removed and the cells were washed twice with PBS. The amount of dye retained by the hSkMCs was extracted with ethanol/water 1/1 by moderate shaking the plate for 10 minutes using TITRAMAX 1000 (Heidolph instruments, NJ, USA). Fluorescence in the ethanol/water mixture was measured with a Cytofluor 2300 from Minipore, with an excitation wavelength of 485 nm and an emission wavelength of 530 nm.

2.4.4 Determination of nuclear morphology

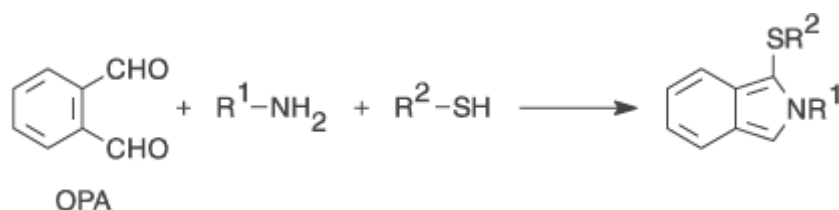
Hoechst dyes are cell membrane permeable and stain DNA to emit intense blue fluorescence. They bind to DNA in the minor groove of poly-AT sequence rich areas. Hoechst 33342 is water-soluble and stable in aqueous solutions. The excitation and emission wavelengths of Hoechst-DNA complex are 350 nm and 461 nm, respectively.

A stock solution of 1mg/ml Hoechst 33342 dye (Molecular Probes, Eugene, OR) was prepared freshly in PBS and stored at 4°C in the dark until use. Approximately 10^5 cells/ml were placed into each well of 24 well plates (500 μ l) and incubated with respective substances for 72 hours. 10 μ l of Hoechst 33342 dye solution (1 μ g/ml) were added to each well to result in a final concentration of 0.3 μ M. After 30 min incubation at 37°C in 5% CO₂, 255 μ l of fixation solution (12% formaldehyde in wash buffer) were directly added to each well without removing medium and incubated in a fume hood at room temperature for 10 minutes. Fixation solution was removed and cells were washed twice with washing buffer (Cellomic Kit). The fluorescence was measured in the Cellomics ArrayScan (Pittsburgh, PA; USA) using the filter set XF-93.

2.4.5 Determination of protein concentration

Protein content was determined using the FluoraldehydeTM *o*-Phthalaldehyde reagent Solution (OPA) (PIERCE, Lausanne, Switzerland) according to Jones and Gilligan (1983). The combination of OPA and 2-mercaptoethanol provides a rapid and simple method of determining protein concentrations in the range of 0.2 μ g/ml to 25 μ g/ml. As compared to fluorescamine, OPA is more soluble and stable in aqueous buffers and its sensitivity for detection of peptides is reported to be 5–10 times better. In the presence of reduced sulfhydryl groups, OPA reacts with the primary amino groups found in terminal amino acids and the ϵ amino group of lysine to form fluorescent moieties. Here, a fluorescent assay with OPA is described to quantitate total protein in the 96-well microplate using a multi-well reader (CytoFluor).

Fluorogenic amine-derivatization reaction of *o*-phthalaldehyde (OPA)



BSA (bovine serum albumin) was used as a standard. A series of dilutions ranging from 0.0 to 1000 $\mu\text{g/ml}$ of bovine serum albumin (BSA) were made using phosphate buffered saline (PBS) pH 7.4 as the diluents. Samples and standards were placed in microplate wells (200 μl per well) and 20 μl of OPA reagent solution (complete) was added to each well. Samples were allowed to incubate for 2 minutes with moderate shaking at room temperature using TITRAMAX 1000 (Heidolph instruments, NJ, USA), and fluorescence was measured at excitation 360 nm and emission 460 nm in a multi-well reader (CytoFluor).

2.4.5 Determination of total antioxidant capacity

Total antioxidant capacity (TAC) was measured using a colorimetric assay (Randox Laboratories, Crumlin, U.K.). The chromogen ABTS[®] (2, 2'-Azino-di [3-ethylbenzthiazoline sulphonate]) was incubated with a peroxidase (metmyoglobin) and hydrogen peroxide to produce the ABTS radical cation. The ABTS radical is detectable due to its blue-green color which is measured at 600 nm at 37°C. Antioxidants in the sample suppress the formation of the radical cation to a degree which is proportional to their concentration. At 37°C, 10 μl of distilled water (blank), trolox-c (6-hydroxyl-2, 5, 7, 8-tetramethylchroman-2-carboxylic acid [1, 6 mmol/ml]) (standard), or compound to be analyzed were pipetted into a 96-well-plate. 200 μl of metmyoglobin (6.1 $\mu\text{mol/L}$) combined with ABTS (610 $\mu\text{mol/L}$) were added into each well. After mixing, the initial absorbance (A_1) was read at 600 nm using a spectrophotometer, and 40 μl of substrate (hydrogen peroxide [500 $\mu\text{mol/L}$]) were added. After 2 minutes incubation and any minute a second absorbance (A_2) was determined using UV-visible spectrophotometer (Hewlett-Packard[®] Laboratories, CA, USA). Changes in absorbance (A) were calculated ($A = A_2 - A_1$) and TAC was determined using the following calculation: $\text{TAC} = (1.6 / [A_{\text{blank}} - A_{\text{standard}}]) \times (A_{\text{blank}} - A_{\text{sample}})$. Values were expressed as mmol/L.

2.5 Gene expression analysis

cDNA synthesis and PCR set up were performed using the liquid handling robot Microlab STAR^{let} from Hamilton.

2.5.1 RNA extraction

Human skeletal muscle cells were treated with different statins at different times. Medium was removed, cells were washed with PBS, lysated in trizol and stored at -80°C. The RNA extractions were performed using the MagNA Pure LC robot (Roche) with the High Performance RNA Isolation Kit (Roche).

2.5.2 cDNA synthesis

Total RNA was reverse transcribed to cDNA using the High Capacity cDNA Archive Kit (Applied Biosystems) according to the manufacturer instructions, using the DNA Engine PTC-200 (Bioconcept).

cDNA was synthesized starting from 5 µl of total RNA and adding 95 µl of mix preparation. The solutions were stored at -80°C.

	Volume (µl / well)
10X RT Buffer	20
25X dNTP mixture	8
10X Random primers	20
Multiscribe RT	10
RNase-free water	37
sum	95

Tab. 6: Reverse transcription mix preparation

2.5.3 Real-time PCR

Real-time PCR was performed using ABI prism™ 7900HT (Applied Biosystems) in combinations with TaqMan® PCR Master Mix (Applied Biosystems) according to assay design (Table 1-3). For all of genes TaqMan® assay were available in Applied Biosystems database in a form of an Assay on Demand (AoD) (Table 1-4).

The PCR conditions consisted in one cycle at 50°C for 2 min, followed by one cycle of denaturation at 95°C for 10 min and 40 cycles of amplification: a denaturation step at 95°C for 15s and annealing/elongation step at 60°C for 1 min.

	Volume (µl/ well)
Master Mix	10
AoD	1
NF Water	7
sum	18

Tab. 7: TaqMan® Master Mix preparation

Gene Name	Gene symbol	Accession #	Gene symbol
Actin beta	ACTB	NM_001101	Hs99999903_m1
18s	18s	X03205	Hs99999901_s1
6-phosphofructo-2-kinase / fructose-2, 6-bisphosphatase 2	PFKFB-2	MN_006212	Hs00359506_g1
6-phosphofructo-2-kinase / fructose-2, 6-bisphosphatase 3	PFKFB-3	MN_004566	Hs00190079_m1
Pyruvate dehydrogenase kinase, isoenzyme 4	PDK-4	MN_002612	Hs00176875_m1
Pyruvate dehydrogenase phosphatase, isoenzyme 2	PDP-2	MN_020786	Hs00380020_m1
Fructose-1, 6-bisphosphatase 1	FBP-1	MN_000507	Hs00166829_m1
Peroxisome proliferative activated receptor, alpha	PPARa	MN_032644	Hs00231882_m1
Superoxide dismutase 2, mitochondrial	SOD-2	MN_000636	Hs00167309_m1
Forkhead box O3A	FOXO3A	MN_201559	Hs00818121_m1

Tab. 8: ABI TaqMan[®] Gene Expression Assay

2.5.4 Calculation of results

An absolute quantification of mRNA was performed using a standard curve:

A commercial total RNA of human (Ambion) was reverse transcribed to obtain a cDNA which will be used as standard: the cDNA was serial diluted one to ten up to have a serie of 8 dilutions. This standard curve was only done on housekeeping gene. The efficiency of the reaction was calculated from the slope of the standard curve: efficiency = $10^{-1/\text{slope}} - 1$. As each dilution of standard cDNA had a known concentration, we could determinate a quantity (copy number) of cDNA in each sample, according to

the CT values. The normalization of the samples was performed by calculating a ratio gene of interest / housekeeping gene.

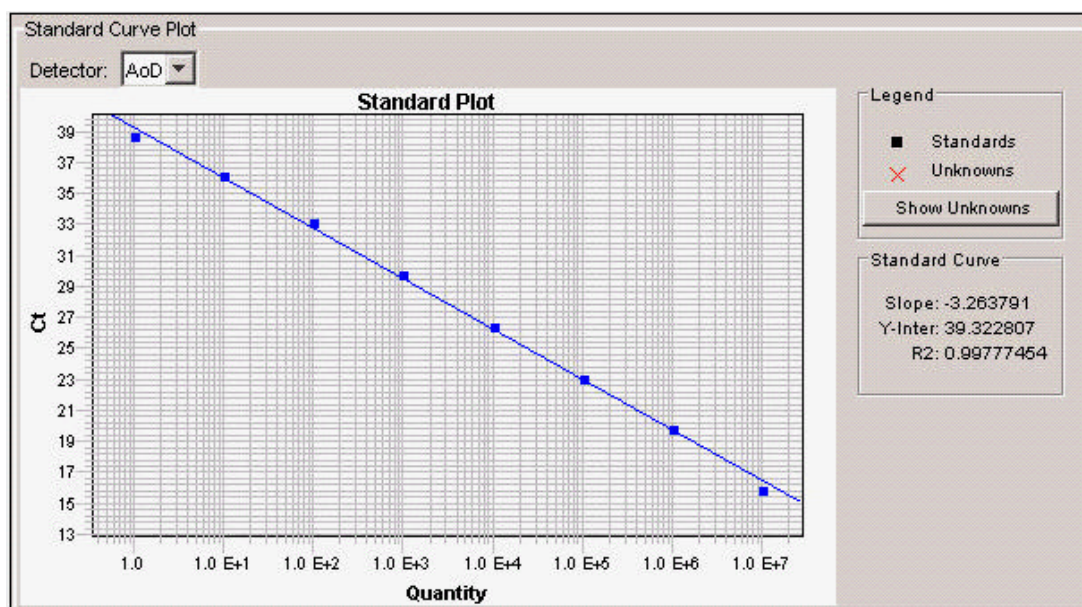


Fig. 8: standard curve of cDNA

2.6 Statistical evaluation

First, one-way analyses of variance (ANOVA) were performed to compare the effects of different concentrations of a compound with the response. Second, the effects of combinations of a compound and a protective substance on the response were compared with a) the "overall control" (no compound, no protective substance) and b) the "compound control" (same concentration of the compound, but no protective substance). For different time points, separate analyses were performed.

For all responses, plots of the log average response versus the logarithmized standard deviation per compound concentration group reveal that the variance increases with the response. A logarithmic transformation removes this trend. Thus, values were logarithmized before the analysis.

As a general rule, comparisons of a "treatment" were adjusted for multiple comparisons by Dunnett's method, if they shared a common control. Thus, depending on the response and the experiment, the term *treatment* may refer to a) different concentrations of the same compound, b) different compounds, each with one specific concentration, c) different compound and concentration combinations or d) different compound and protective substance combinations.

Some of the responses were given as the percentage of control, whereas for others, the responses to treatment and control were given separately. These two types of responses were analysed in slightly different ways.

If the responses to treatment and control were given separately, the log response was analyzed by the usual Dunnett's t-test for multiple comparisons in a one-way ANOVA (Dean and Voss, 1999). Calculations were performed with SAS version 8.2, procedure GLM. The test were repeated for levels 5%, 1% and 0.1% and significance is reported as *not significant (n.s.)*, *, **, and ***, respectively.

If the responses were given as the percentage of control, the usual Dunnett's t-test is not directly applicable. However, if the log original responses were normally distributed, it could be shown that the log ratios were also normally distributed with a certain correlation structure that arose from the fact that the treatments were compared with the same control. From this fact, it was possible to derive a ttest statistic for the multiple hypothesis that the log ratios are zero. The joint distribution of the ttest statistics for different treatments was a multivariate t-distribution to which Dunnett's method of α -adjustment could be applied (Dunnett, 1955). This was done with an SAS IML program. In this case, an adjusted p-value was calculated.

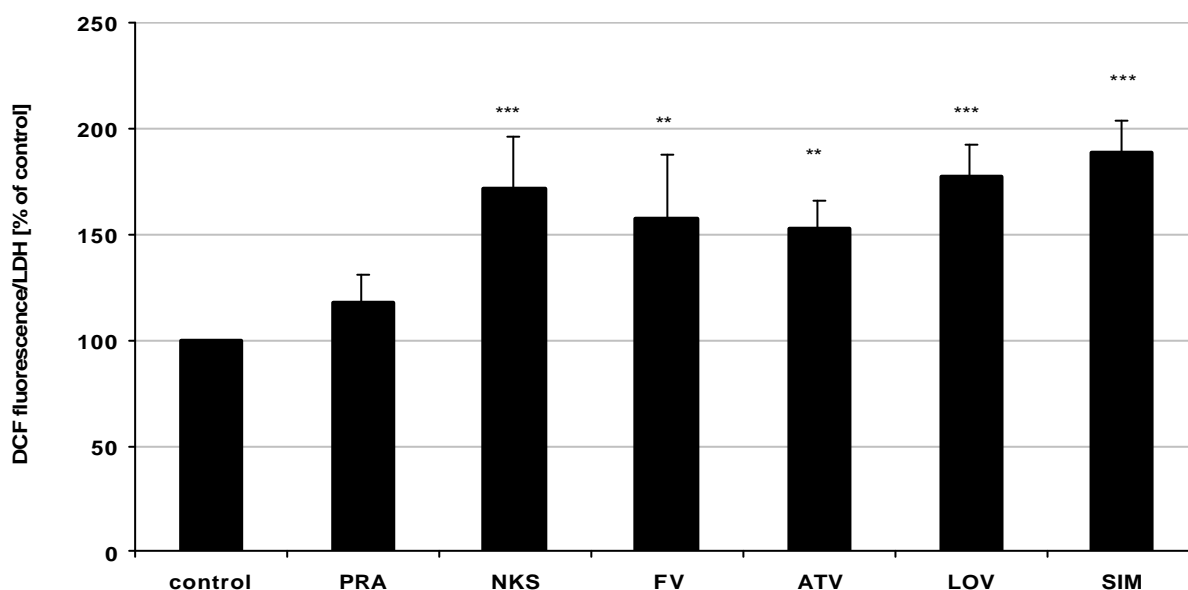
3 RESULTS AND DISCUSSION

3.1 Time- and concentration-dependent changes of statin-induced cellular events

3.1.1 Oxidative stress

3.1.1.1 Formation of reactive oxygen species

The intracellular formation of reactive oxygen species (ROS) was measured in order to study the role of oxidative stress in statin induced skeletal muscle toxicity. HSkMCs were incubated with the different statins, and ROS were determined fluorimetrically by measuring the oxidation of DCF. Already after 30 minutes incubation of hSkMCs with 10 μ M of statins there was an increase in ROS formation, which was statistically significantly different from controls except for PRA (Fig. 9). The extent of increase in ROS at this time point and concentration was similar for all statins.

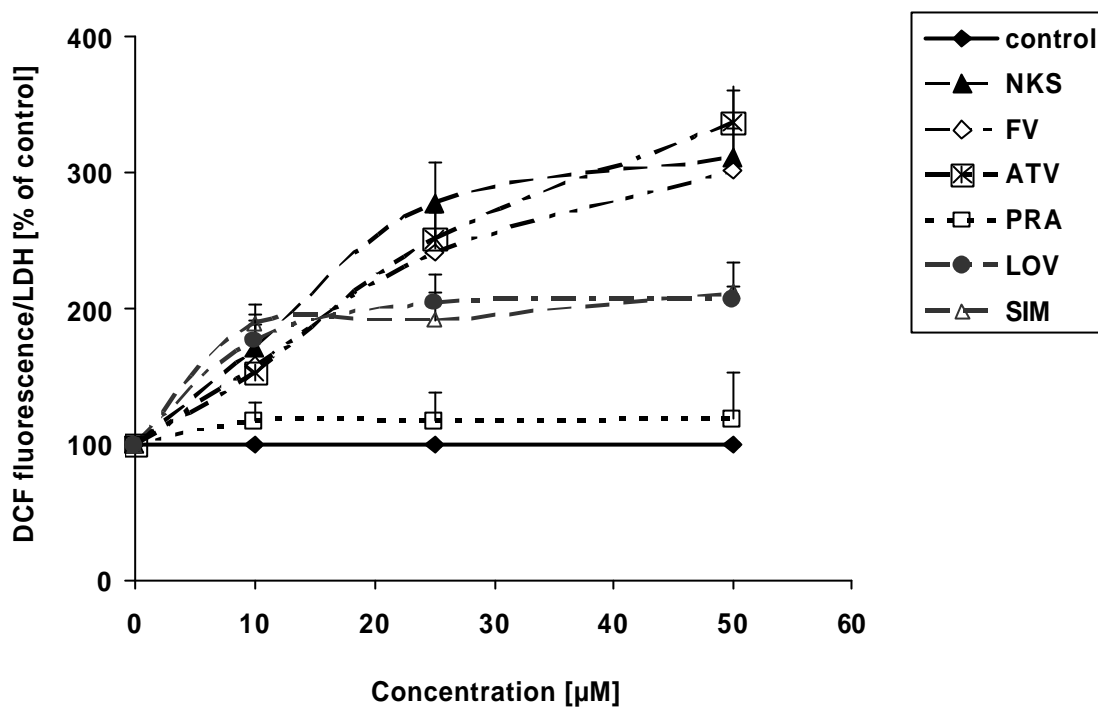


[Control values: ROS formation: 100% = 0.8-1.6 LU/LDH cells]

Fig. 9: Effect of 10 μ M of statins on intracellular ROS formation.

HSkMCs were incubated 30 min with 10 μ M of statins. Data are expressed as means \pm SD from three independent experiments (n=3). Statistically significant differences versus the control group are expressed as **P<0.01 and ***P<0.001.

NKS, FV and ATV induced a concentration dependent increase in ROS up to 50 μM , whereas the ROS levels induced by 10 μM LOV and SIM remained nearly the same even with increasing concentrations of 25 and 50 μM (Fig. 10). ROS were produced continuously during the experiment, as long as cells were viable.



[Control values: ROS formation: 100% = 0.8-1.6 LU/LDH cells]

Fig. 10: Concentration-dependency of statin-induced formation of intracellular ROS.

HskMCs were incubated 30 min with 0, 10, 25 and 50 μM of statins. Data are expressed as means \pm SD from three independent experiments (n=3).

3.1.1.2 Cellular glutathione levels

Decreased cellular glutathione (GSH) levels is an indicator of oxidative stress (Jones and Kennedy, 1983). Intracellular GSH was measured using the enzymatic method of Tietze (1969). HSkMCs cultures were incubated with FV, ATV, PRA and NKS at concentrations of 0, 100, 200 and 400 μM , with LOV at concentrations of 0, 50 and 100 μM and with SIM concentrations of 0, 25, 50 μM for 4 or 24 hours. All statins except PRA caused a concentration dependent decrease of intracellular GSH levels, reaching statistically significant differences versus respective controls after 4 hours of incubation (Fig. 11). This decrease was more pronounced after 24 hours (Fig. 12). There was no significant decrease of GSH detectable with PRA.

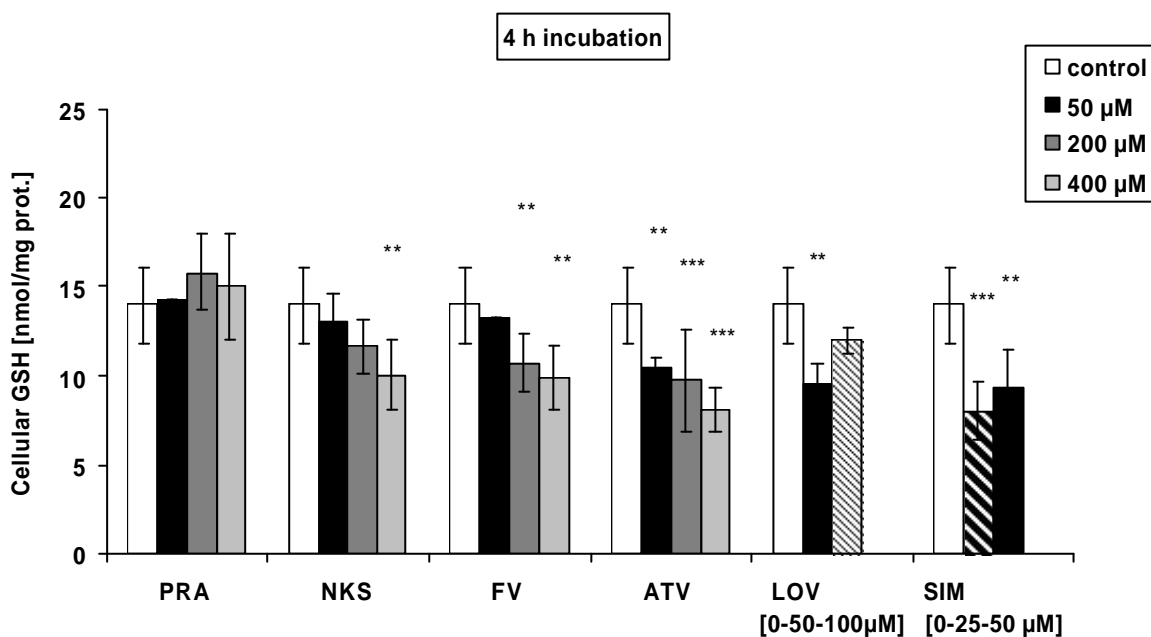


Fig. 11: Concentration-dependency of statin-induced changes of GSH on hSkMCs after 4 hours. Data are expressed as means \pm SD from three independent experiments (n=3). Statistically significant differences versus the control group are expressed as *P<0.05, **P<0.01 and ***P<0.001.

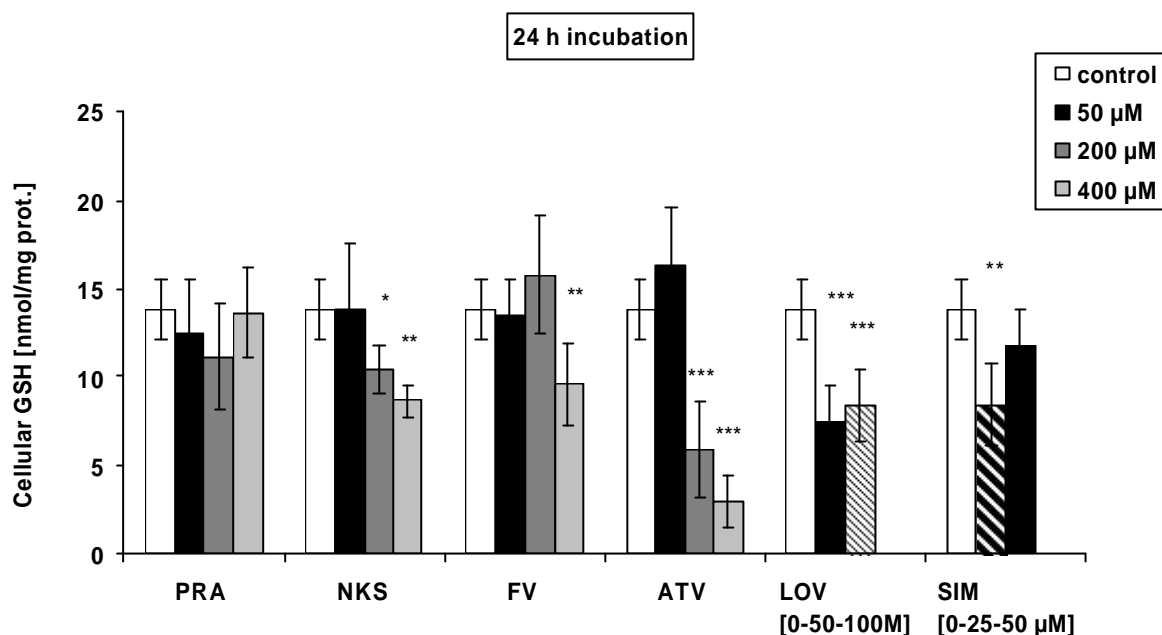


Fig. 12: Concentration-dependency of statin-induced changes of GSH on hSkMCs after 24 hours. Data are expressed as means \pm SD from three independent experiments (n=3). Statistically significant differences versus the control group are expressed as *P<0.05, **P<0.01 and ***P<0.001.

A direct comparison of the effects of different statins on intracellular GSH levels at incubation concentrations of 50 μ M revealed, that after 4 and 24 hours, SIM and LOV caused the strongest decrease of GSH. The effect of 50 μ M ATV was different after 4 and 24 hours of incubation. While there was a significant decrease of GSH after 4 hours at 50 μ M, no statistically significant decrease was found after 24 hours. Under the experimental conditions, cellular GSSG could not be measured, because it was below the detection limit.

3.1.1.3 TBARS assay for lipid peroxidation

TBARS (thiobarbituric acid reactive substances) were determined in hSkMCs and in the cell culture supernatant after treatment with statins by the fluorimetric method of Yagi (1984).

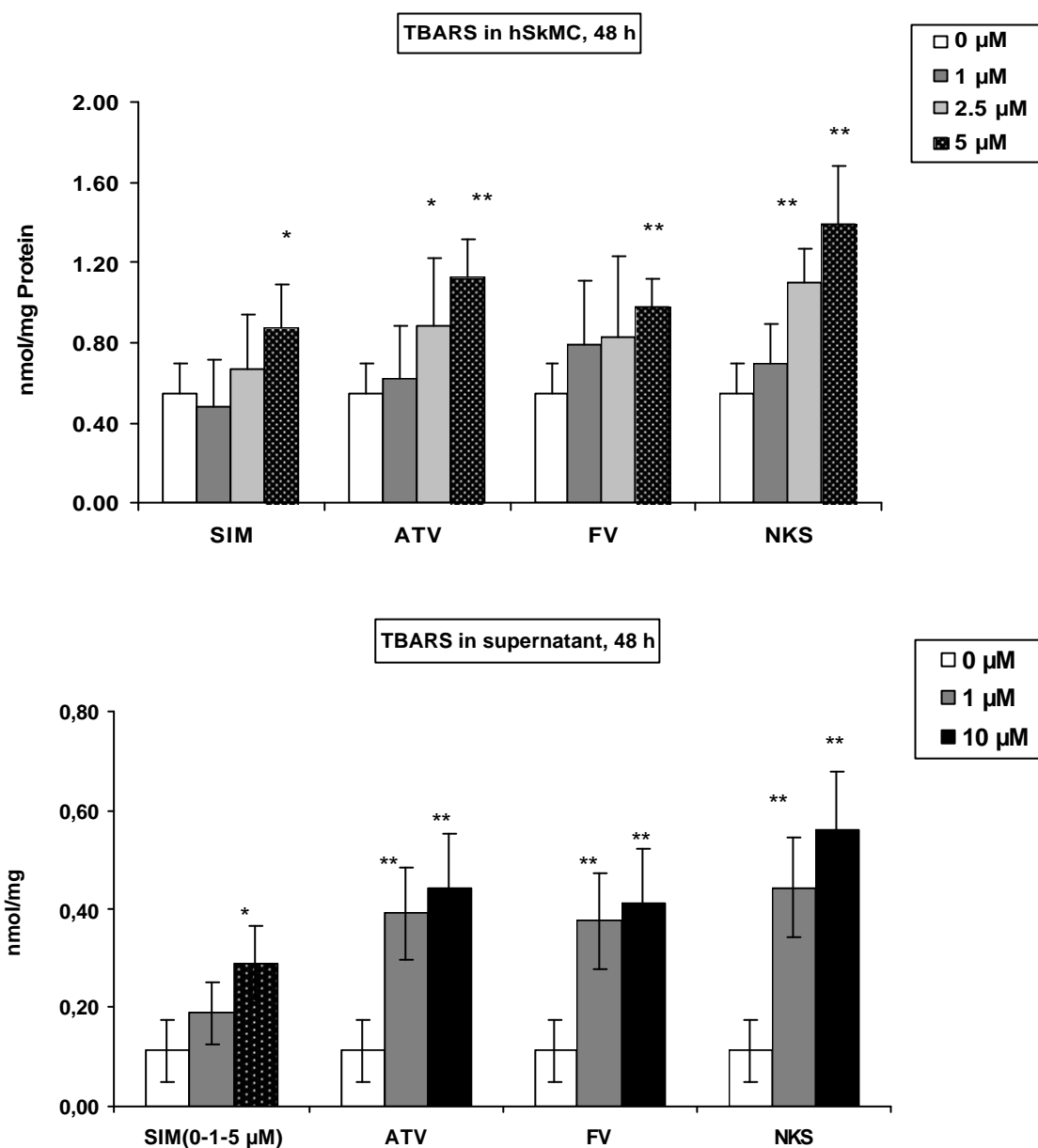


Fig. 13: Concentration dependency of statin-induced intracellular and extracellular TBARS formation on hSkMCs after 48 h.

hSkMCs cultures were incubated with FV, ATV, and NKS at concentrations of 0, 1, 2.5, 5, 10 µM, and with SIM at the concentrations of 0, 1, 2.5 and 5 µM for 48 hours. Data are expressed as means \pm SD from two independent experiments (n=2). Statistically significant differences versus the control group are expressed as *P<0.05, **P<0.001.

HSkMCs cultures were incubated with FV, ATV and NKS at concentrations of 0, 1, 2.5, 5 or 10 μM and with SIM at the concentration of 0, 1, 2.5 and 5 μM for 48 or 72 hours. All statins caused concentration-dependent statistically significantly increase of TBARS in the culture supernatant and in the cells after 48 and 72 hour's incubation (Fig. 13 and 14).

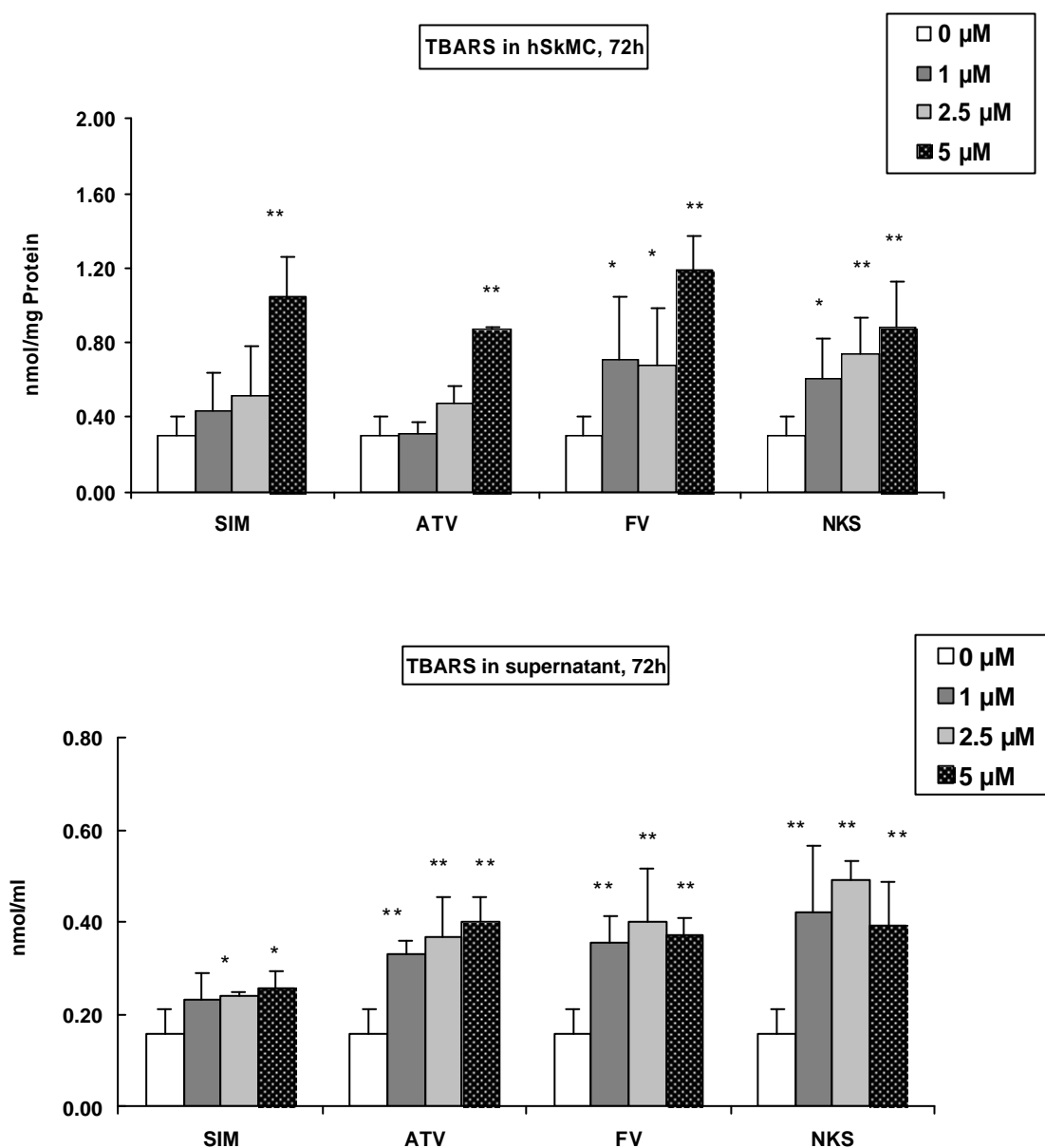


Fig. 14: Concentration dependency of statin-induced intracellular and extracellular TBARS formation on hSkMCs after 72 h.

HSkMCs cultures were incubated with FV, ATV, and NKS at concentrations of 0, 1, 2.5, 5, 10 μM , and with SIM at the concentrations of 0, 1, 2.5 and 5 μM for 72 hours. Data are expressed as means \pm SD from two independent experiments ($n=2$). Statistically significant differences versus the control group are expressed as * $P<0.05$, ** $P<0.001$.

3.1.2 Apoptosis

3.1.2.1 Mitochondrial membrane potential

Disturbance of the mitochondrial membrane potential is an early event in the process of apoptosis. Mitochondrial membrane potential was determined spectrofluorimetrically by rhodamine 123 uptake. Rhodamine 123 is taken up into the cells by passive diffusion and accumulates in mitochondria with intact membrane potential. Incubation of hSkMCs for one hour with NKS, FV, and ATV at 400 μM , LOV at 100 μM and SIM at 50 μM resulted in a decrease of the mitochondrial membrane potential by 12, 18, 16, 47, and 50% of control values, respectively. The decreased membrane potential then remained stable during the 4 h of incubation. The decrease in mitochondrial membrane potential was more pronounced with LOV and SIM. No significant change has been shown after treatment with PRA (Fig. 15).

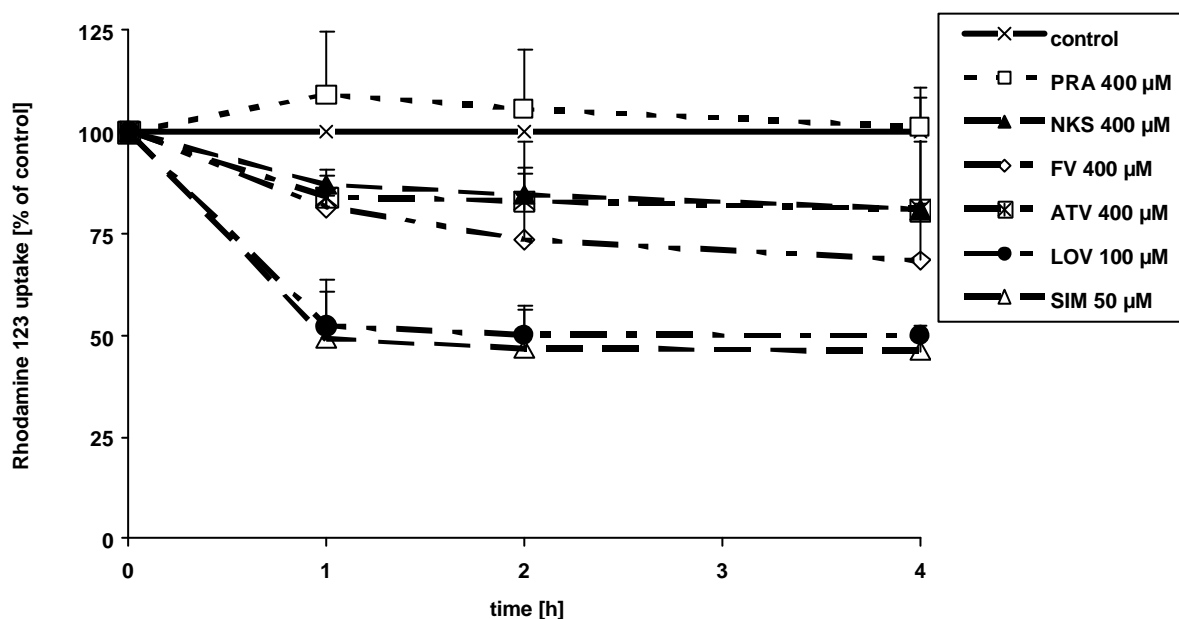


Fig. 15: Time course of statin-induced decrease of mitochondrial membrane potential in hSkMCs.

hSkMCs cultures were incubated with FV, ATV, PRA and NKS at concentration of 400 μM , with LOV at concentration of 100 μM and with SIM concentration of 50 μM for 1, 2 or 4 hours. Data are expressed as means \pm SD from three independent experiments (n=3).

The decrease of rhodamine 123 uptake was concentration dependent and statistically significantly different from controls at 50 μM for LOV, at 25 μM for SIM, and at high concentrations of 400 μM for NKS, FV and ATV (Fig. 16).

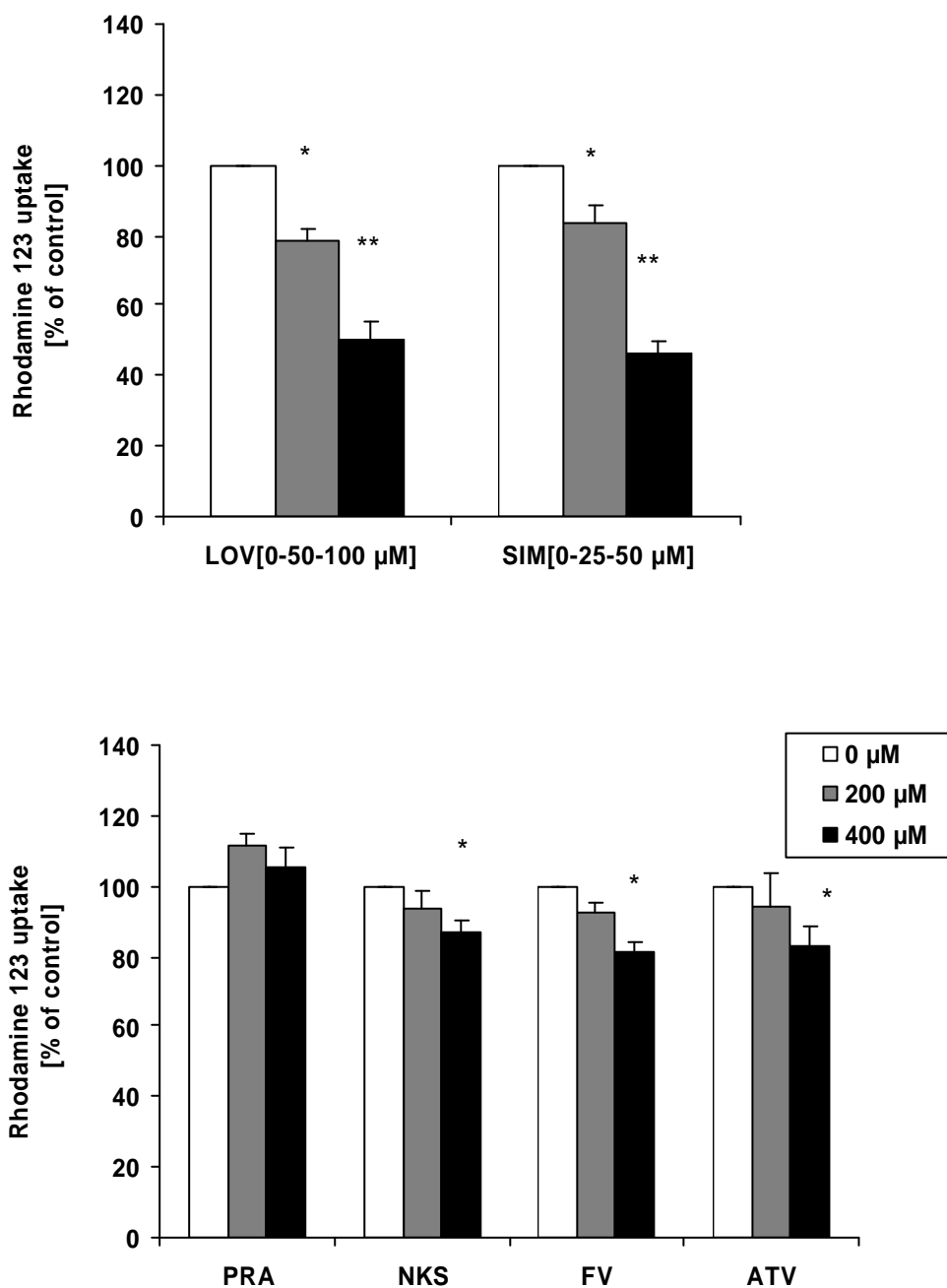


Fig. 16: Concentration dependent effect of statins on hSkMCs mitochondrial membrane potential.

HskMCs cultures were incubated with FV, ATV, PRA and NKS at concentrations of 0, 200 and 400 μM , with LOV at concentrations of 0, 50 and 100 μM , and with SIM at concentrations of 0, 25, 50 μM for 1 hour. Data are expressed as means \pm SD from three independent experiments (n=3). Statistically significant differences versus the control group are expressed as *P<0.05 and **P<0.01.

Effects on the mitochondrial membrane potential were additionally investigated using confocal laser scanning microscopy for determination of fluorescence intensity after double staining of hSkMCs with MitoTracker green FM dye and MitoTracker deep red 633. MitoTracker green FM dye becomes fluorescent once it accumulates in the lipid environment of mitochondria and MitoTracker deep red 633 stains all functional active mitochondria. Staining of hSkMCs with MitoTracker green and MitoTracker red with and without statins treatment is shown in Fig. 17. Control cells show clearly that almost all mitochondria, that are present (green) are also active (red). The overlay image appeared yellow when both mitochondrial dyes stained the same structures. Treatment of hSkMCs with 25 μM SIM for 24 hours strongly decreased the number of active mitochondria as shown with the Mito Tracker red staining and the overlay image (Fig. 17).

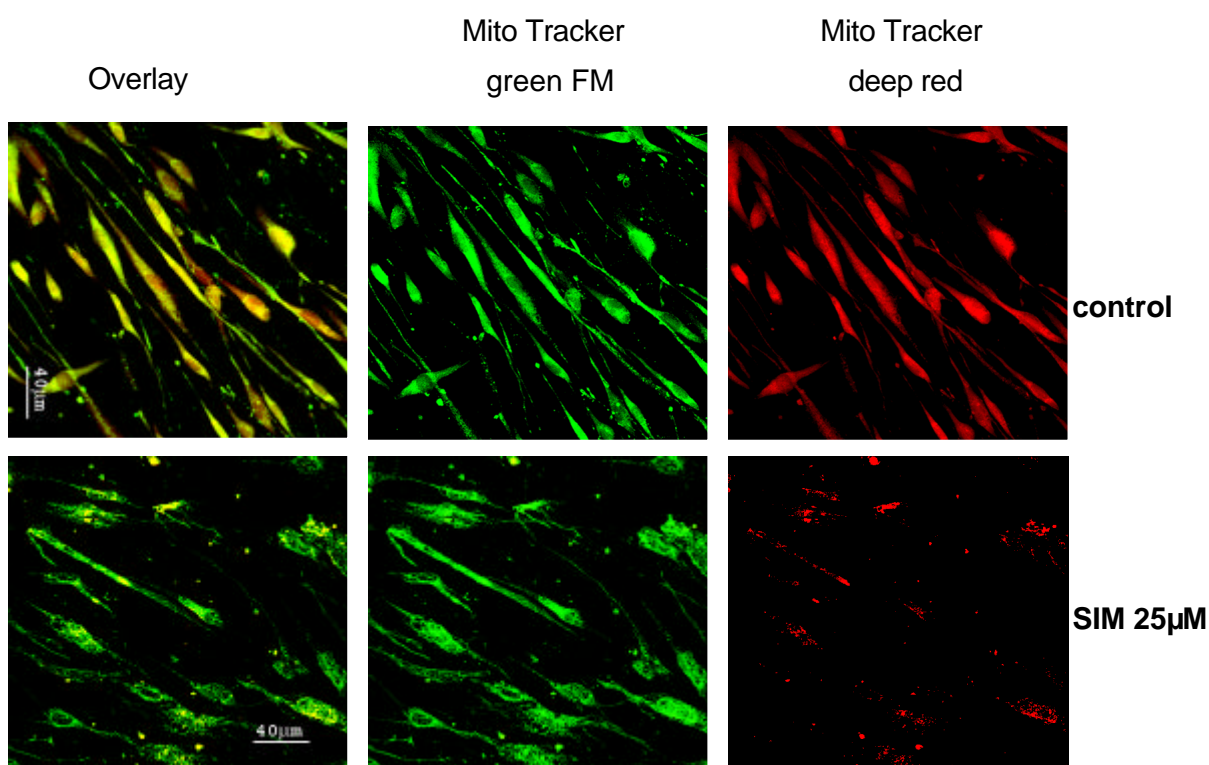


Fig. 17: Representative micrographs of the distribution of the MitoTracker fluorescence.

hSkMCs were grown on cover slips and treated with 25 μM SIM for 24 hours. Cells were incubated with Mito Tracker Red and co-stained with Mito Tracker Green (see "Material and methods"). The scale bar was 40 μm .

Quantitative determination of the ratios of the MitoTracker red vs. MitoTracker green fluorescence intensities in hSkMCs treated with statins confirmed data from rhodamine 123 uptake showing that the decreases of the membrane potential was more effective with LOV and SIM as compared to the others statins (Fig. 18). There was no significant decrease of the membrane potential with PRA.

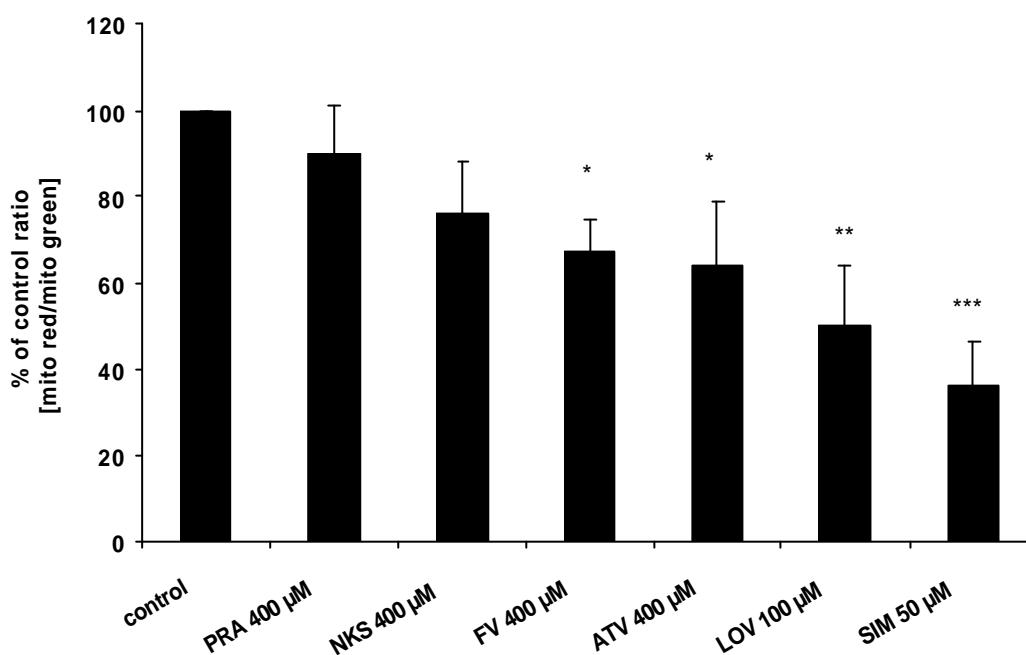
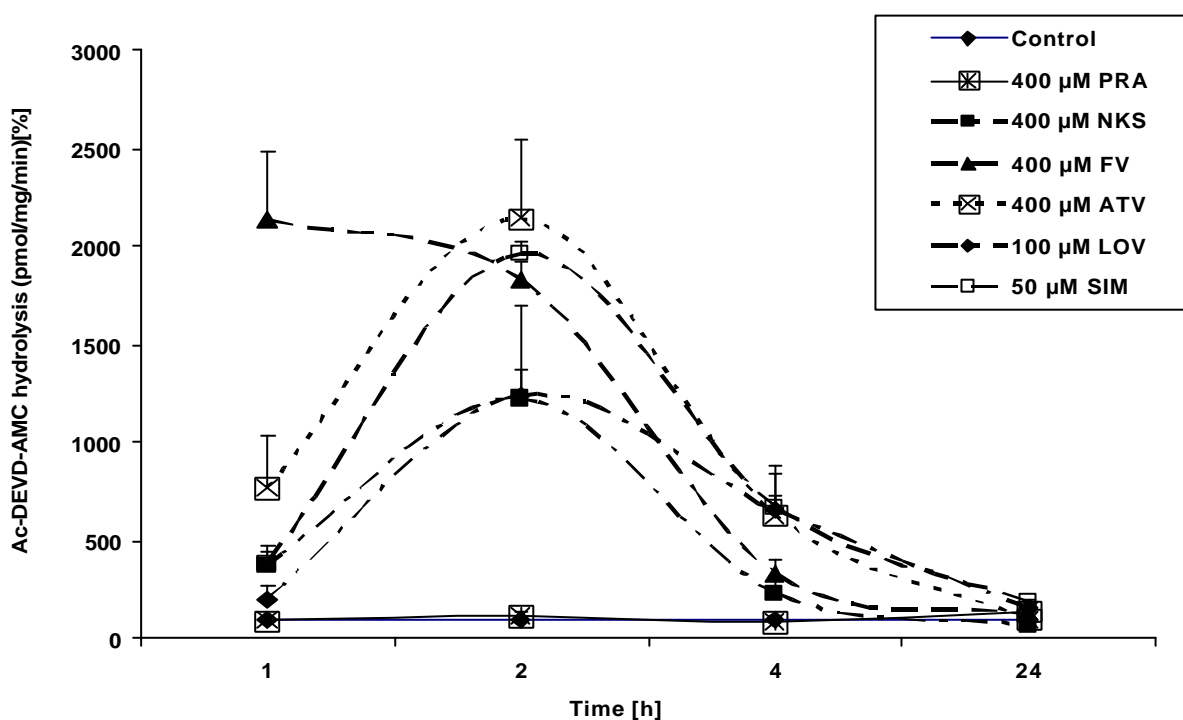


Fig. 18: Effect of statins on the mitochondrial membrane potential determined by MitoTracker Red and MitoTracker Green fluorescence intensities after 1 hour incubation.

HSkMCs cultures were incubated 1 hour with 400 µM NKS, FV, ATV, PRA, 100µM LOV and 50 µM SIM. Data are expressed as means \pm SD from three independent experiments (n=3). Statistically significant differences versus the control group are expressed as *P<0.05, **P<0.01 and ***P<0.001.

3.1.2.2 Caspase-3 activity

The increase of the cytosolic cytokine protease caspase-3 is a strong indication for apoptosis. Therefore hSkMCs were incubated with the different statins and caspase-3 activity was determined enzymatically in the cell homogenate. Short-term treatment of hSkMCs with different statins significantly increased the activity of caspase-3. The data showed that FV (400 μ M) increased the caspase-3 activity as early as after 1 hour incubation to about 21 times of that of the control. After 2 hours, FV, NKS and ATV treatment at 400 μ M resulted in 18, 12 and 21 fold increased caspase-3 activity, respectively. At the same time, 50 μ M SIM and 100 μ M LOV increased the caspase-3 activity 19 and 12 fold, respectively. After 24 hours of incubation, no statistically significant increase in caspase-3 activity was seen with any statin (Fig. 19).

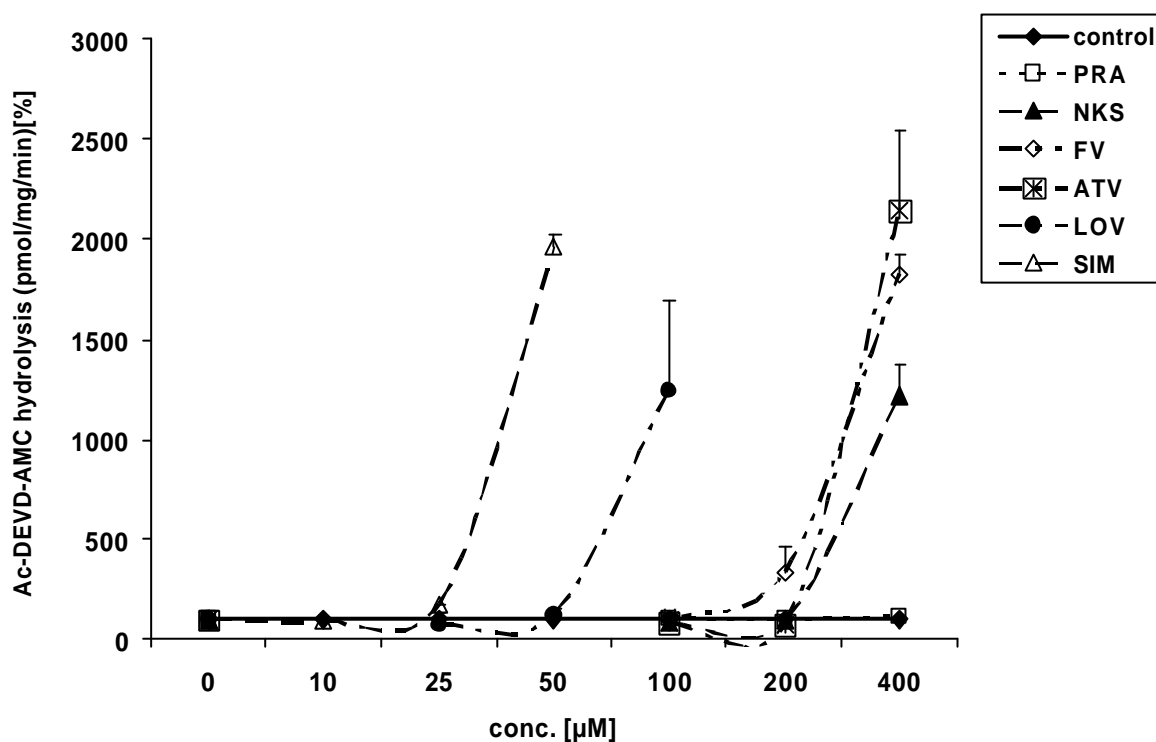


[Control values: Caspase-3 activity: 100%= 4.5-9 pmolAMC/min/mg protein]

Fig. 19: Time course of statin-induced caspase-3 activity in hSkMCs cultures.

hSkMCs cultures were incubated with FV, ATV, PRA and NKS at concentrations of 400 μ M, and with LOV at the concentration of 100 μ M, and with SIM at the concentration of 50 μ M for 1, 2 or 4 hours. Data are expressed as means \pm SD from three independent experiments (n=3).

Increases in caspase-3 activity were concentration dependent. SIM was more potent than all others statins, having effects at concentrations of 50 μM , whereas effects of LOV started at 100 μM . All other statins, except PRA, showed effects at concentrations greater than 200 μM . There was not significant changes on caspase-3 activity in hSkMCs culture treated with PRA as compare to the controls and to the others statins (Fig. 20).



[Control values: Caspase-3 activity: 100%= 4.5-9 pmolAMC/min/mg protein]

Fig. 20: Concentration-dependency of statin-induced caspase-3 activity on hSkMCs.

hSkMCs cultures were incubated with FV, ATV, PRA and NKS at concentrations of 0, 100, 200 and 400 μM , and with LOV at concentrations of 0, 25, 50 and 100 μM , and with SIM at concentrations of 0, 10, 25, 50 μM for 2 hours. Data are expressed as means \pm SD from three independent experiments (n=3). Data are expressed as mean \pm SD from three independent experiments (n=3).

3.1.2.3 Nuclear morphology

Changes in cell nuclear morphology, such as condensation and fragmentation are considered late events of apoptosis. In order to identify the changes on cell nuclei in hSkMCs after treatment with statins, cells were stained with the fluorescent DNA stain Hoechst 33342 and nuclear morphology as well as fluorescence intensity was determined using the Cellomics ArrayScan. Results were expressed as percentage of cells with shrunk nuclei compared to the total cell population. Long term incubation (72 h) of hSkMCs culture with 5 and 10 μM of NKS, FV, ATV, LOV and SIM resulted in a concentration-dependent increase of cells with smaller nuclei. The number of cells with changed nuclei was between 20 and 36% as compared with control values. Effects were strongest with 10 μM of NKS. No significant changes were found after incubation with PRA under the same conditions (fig. 21). Incubation for shorter time periods such as 4, 24, or 48 hours did not reveal any changes in cell nuclear morphology (data not shown).

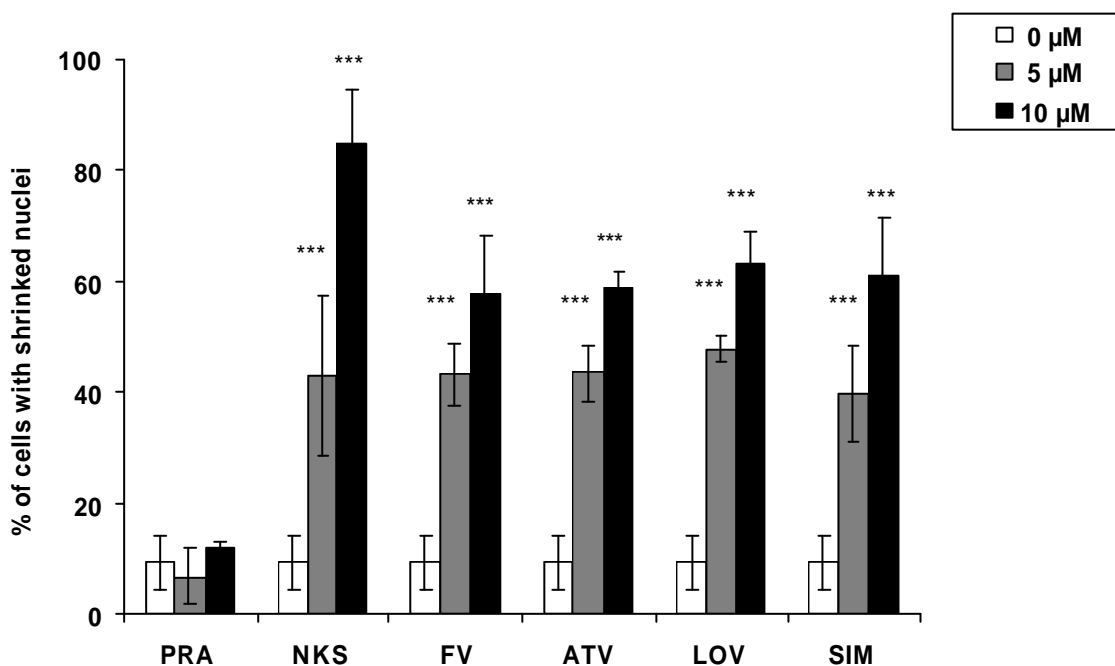


Fig. 21: Effect of statins on hSkMCs nuclear morphology.

hSkMCs cultures were incubated with NKS, FV, ATV, PRA, LOV and SIM at concentrations of 0, 5 and 10 μM , for 72 hours. Data are expressed as means \pm SD from three independent experiments (n=3). Statistically significant differences versus the control group are expressed as ***P<0.001.

Representative pictures of hSkMCs stained with Hoechst after treatment with 10 μM of different statins for 72 hours are shown in figure 22. Nuclear changes of the treated cells are very obvious by the bright fluorescence and reduced diameter.

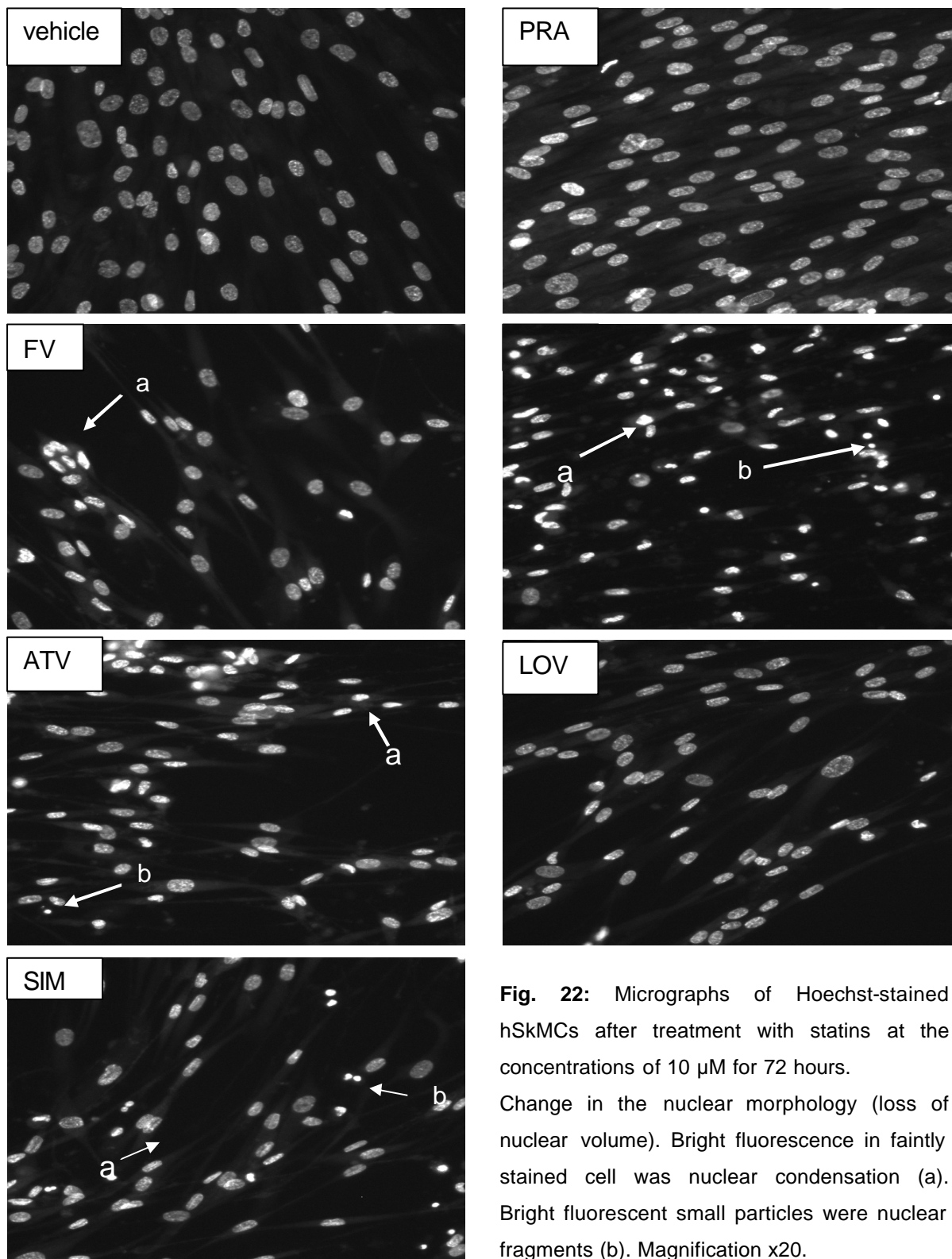


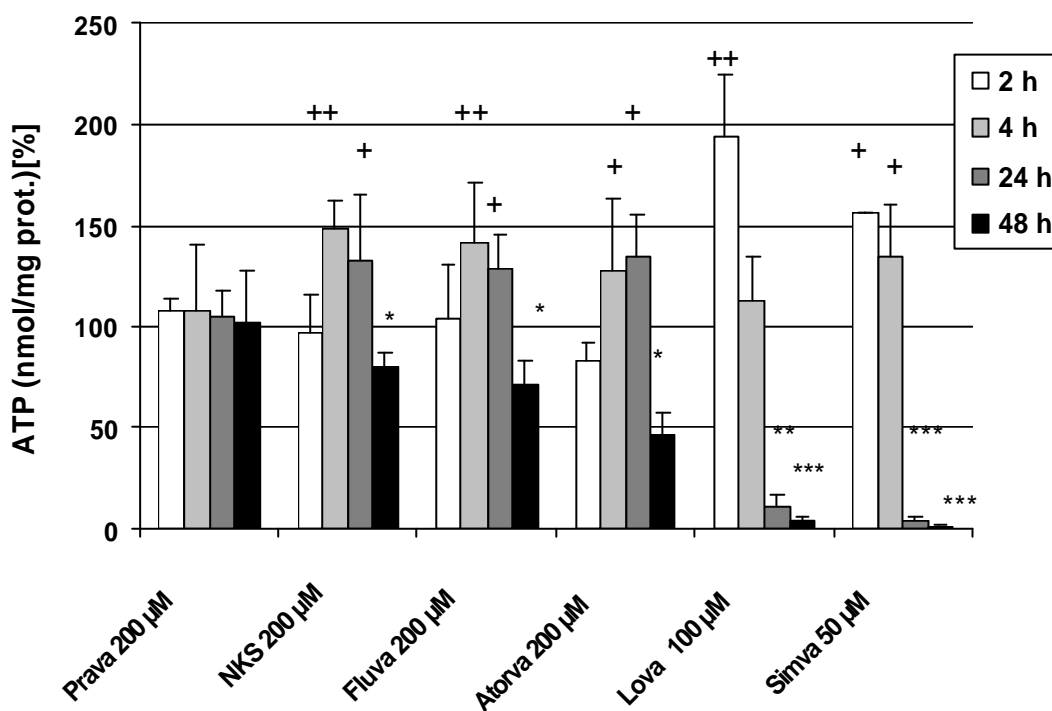
Fig. 22: Micrographs of Hoechst-stained hSkMCs after treatment with statins at the concentrations of 10 μM for 72 hours.

Change in the nuclear morphology (loss of nuclear volume). Bright fluorescence in faintly stained cell was nuclear condensation (a). Bright fluorescent small particles were nuclear fragments (b). Magnification x20.

3.1.3 Cytotoxicity

3.1.3.1 Intracellular ATP

Intracellular ATP was determined as an index of cell viability because of its importance in mitochondria activity. Treatment of hSkMCs cultures with 200 μ M of NKS, FV and ATV, 100 μ M of LOV and 50 μ M of SIM significantly increased the cellular ATP content after 2 hours incubation. Later, the ATP content continuously decreased. At 48 hours, ATP levels were statistically significantly decreased as compared to the controls. The extent of decrease was different for the different statins (Fig. 23).



[Control values: ATP 100% = 140-350 nmol/mg protein (depends on time and confluence)]

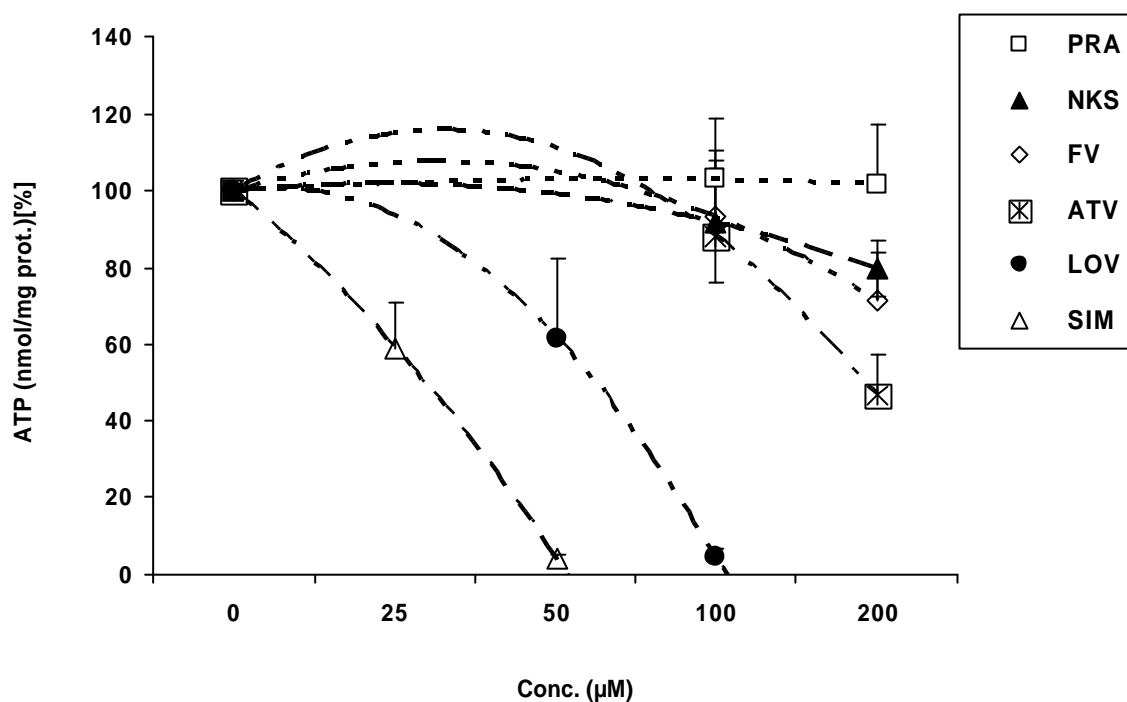
Fig. 23: Time course of effect of statins on hSkMCs intracellular ATP.

HskMCs cultures were incubated with FV, ATV, PRA and NKS at concentrations of 200 μ M, and with LOV at concentrations of 100 μ M, and with SIM concentrations of 50 μ M for 2, 4, 24 and 48 hours.

Data are expressed as means \pm SD from three independent experiments (n=3). Statistically significant differences versus the respective control group (0 μ M statins) are expressed as *P<0.05, **P<0.01 and

***P<0.001. Statistically significant differences versus the respective control group (2h incubation) are expressed as +P<0.05 and ++P<0.01.

HSkMCs cultures were treated with NKS, FV, ATV, LOV and SIM at different concentrations for 48 hours. The results showed that the decrease of ATP content in the cells was concentration-dependent (Fig. 24). SIM and LOV were more potent than the other statins, having effects at lower concentration and after shorter incubation times. There were no significant changes on ATP content in hSkMCs cultures treated with PRA.

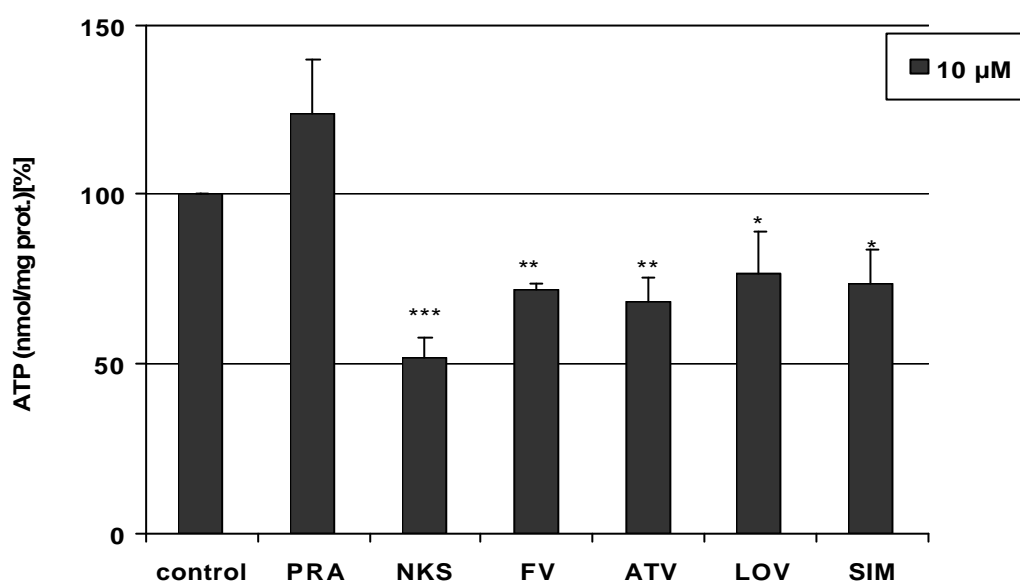


[Control values: ATP 100% = 140-350 nmol/mg protein (depends on time and confluence)]

Fig. 24: Concentration-dependent effects of statins on hSkMCs intracellular ATP.

HSkMCs cultures were incubated with FV, ATV, PRA and NKS at concentrations of 0,100, 200 µM, and with LOV at concentrations of 0, 50 and 100 µM, and with SIM concentrations of 0, 25, 50 µM for 48 hours. Data are expressed as means ±SD from three independent experiments (n=3).

In order to compare the effects of different statins on intracellular ATP levels hSkMCs were incubated with the same concentrations of all statins, 10 μ M. After 72 hours, the intracellular ATP decreased to similar levels with ATV, FV, LOV and SIM. NKS caused the strongest decrease of intracellular ATP, whereas no effect was found with PRA (Fig. 25).



[Control values: ATP 100% = 140-350 nmol/mg protein (depends on time and confluence)]

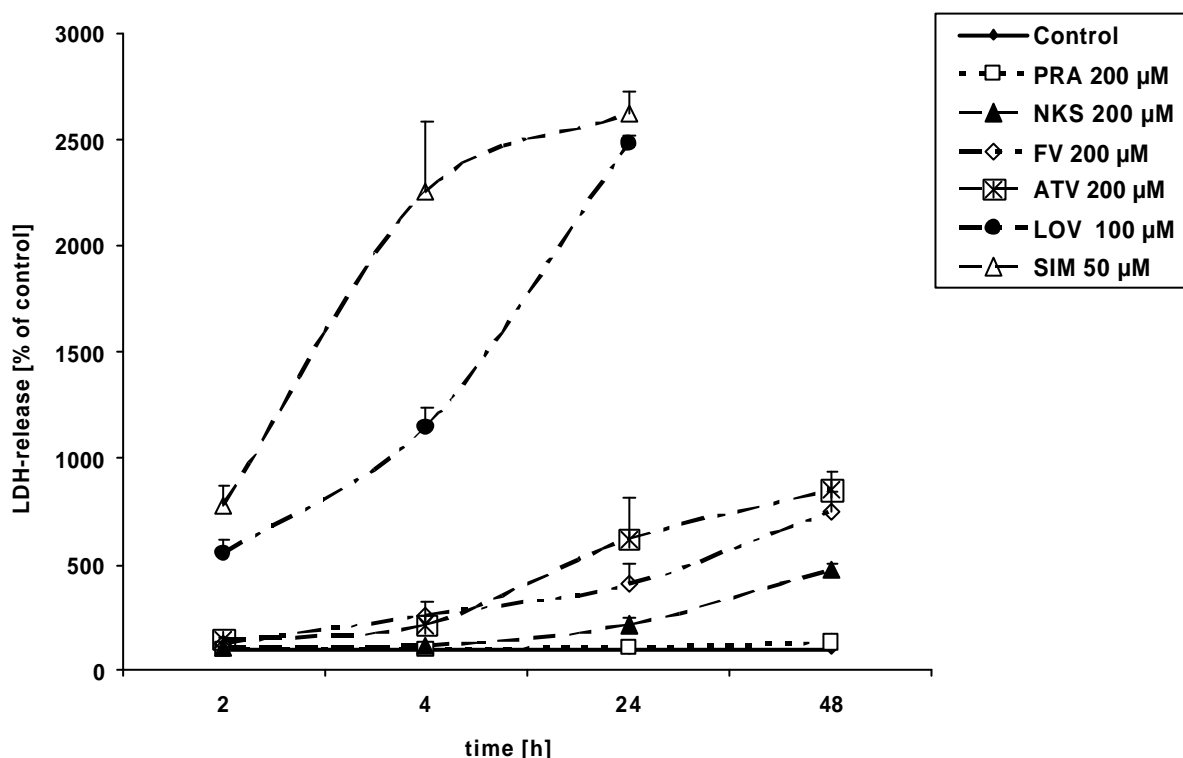
Fig. 25: Effect of 10 μ M statins on intracellular ATP after 72 h incubation of hSkMCs.

HSkMCs cultures were incubated with NKS, FV, ATV, PRA, LOV and SIM at concentrations of 10 μ M for 48 hours. Data are expressed as means \pm SD from two independent experiments (n=2). Statistically significant differences versus the control group are expressed as *P<0.05, **P<0.01 and ***P<0.001.

3.1.3.2 Lactate dehydrogenase release

Extracellular lactate dehydrogenase (LDH) activity was measured spectrophotometrically as an index of plasma membrane damage and loss of membrane integrity (Welder *et al.*, 1994, Tyson *et al.*, 1987).

The treatment of hSkMCs with statins resulted in a time-dependent induction of LDH release into the culture medium. LOV and SIM, at concentrations of 100 and 50 μM , respectively, statistically significantly increased LDH-release starting after 2 hours to reach 25 times the control values after 24 hours of incubation. While NKS, FV and ATV were not significantly cytotoxic after 2 and 4 hours, LDH-release was increased after 24 and 48 hours incubation (Fig. 26).

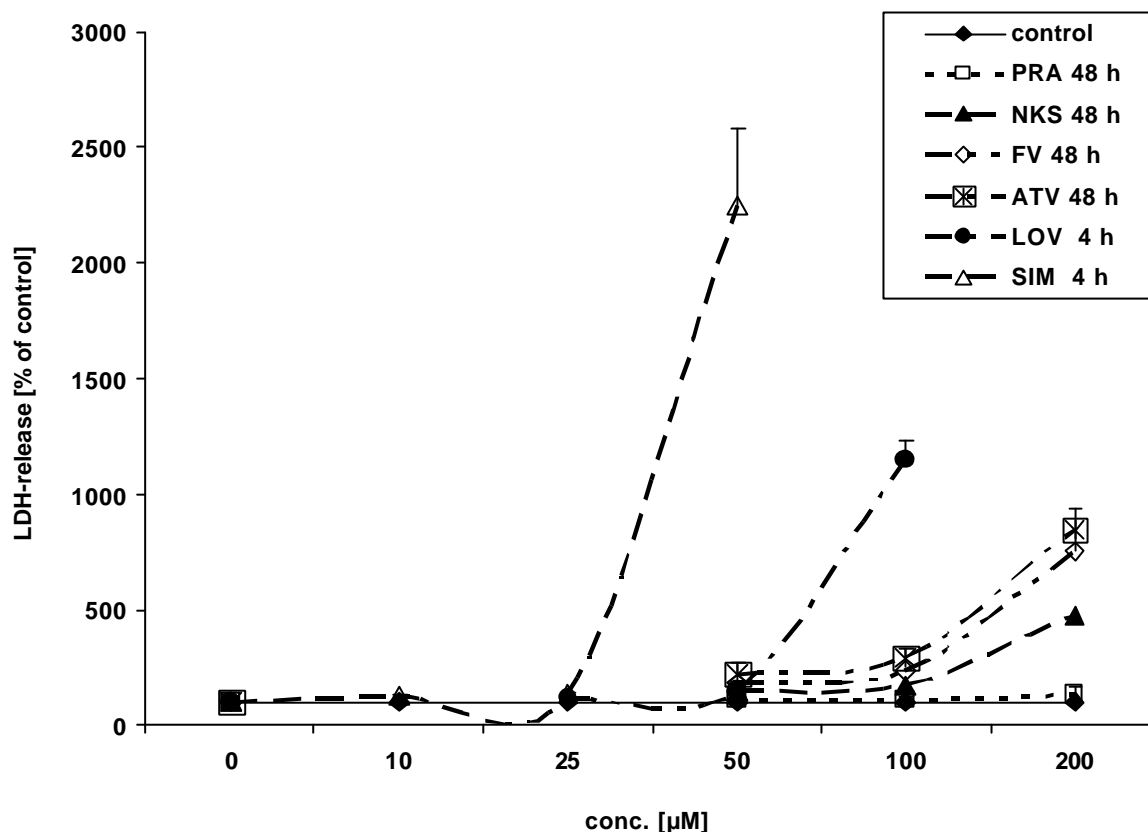


[Control values: LDH-release100% = 750-1100 IU/L (depends of the confluence)]

Fig. 26: Time course of statin-induced cytotoxicity in hSkMCs cultures.

HskMCs cultures were incubated with FV, ATV, PRA and NKS at concentrations of 200 μM , with LOV at concentrations of 100 μM , and with SIM concentrations of 50 μM for 2, 4, 24 and 48 hours. Data are expressed as means \pm SD from three independent experiments (n=3).

Cytotoxic effects of statins in hSkMCs cultures were concentration and time-dependent (Fig. 27). In general, SIM was more potent than the other statins, having effects at lower concentration and after shorter incubation times. There was no significant change of LDH-release in hSkMCs culture treated with PRA compared to the controls.

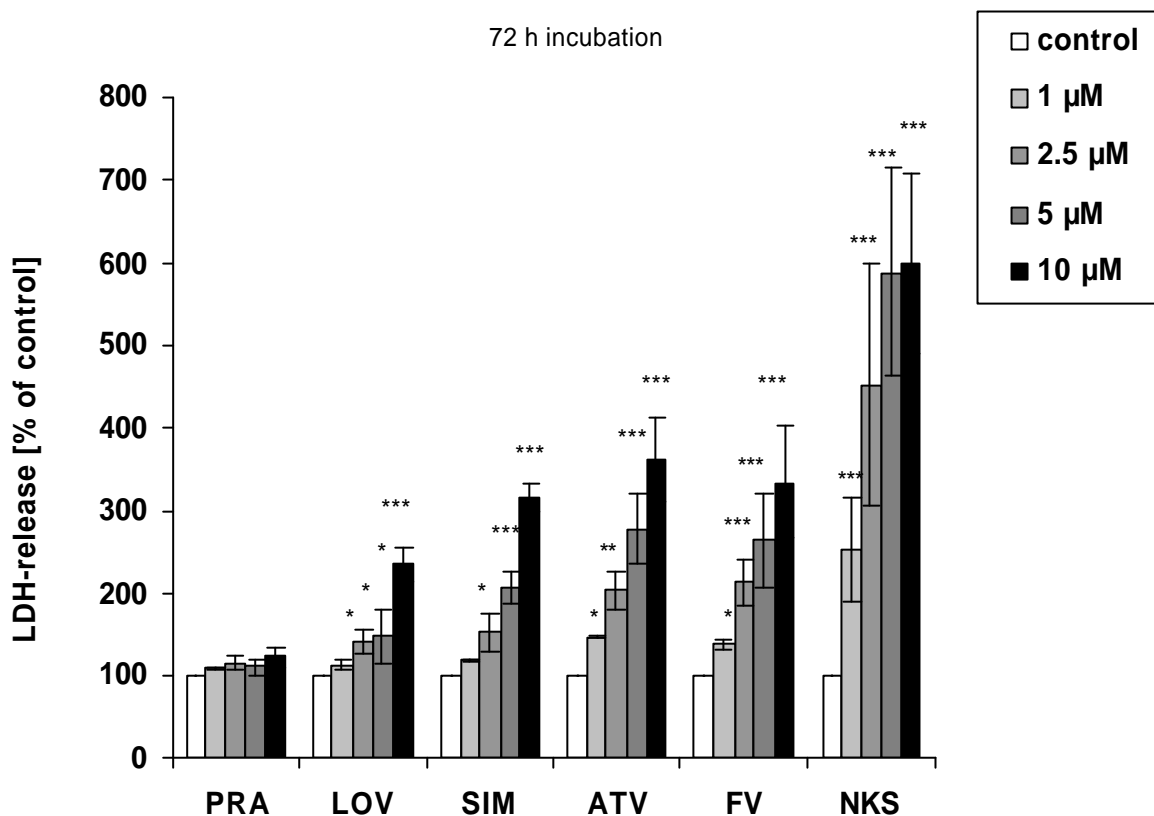


[Control values: LDH-release 100% = 750-1100 IU/L (depends of the confluence)]

Fig. 27: Concentration-dependency of statin-induced cytotoxicity on hSkMCs.

HskMCs cultures were incubated with FV, ATV, PRA and NKS at concentrations of 0, 50, 100, 200 µM, for 48 hours. With LOV at concentrations of 0, 25, 50 and 100 µM, and SIM concentrations of 0, 10, 25, 50 µM for 4 hours. Data are expressed as means \pm SD from three independent experiments (n=3).

HskMCs were treated also with low concentrations of NKS, FV, ATV, PRA, LOV and SIM at 1, 2.5, 5, and 10 μM , but then for long time such as 72 hours. The treatment with statins resulted in a concentration-dependent induction of LDH release into the culture medium. Under these conditions, NKS was found to be most potent, while PRA was again not cytotoxic at all (Fig. 28).



[Control values: LDH-release100% = 750-1100 IU/L (depends of the confluence)]

Fig. 28: Concentration-dependency of cytotoxicity after 72 hours incubation of hSkMCs with statins.

HskMCs cultures were incubated with NKS, FV, ATV, PRA, LOV and SIM at concentrations of 0, 1, 2.5, 5 and 10 μM , for 72 hours. Data are expressed as means \pm SD from three independent experiments (n=3). Statistically significant differences versus the respective control group are expressed as *P<0.05, **P<0.01 and ***P<0.001.

3.1.4 Discussion

In the current studies DCF-dAc (2', 7'-dichlorofluorescein diacetate) was used as an indicator of intracellular ROS formation (LeBel *et al.*, 1992). After passing the outer cell membrane, DCF-dAc is cleaved by cytosolic esterases into its active fluorophore DCFH, which, by the reaction with hydrogen peroxide and other hydroperoxides, such as lipid hydroperoxides results in a fluorescence molecule with an excitation wavelength of 475 nm and an emission wavelength of 525 nm. We have demonstrated for the first time that statin treatment of hSkMCs is leading to increase intracellular levels of ROS. The statin-induced formation of ROS is a very early event that occurred after only 30 min of incubation with hSkMCs, starting to be significantly different from controls at 10 μ M. All statins behaved nearly in the same way, except PRA, which, because of its hydrophilic property, was not very well taken-up into the cells and thus showed no increase of ROS formation.

Depletion of intracellular GSH level and increased GSSG formation are markers of increased ROS formation. The consumption of GSH is facilitated by GSH-peroxidase which is leading to the detoxification of reactive oxygen species like hydrogen peroxides. We could demonstrate that GSH was decreased at non-toxic concentrations of NKS, FV and ATV. However there was an overlap of cytotoxicity and GSH depletion at the applied LOV and SIM concentrations. In general the concentrations used to decrease GSH were higher than that in the DCF-dAc assay in order to show increased ROS formation. Since the GSH metabolism is adapting very rapidly by enzyme induction to ROS stress, a decrease of GSH at low ROS stress, which occurs with low statin concentrations and short incubation times, may not become visible.

Confirmation of ROS formation by the depletion of GSH is still not sufficient since there was no increased GSSG found in any of the samples treated with either statins. By the applied method of Tietze (1969), we could not confirm GSSG formation in hSkMCs, since GSSG levels for control samples were below detection level. Since we did not see an increase of GSSG in the cells, it is possible that GSSG is excreted immediately into the cell culture supernatant once it is formed. Formation of GSH-adducts by reactive electrophile drug metabolites would be another mechanism of GSH depletion, which is unlikely however, since statins are not known to form GSH-adducts.

TBARS is another indirect parameter for oxidative stress. TBARS forms intermediates with lipid peroxidation products, such as reactive aldehydes, thus it was supposed to be a specific marker for lipid peroxidation. However in recent investigations it turned out that TBA (thiobarbituric acid) also shows reactivity for oxidized proteins, sugars and ribonucleic acids. In the present studies we could demonstrate that treatment with statins is leading to increased TBARS after 48 and 72 hours in cells as well as in the cell culture supernatant. Increased TBARS formation in the cell culture supernatant was also reported for other pro-oxidative compounds (Fariss 1990, Wolf *et al.*, 1997). One can assume that the increase of TBARS in the cell culture medium may be the result of increased lipid repair as part of a defense mechanism against oxidative stress. Oxidized lipids are cleaved from the membranes and then released into the extracellular medium.

By means of three different methods we provided evidence that statins induce an oxidative stress situation, which is starting already after only 30 min after incubation with hSKMCs, by formation of free reactive oxygen species which continue over the complete observation period of 72 hours. It is interesting to note that significant increases of TBARS occurred at 1 μM of the statin, which is very close to patient's plasma C-max. In vivo study showed an increase in lipid peroxidation in the urine of patients with rhabdomyolysis (Holt *et al.*, 1999).

ROS have been implicated in the pathophysiology of a large number of diseases and this role has been attributed to their high reactivity and deleterious effects on cell structures (Baynes, 1991; Van Dam *et al.*, 1995). ROS may damage skeletal muscle cells in a number of pathological conditions and may contribute to skeletal muscle degeneration in chronic heart failure (Tsutsui *et al.*, 2001), muscular dystrophies (Ragusa *et al.*, 1997), ischemia-reperfusion (Pattwell *et al.*, 2001), and exercise-induced muscle injuries (Zerba *et al.*, 1990). It had been shown that ROS may play an important role during the induction of apoptosis (Jung *et al.*, 2001). Statin-induced apoptosis via the formation of ROS in hSkMCs has not been shown before.

Apoptosis is an organized and regulated cellular death process which controlling the development and homeostasis of multicellular organisms which occurs under pathological and physiological conditions (Arends and Wyllie, 1991). It is widely recognized that mitochondria play a central role in the apoptotic process. A principal feature within apoptosis cascades is disruption of mitochondrial transmembrane

potential and release of apoptogenic protein, induced by opening of the permeability transition pore (Mayer and Oberbauer, 2003).

The loss of mitochondria membrane potential is discussed in current literature as early events in the apoptotic cascade. Our data strongly suggest that statin treatment induced apoptosis by decreasing mitochondrial membrane potential after 1 hour of incubation, which remained stable during 4 hours of observation. The results, which were obtained by Rhodamine 123 uptake, were also confirmed by means of confocal laser scanning microscopy using double staining with Mito Tracker green FM and Mito Tracker deep red 633.

Caspase-3 plays an important role in the executive phase of apoptosis. Caspase-3 cleaves many important cellular substrates that are directly or indirectly involved in the breakage of DNA strands and leading to apoptosis (Nicholson and Thornberry, 1997; Salvesen and Dixit, 1997). The activity of caspase-3 is energy-dependent. In our experiments statin-induced caspase-3 activation was followed for all statins except PRA by an increase of intracellular ATP levels. When cells became necrotic, ATP dropped below the control levels.

Nuclear condensation and fragmentation are late events of apoptosis. In the current studies we determined the number of cells with shranked nuclei by means of light microscopy after staining with Hoechst 33342 dye. The results showed that statins at low concentrations specifically caused changes in the nuclear morphology after 72 hours incubation. With the current results, however, it is not possible to clearly establish whether these effects are related to apoptosis or necrosis.

Overall we provide evidence for the induction of apoptosis in hSkMCs by statins at different levels, in the mitochondria, by cytosolic caspase-3 activity and nuclear morphology changes. This is in accordance with the current literature, which shows that statin can induce apoptosis in a variety of cell types, including vascular smooth muscle (Guijarro *et al.*, 1998), neonate cardiac myocytes (Ogata *et al.*, 2002), proximal tubular cells (Limura *et al.*, 1997), prostate (Padayatty *et al.*, 1997) and other tumor cells (Marcelli *et al.*, 1998; Wong *et al.*, 2001). Cerivastatin induced apoptosis was shown in human myotubes (Johnson *et al.*, 2004).

Necrosis is the type of cell death in which cells die due to swelling and membrane damage. We used the release of the cytosolic enzyme LDH as a marker of irreversible membrane breakage. Once the membrane is broken, LDH is leaking into the cell culture supernatant. The result indicated that all statins except PRA induced

damage in the plasma membrane, thus suggesting a necrotic process. The induction of the necrotic type of cell damage was dependent on the incubation time and on the applied statin concentration.

The time course and the sequence of the statin-induced events suggest a possible mechanistic relationship. The sequence of events is starting with ROS formation, the induction of apoptosis and necrosis. Necrosis may be secondary to apoptosis. ATP may serve as a possible switching element between apoptosis and necrosis. Intracellular ATP is an indicator of energy state and thus can regulate the transition from apoptosis to necrosis. It had been shown that high cellular ATP levels protect against apoptosis whereas low intracellular ATP levels inhibit apoptosis (Leist and Nicotera, 1997, Leist *et al.*, 1997). Since apoptosis is an active process, which involves various cellular reconstructions, energy is needed. Our results showed an increase of the intracellular ATP pool in hSkMCs after short term incubation. The later decrease of intracellular ATP pool levels after long term incubation can drive cells into necrosis.

In general, statins showed two types of effects: Effects at high concentrations (up to 400 μ M) within a short period of time (2-4 hours) and effects at low concentrations (from 1 to 10 μ M) mainly after long term incubation (48 till 72 hours). The results reached after long term and at low concentrations may be considered as more relevant for the situation for man, whereas the results at high level and short term may be less specific. Effects at high concentrations and after short incubation times showed in principle the specific low-dose effect, which, however, is superposed by unspecific cytotoxicity. In our experiments, high concentrations were used mainly in order to exaggerate reactions which were not seen at low concentrations and short incubation times. The relevance of the high dose effects was further investigated by performing experiments with specific inhibitors (next chapter).

Our results demonstrate in principle that SIM and LOV were the most potent cytotoxic compounds, whereas FV, NKS and ATV were better tolerated in short term experiments. In long term experiments with physiologically relevant concentrations, the ranking of effects changed. In these studies NKS was revealed as the most potent statin, whereas ATV, FV, SIM and LOV were similarly less potent. PRA was markedly non-toxic, at both high concentrations and longer treatment periods. This is in accordance with Masters *et al.* (1995) who showed that PRA was less myotoxic to cultures of neonatal rat skeletal muscle cells than either SIM or LOV (Masters *et al.*,

1995). The difference in toxicity is mainly due to factors including the lipophilicity and the diversity of their physical and chemical properties.

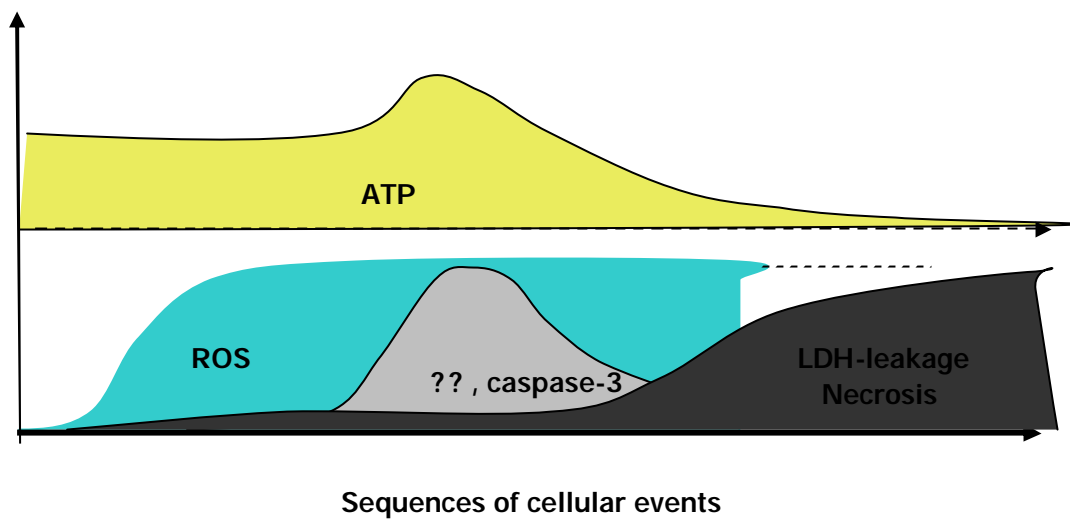


Fig. 29: Postulated causal relation between ROS formation, apoptosis and necrosis and sequence of events.

3.2 Interaction between the cellular events-induced by statins

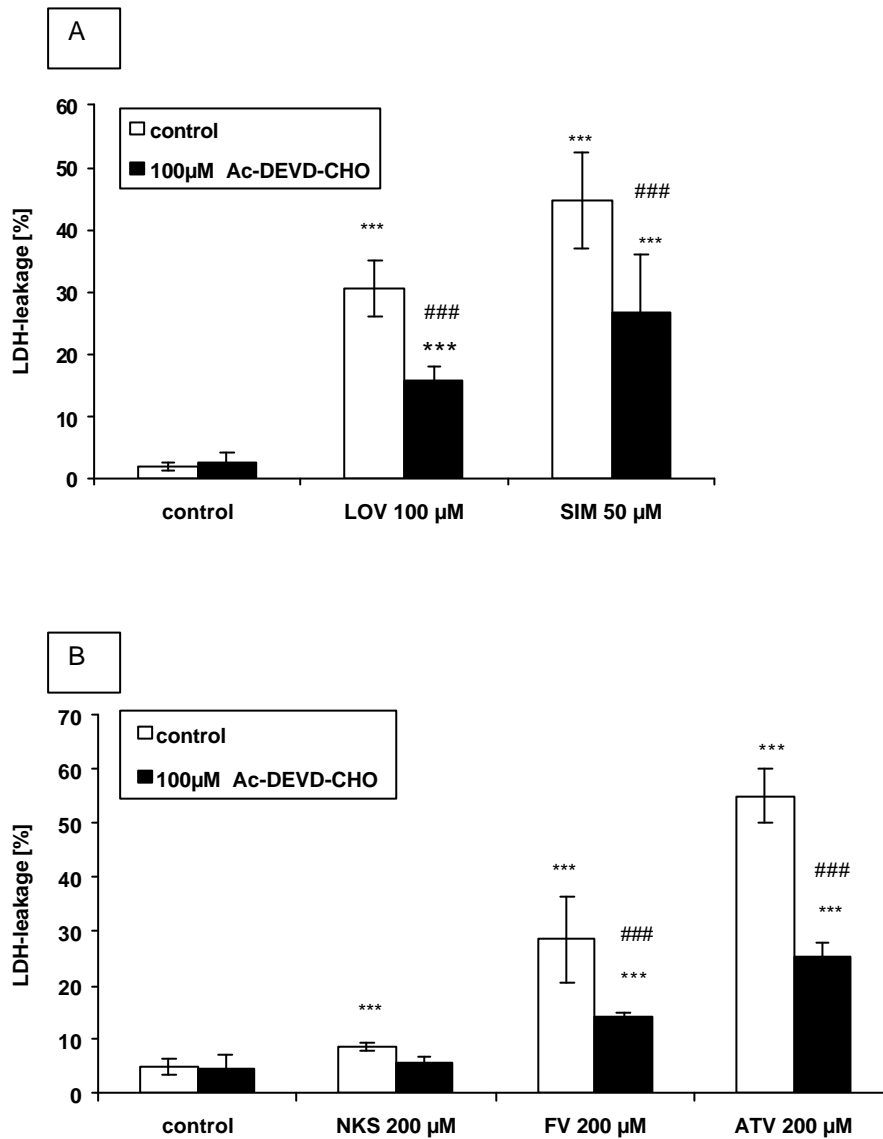
The results presented in the previous chapter suggest a possible link between ROS formation, apoptosis and necrosis. The direct link between these cellular events however has not been demonstrated. In the following the interaction between these events shall be discussed by means of results from experiments with a specific inhibitor of caspase-3, various antioxidants, a pro-oxidant, HMG-CoA downstream metabolites and an intracellular Ca²⁺ chelator.

3.2.1 Role of caspase-3 inhibitors on statin-induced cellular events

3.2.1.1 Cytotoxicity

Human SkMCs were pre-incubated with the specific inhibitor of caspase-3 (Ac-DEDV-CHO) at the concentration of 100 µM for 2 hours before co-incubated with or without 100 µM LOV and 50 µM SIM for 4 hours and with 200 µM NKS, FV and ATV for 24 hours. LDH-leakage was measured at the end of the experiments.

After 4 hours, Ac-DEDV-CHO statistically significantly inhibited LDH-leakage induced by LOV and SIM to between 45% and 50%. After 24 hours incubation, caspase-3 inhibitor reduced LDH-leakage caused by FV and ATV between 40% and 55%. In the case of NKS, the inhibitory effect was about 25% (Fig. 30).



[Control values: LDH-leakage: % of total= LDH supernatant/ LDH total]

Fig. 30: Effect of caspase-3 inhibitors on SIM and LOV (A), NKS, FV and ATV (B)-induced LDH-leakage.

HSkMCs were preincubated 2 hours with 100 µM Ac-DEVD-CHO before adding the statins in combinations with inhibitor. Data are expressed as means \pm SD from three independent experiments (n=3). Statistically significant differences versus the control group are expressed as ***P<0.001. Statistically significant differences in comparison with the statins group are indicated by ###P<0.001.

3.2.1.2 Nuclear morphology

The numbers of nuclei with changed morphology were measured in hSkMCs culture pre-incubated with the caspase-3 inhibitor, Ac-DEDV-CHO, at concentration of 100 μ M for 2 hours before co-incubated with and without 10 μ M of the statins for 72 hours. The addition of Ac-DEDV-CHO inhibited the statins-induced changes in the nuclear of hSkMCs in the range of 12-35 % (Fig. 31). The inhibitory effect was statistically significant different from the incubation without Ac-DEDV-CHO in the case of FV, LOV and SIM.

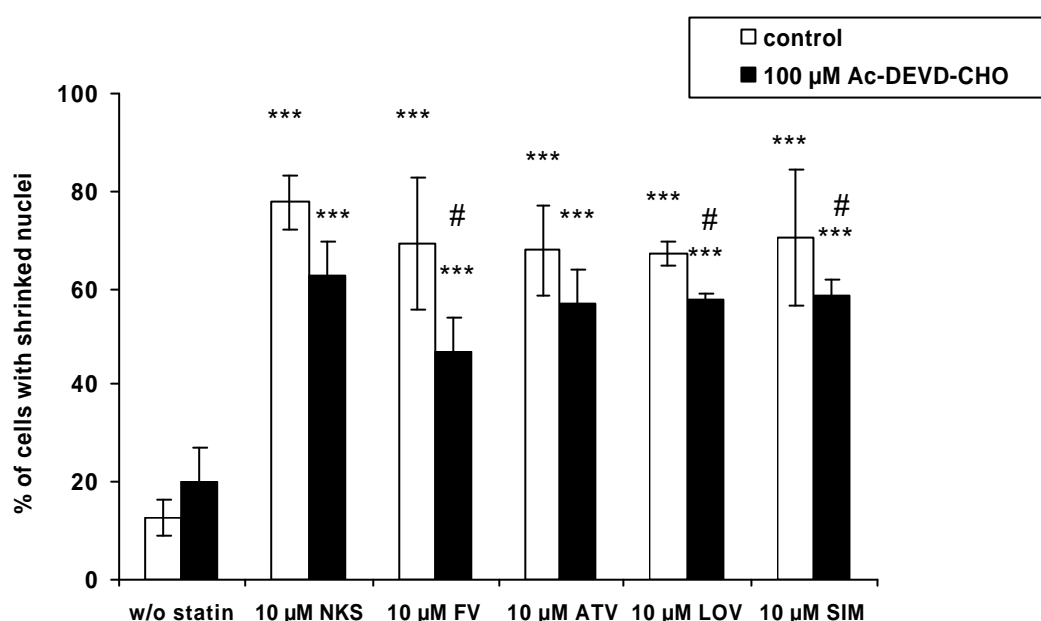


Fig. 31: Effect of caspase-3 inhibitor on statin-induced nuclear morphology change.

hSkMCs were incubated 72 hours with the different statins with or without 100 μ M Ac-DEDV-CHO and the change on nuclear morphology was measured after Hoechst dye staining. Data are expressed as means \pm SD from three independent experiments (n=3). Statistically significant differences versus the control group are expressed as ***P<0.001. Statistically significant differences in comparison with the statins group are indicated by #P<0.05.

3.2.1.3 Discussion

Our previous results showed that apoptosis precedes the membrane damage as measured by LDH leakage, a property of necrosis. By means of the specific caspase-3 inhibitor, Ac-DEVD-CHO, which completely inhibited the caspase-3 activity, however only partial protection of about 50 % against the statin-induced LDH-leakage was achieved. In general, this result demonstrates that caspase-3, as an early event in the apoptotic pathways is involved in the later occurring necrosis.

Necrosis secondary to apoptosis is also discussed in the current literature. ATP might serve as a cellular checkpoint for shifting apoptosis into necrosis. It is described that the decreased cellular ATP level induces a switch from apoptosis to necrosis (Lemaire *et al.*, 1998).

In our experiments, the inhibition of LDH-leakage by Ac-DEVD-CHO was not totally achieved. This indicates that statins not exclusively induce cell death by an apoptotic mechanism. The high concentrations used may favor unspecific cytotoxicity which is overlapping with the apoptotic events

The changes in the nuclear morphology observed after the statin treatment also indicates characteristics of apoptosis or necrosis. We could demonstrate that cells, when treated at low concentrations for 72 hours showed decreased nuclei sizes. By means of co-treatment with the caspase-3 inhibitor, Ac-DEVD-CHO, we saw that the number of nuclei exhibiting these properties was reduced. The inability to reduce the statin-mediated apoptotic picture completely up to the level of the untreated controls after 72 hours may be the result of too low caspase-3 inhibitor concentrations during long term incubations. It may be also possible that statins induce apoptosis by mechanisms different from caspase-3 activation. We can further not exclude that the nuclear morphology after 72 hours statin treatment is the results of other unspecific effects.

3.2.2 Role of pro-oxidants and anti-oxidants on statin-induced cellular events

Statins alone cause statistically significant increased ROS formation, caspase-3 activity and LDH-leakage. This study was carried out to evaluate the effects of pro-oxidant or anti-oxidants on the statin-induced cellular events.

3.2.2.1 Effect of BSO on statin-induced ROS formation, caspase-3 activity and LDH-leakage

DL-buthionine-(S,R)-sulfoximine (BSO) (2 mM) is an inhibitor of glutathione synthesis. In controls human SkMCs cultures BSO has no significant effect on ROS formation, caspase-3 activation and LDH-leakage. After co-incubation with statins, the pro-oxidant BSO increased the statin-induced ROS production, caspase-3 activity and LDH-leakage. Increases were by mean values, which however were not statistically significant different as compared to incubations without BSO (Tab. 9).

	ROS (30 min) (% of control)		Caspase-3 activity (2h) (% of control)		LDH-leakage (4h) (% of total)	
	w/o BSO	+ BSO	w/o BSO	+ BSO	w/o BSO	+ BSO
w/o statin	100 ± 0.0	132.3 ± 32	100 ± 0.0	97.2 ± 16.1	1.43 ± 0.2	1.87 ± 0.3
NKS	254.5 ± 16 ***	270.3 ± 34 ***	1083.2 ± 108 ***	1192 ± 79 ***		
FV	199.5 ± 11 ***	232.4 ± 15 ***	1902.4 ± 405 ***	2013.1 ± 123 ***		
ATV	328.4 ± 45 ***	333.1 ± 30 ***	2077.1 ± 105 ***	2330 ± 383 ***		
LOV	214.2 ± 17 ***	241.4 ± 36 ***	788.8 ± 302 ***	1231.8 ± 119 ***	29.0 ± 2.5 ***	37.9 ± 9.6 ***
SIM	208.6 ± 19 ***	223.3 ± 64 ***	1225.7 ± 422 ***	1300.1 ± 292 ***	41.9 ± 2.1 ***	51.2 ± 9.7 ***

[Control values: ROS formation: 100% = 0.8-1.6 DCF fluorescence/LDH in cells, Caspase-3 activity: 100%= 4.5-9 pmolAMC/min/mg protein, LDH-leakage: % of total= LDH supernatant / LDH total]

Tab. 9: Effect of BSO on statin-induced ROS formation, caspase-3 activity and LDH-Leakage.

Incubation conditions: HSkMCs were pre-incubated with 2mM BSO before adding the statins in combination with BSO. ROS formation: after 30 min incubation with 50 µM statins. Caspase-3 activity: after 2 hours incubation with 100 µM LOV, 50 µM SIM or 400 µM others statins. LDH-leakage: after 4 hours incubation with 100 µM LOV or 50 µM SIM. Data are expressed as means ±SD from three independent experiments (n=3). Statistically significant differences versus the control group are expressed as ***P<0.001.

3.2.2.2 Effect of NAC on statin-induced ROS formation, caspase-3 activity and LDH-leakage

NAC is a precursor of glutathione synthesis and a potent antioxidant, showing protective effects against various toxic compounds. NAC at concentration of 2 mM reduced statin-induced ROS production in the range of 25 and 30%. The presence of NAC statistically significant inhibited caspase-3 activity between 55 and 75% of the control value and the protective effect of NAC on LDH-leakage was 53 % for LOV and 68 % for SIM (Tab. 10).

	ROS (30 min) (% of control)		Caspase-3 activity (2h) (% of control)		LDH-leakage (4h) (% of total)	
	w/o NAC	+ NAC	w/o NAC	+ NAC	w/o NAC	+ NAC
w/o statin	100 ± 0.0	101.9 ± 11	100 ± 0.0	88 ± 25	1.43 ± 0.2	2.0 ± 0.5
NKS	254.5 ± 16 ***	190.9 ± 1 #	1083.2 ± 108 ***	253.4 ± 81 ###	nd	nd
FV	199.5 ± 11 ***	144.2 ± 8 #	1902.4 ± 405 ***	755.9 ± 158 ###	nd	nd
ATV	328.4 ± 45 ***	257 ± 44.7 #	2077.1 ± 105 ***	637.9 ± 302 ##	nd	nd
LOV	214.2 ± 17 ***	150.7 ± 30 #	788.8 ± 302 ***	367 ± 156 #	29.0 ± 2.5 ***	13.5 ± 6.2 ###
SIM	208.6 ± 19 ***	155.7 ± 20 #	1225.7 ± 422 ***	337.2 ± 125 ##	41.9 ± 2.1 ***	13.2 ± 2.1 ###

[Control values: ROS formation: 100% = 0.8-1.6 DCF fluorescence/LDH in cells, Caspase-3 activity: 100%= 4.5-9 pmolAMC/min/mg protein, LDH-leakage: % of total= LDH supernatant / LDH total]
nd: not determined

Tab. 10: Effect of NAC on statin-induced ROS formation, caspase-3 activity and LDH-Leakage.

Incubation conditions: HSkMCs were pre-incubated with 2mM NAC before adding the statins in combination with NAC. ROS formation: after 30 min incubation with 50 µM statins. Caspase-3 activity: after 2 hours incubation with 100 µM LOV, 50 µM SIM or 400 µM others statins. LDH-leakage: after 4 hours incubation with 100 µM LOV or 50 µM SIM. Data are expressed as means ±SD from three independent experiments (n=3). Statistically significant differences versus the control group are expressed as ***P<0.001. Statistically significant differences in comparison with the statins group are indicated by #P<0.05, ##P<0.01 and ###P<0.001.

3.2.2.3 Effect of DTT on statin-induced ROS formation, caspase-3 activity and LDH-leakage

DL-dithiothreitol (DTT) is a GSSG-reducing agent. The presence of 2 mM DTT statistically significant inhibited ROS formation, caspase-3 activity and LDH-leakage induced by the different statins. The inhibitory effect of DTT on ROS formation by the different statins was between 40 and 55%. Caspase-3 activity was reduced in between 22 and 87% and the protective effect of DTT on LDH-leakage was 44 % for LOV and 59 % for SIM (Tab. 11).

	ROS (30 min) (% of control)		Caspase-3 activity (2h) (% of control)		LDH-leakage (4h) (% of total)	
	w/o DTT	+ DTT	w/o DTT	+ DTT	w/o DTT	+ DTT
w/o statin	100 ± 0.0	120.2 ± 30	100 ± 0.0	212.2 ± 86	1.43 ± 0.2	2.0 ± 0.8
NKS	254.5 ± 16 ***	134.3 ± 17 ###	1083.2 ± 108 ***	143.4 ± 66 ###		
FV	199.5 ± 11 ***	120.5 ± 14 ##	1902.4 ± 405 ***	774.8 ± 277 ###		
ATV	328.4 ± 45 ***	171 ± 61.5 ##	2077.1 ± 105 ***	1629.9 ± 219 ##		
LOV	214.2 ± 17 ***	111.4 ± 20 #	788.8 ± 302 ***	469.9 ± 203 #	29.0 ± 2.5 ***	16.1 ± 7.0 ###
SIM	208.6 ± 19 ***	96.4 ± 9.0 ##	1225.7 ± 422 ***	510.4 ± 192 #	41.9 ± 2.1 ***	17.0 ± 7.6 ###

[Control values: ROS formation: 100% = 0.8-1.6 DCF fluorescence/LDH in cells, Caspase-3 activity: 100%= 4.5-9 pmolAMC/min/mg protein, LDH-leakage: % of total= LDH supernatant / LDH total]

Tab. 11: Effect of DTT on statin-induced ROS formation, caspase-3 activity and LDH-Leakage.

Incubation conditions: HSkMCs were pre-incubated with 2mM DTT before adding the statins in combination with DTT. ROS formation: after 30 min incubation with 50 µM statins. Caspase-3 activity: after 2 hours incubation with 100 µM LOV, 50 µM SIM or 400 µM others statins. LDH-leakage: after 4 hours incubation with 100 µM LOV or 50 µM SIM. Data are expressed as means ±SD from three independent experiments (n=3). Statistically significant differences versus the control group are expressed as ***P<0.001. Statistically significant differences in comparison with the statins group are indicated by #P<0.05, ##P<0.01 and ###P<0.001.

3.2.2.4 Effect TPGS on statin -induced ROS formation, caspase-3 activity and LDH-leakage

DL-&-tocopherol-polyethylene-glycol-1000-succinate (TPGS) is water soluble vitamin E derivative, which showed potent protection against lipid peroxidation mediated toxicity in various experiments reported in the literature (Witting *et al.*, 1999; Bieri *et al.*, 1983). In the hSkMCs culture, co-incubation of statins with 100 μ M TPGS statistically significantly inhibited ROS formation. The inhibitory effect of TPGS on ROS formation by the different statins was between 32 and 46%. Inhibition of ATV, LOV and SIM-induced caspase-3 activity was in the range of 47-74 %. There was no significant inhibition of caspase-3 induced by NKS and FV. The protective effect of TPGS on LDH-leakage was 63 % for LOV and 75 % for SIM (Tab. 12).

	ROS (30 min) (% of control)		Caspase-3 activity (2h) (% of control)		LDH-leakage (4h) (% of total)	
	w/o TPGS	+ TPGS	w/o TPGS	+ TPGS	w/o TPGS	+ TPGS
w/o statin	100 \pm 0.0	131.6 \pm 13	100 \pm 0.0	115.0 \pm 54.6	1.43 \pm 0.2	3.4 \pm 1.3
NKS	254.5 \pm 16 ***	136.7 \pm 38 ###	1083.2 \pm 108 ***	1546.5 \pm 327		
FV	199.5 \pm 11 ***	135.2 \pm 40 ##	1902.4 \pm 405 ***	1679.6 \pm 433		
ATV	328.4 \pm 45 ***	159.3 \pm 26 ##	2077.1 \pm 105 ***	1094.2 \pm 437 #		
LOV	214.2 \pm 17 ***	134.2 \pm 49 ##	788.8 \pm 302 ***	345.1 \pm 148 #	29.0 \pm 2.5 ***	10.8 \pm 3.2 ###
SIM	208.6 \pm 19 ***	121.7 \pm 31 ##	1225.7 \pm 422 ***	319.9 \pm 110 ##	41.9 \pm 2.1 ***	10.7 \pm 3.3 ###

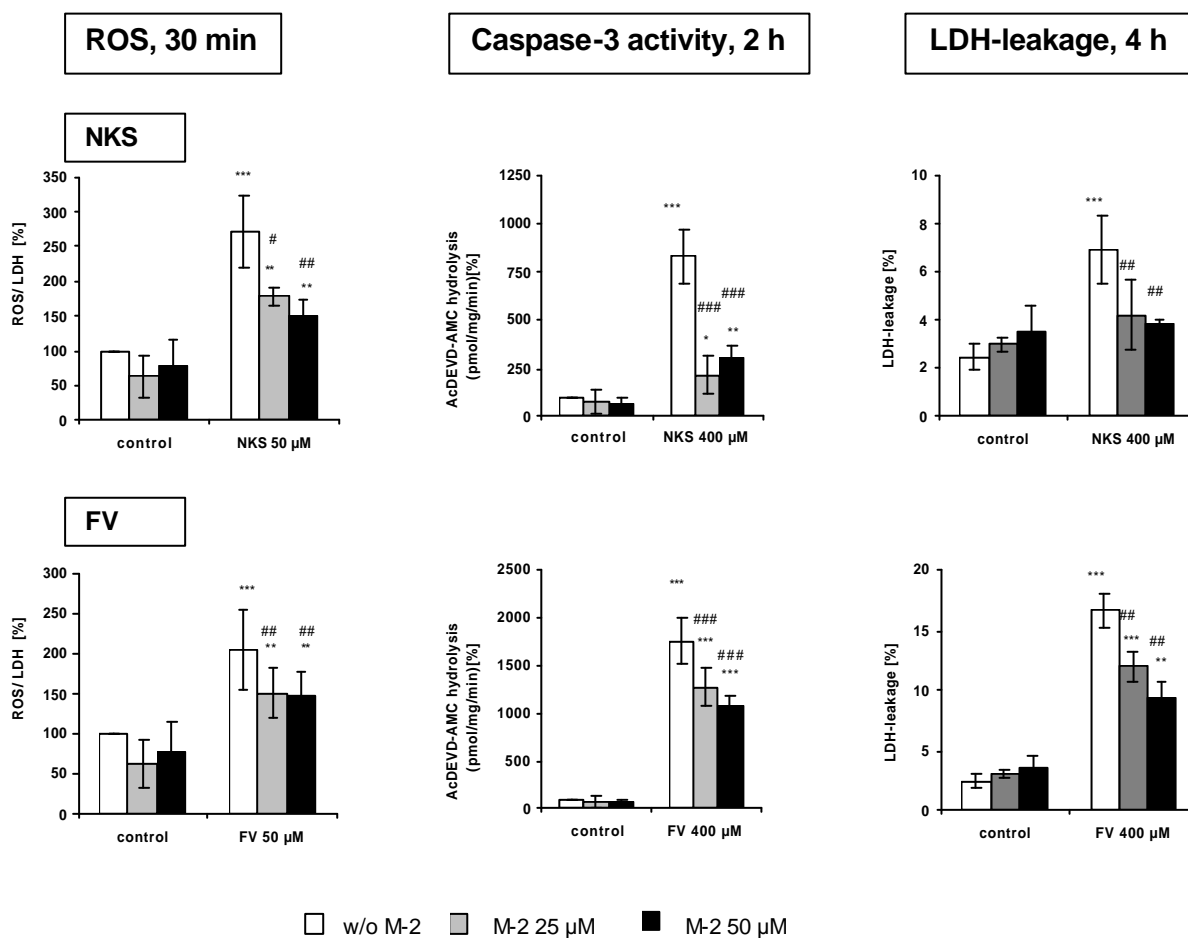
[Control values: ROS formation: 100% = 0.8-1.6 DCF fluorescence/LDH in cells, Caspase-3 activity: 100%= 4.5-9 pmolAMC/min/mg protein, LDH-leakage: % of total= LDH supernatant / LDH total]

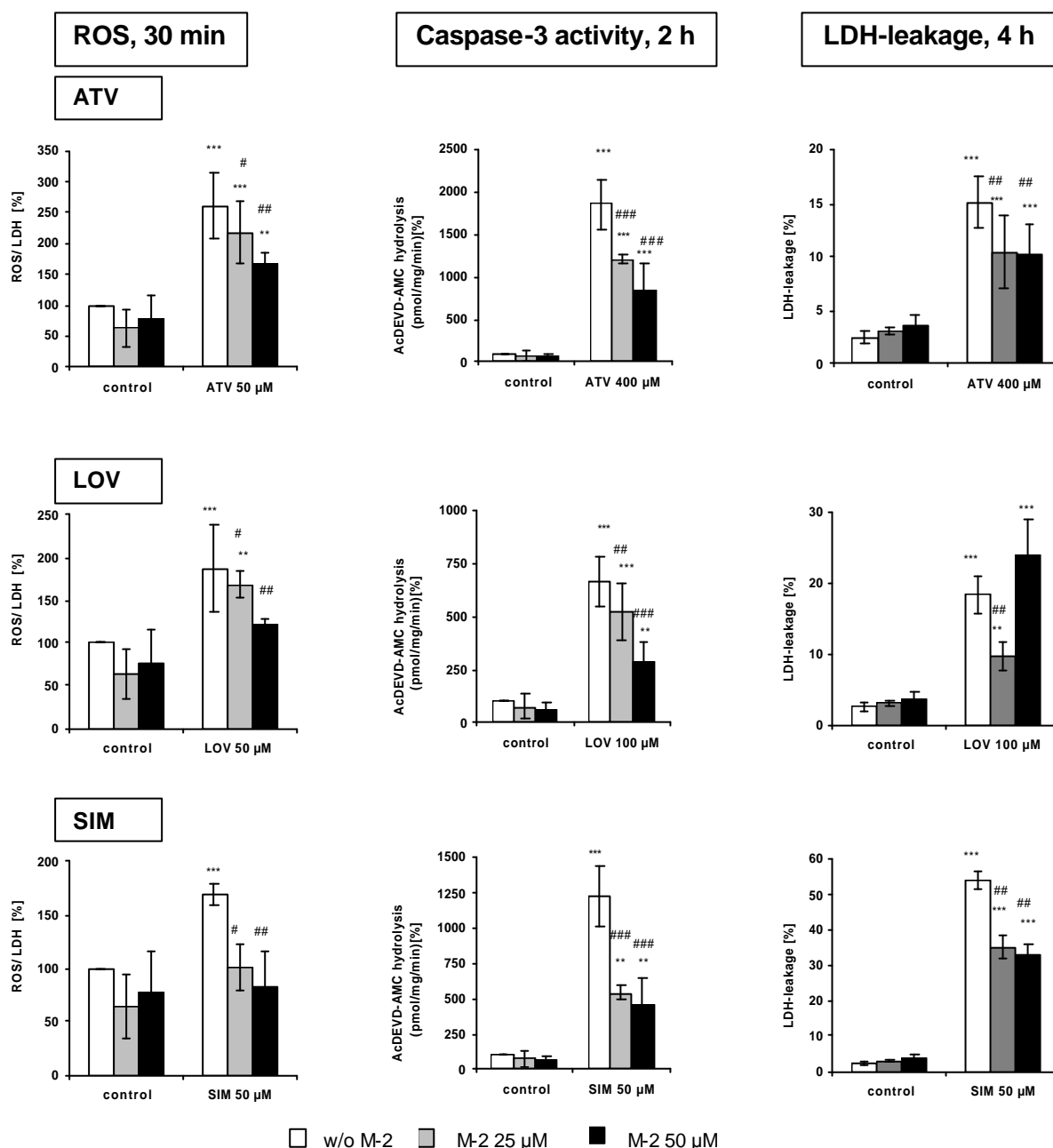
Tab. 12: Effect of TPGS on statin-induced ROS formation, caspase-3 activity and LDH-Leakage.

Incubation conditions: HSkMCs were pre-incubated with 100 mM TPGS before adding the statins in combination with TPGS. ROS formation: after 30 min incubation with 50 μ M statins. Caspase-3 activity: after 2 hours incubation with 100 μ M LOV, 50 μ M SIM or 400 μ M others statins. LDH-leakage: after 4 hours incubation with 100 μ M LOV or 50 μ M SIM. Data are expressed as means \pm SD from three independent experiments (n=3). Statistically significant differences versus the control group are expressed as ***P<0.001. Statistically significant differences in comparison with the statins group are indicated by #P<0.05, ##P<0.01 and ###P<0.001.

3.2.2.5 Effect of 5-OH-fluvastatin on statin-induced ROS formation, caspase-3 activity and LDH-leakage

5-OH-fluvastatin (M-2) is a fluvastatin metabolite reported in the literature which has strong antioxidant properties (Nakashima *et al.*, 1999, 2001; Imaeda *et al.*, 2001a, b, 2002). The addition of M2 to hSKMCs together with statin statistically significantly reduced the ROS formation, caspase-3 activity and LDH-leakage in comparison with the same statin concentration alone. The inhibition of the ROS formation was concentration dependent (Fig. 32). No inhibitory effect of M-2 (50 μ M) after co-administration with lovastatin on LDH-leakage.



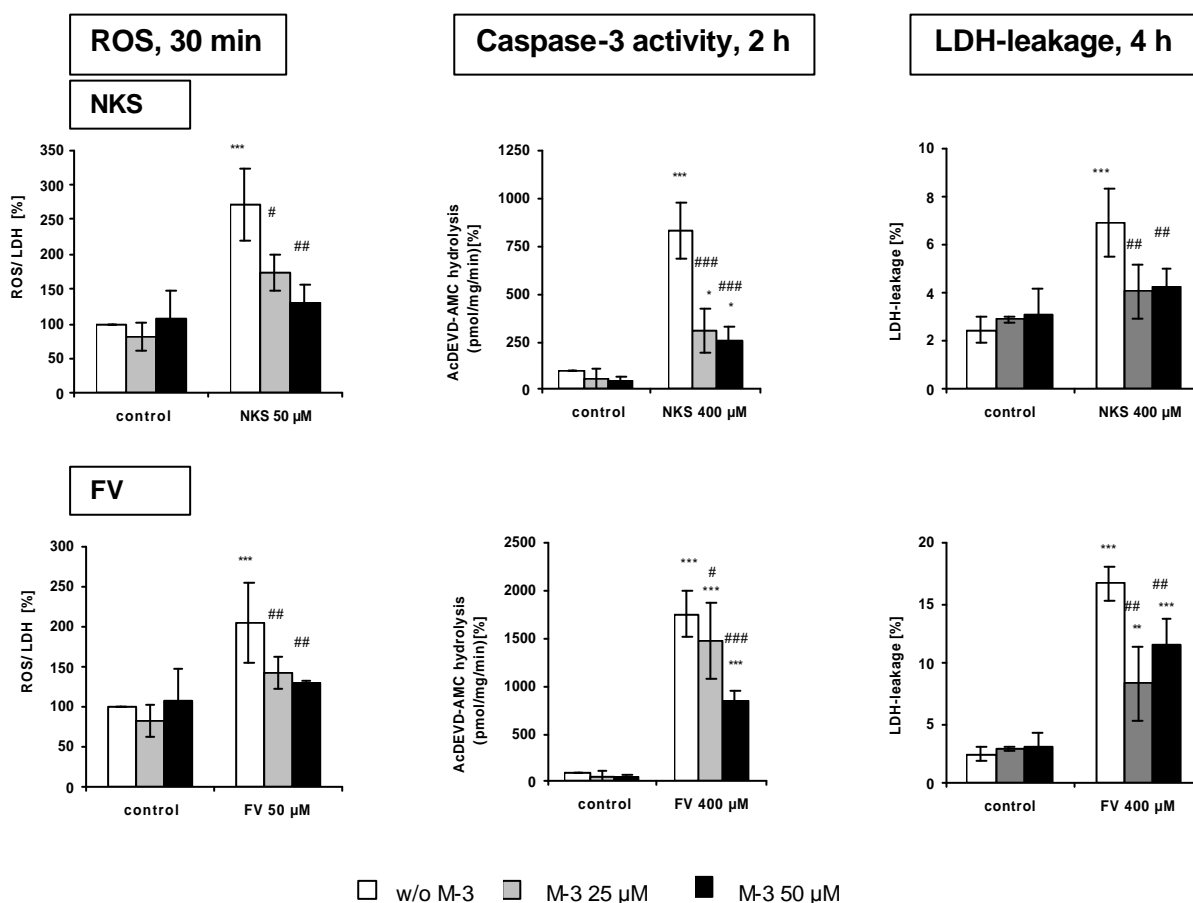


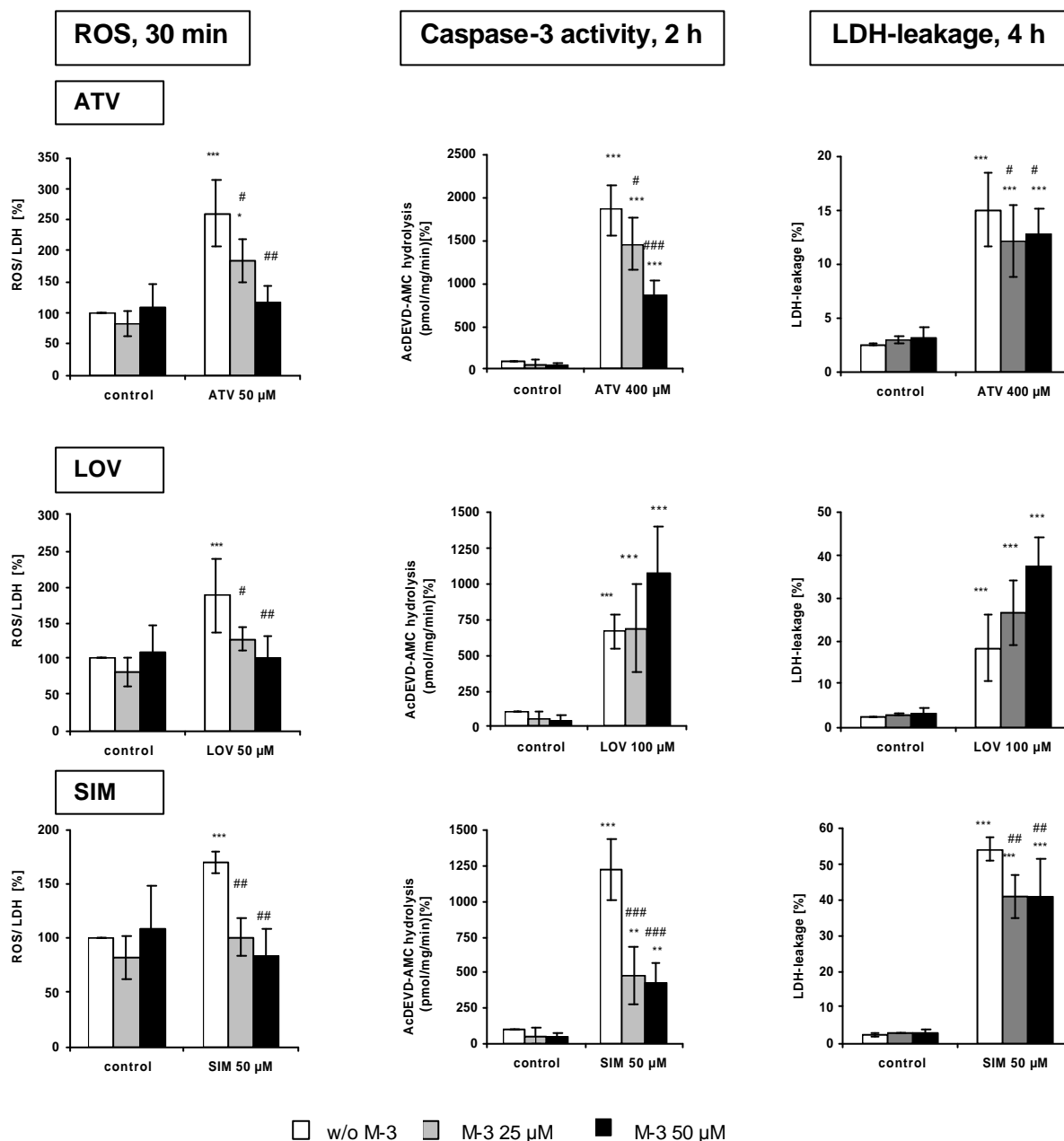
[Control values: ROS formation: 100% = 0.8-1.6 DCF fluorescence/LDH in cells, Caspase-3 activity: 100%= 4.5-9 pmolAMC/min/mg protein, LDH-leakage: % of total= LDH supernatant / LDH total]

Fig. 32: Inhibitory effect M-2 on statin-induced ROS formation, caspase-3 activity and LDH-Leakage. Incubation conditions: HSkMCs were pre-incubated with 25 and 50 μM M-2 before adding the statins in combination with M-2. ROS formation: after 30 min incubation with 50 μM statins. Caspase-3 activity: after 2 hours incubation with 100 μM LOV, 50 μM SIM or 400 μM others statins. LDH-leakage: after 4 hours incubation with 100 μM LOV or 50 μM SIM or 400 μM others statins. Data are expressed as means ± SD from three independent experiments (n=3). Statistically significant differences versus the control group are expressed as *P<0.05, **P<0.01 and ***P<0.001. Statistically significant differences in comparison with the statins group are indicated by #P<0.05, ##P<0.01 and ###P<0.001.

3.2.2.6 Effect of 6-OH-fluvastatin on statin-induced ROS formation, caspase-3 activity and LDH-leakage

M-3 (6-OH-fluvastatin) has also strong reported antioxidant activity (Nakashima *et al.*, 1999, 2001; Imaeda *et al.*, 2001a, b, 2002). In our experiments M-3 statistically significantly, reduced ROS formation, caspase-3 activity and LDH-leakage in comparison with the same statin concentration alone. The inhibition of the ROS formation and caspase-3 activity were concentration dependent (Fig. 33). M-3 inhibited the LDH-leakage stronger than M-2. No inhibitory effect of M-3 on caspase-3 activity and LDH-leakage were observed after co-administration with LOV.





[Control values: ROS formation: 100% = 0.8-1.6 DCF fluorescence/LDH in cells, Caspase-3 activity: 100%= 4.5-9 pmolAMC/min/mg protein, LDH-leakage: % of total= LDH supernatant / LDH total]

Fig. 33: Inhibitory effect M-3 on statin-induced ROS formation, caspase-3 activity and LDH-Leakage. Incubation conditions: HSkMCs were pre-incubated with 25 and 50 μM M-3 before adding the statins in combination with M-3. ROS formation: after 30 min incubation with 50 μM statins. Caspase-3 activity: after 2 hours incubation with 100 μM LOV, 50 μM SIM or 400 μM others statins. LDH-leakage: after 4 hours incubation with 100 μM LOV or 50 μM SIM or 400 μM others statins. Data are expressed as means ± SD from three independent experiments (n=3). Statistically significant differences versus the control group are expressed as *P<0.05, **P<0.01 and ***P<0.001. Statistically significant differences in comparison with the statins group are indicated by #P<0.05, ##P<0.01 and ###P<0.001.

3.2.2.7 Effect of M-2 and M-3 on statin-induced change on nuclear morphology

The changes in the nuclear morphology were measured in hSkMCs culture pre-incubated with M-2 and M-3 at the concentration of 50 μ M for 2 hours before co-incubated with and without 10 μ M of NKS for 72 hours. The medium which contained the FV-metabolites and NKS were renewed daily. M-3 statistically significantly inhibited the nuclear shrinking induced by NKS. M-2 had no effect (Fig. 34). No statistically significant inhibitory effect was also found after co-incubation of FV, ATV, LOV, and SIM with 50 μ M M-2 and M-3 (data not shown).

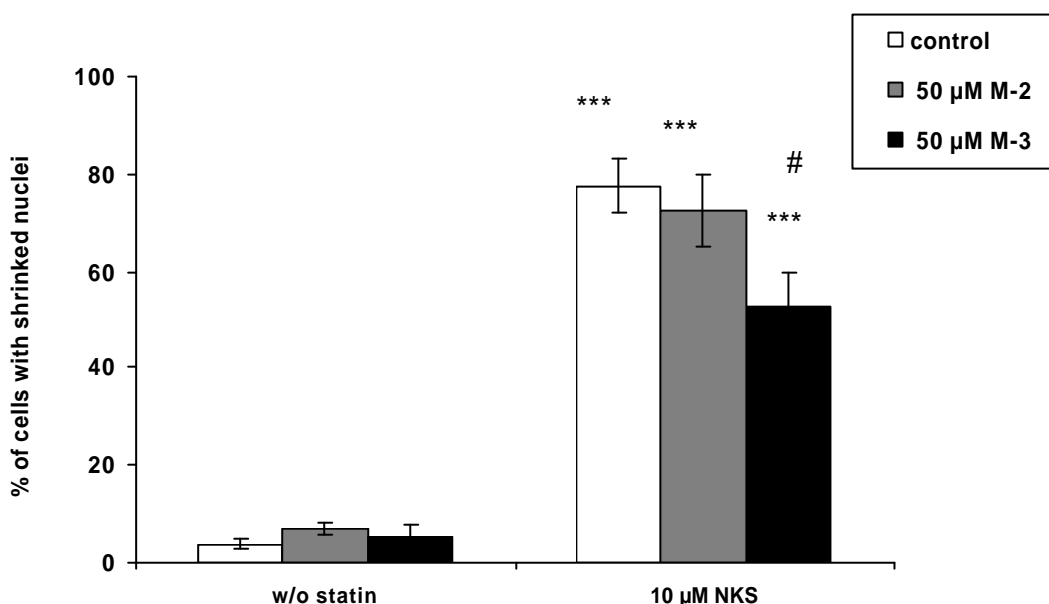


Fig. 34: Effect of M-2 and M-3 on NKS-induced nuclear morphology change on hSkMCs.

hSkMCs were incubated with the different statins with or without M-2 and M-3 for 72 hours and the change on nuclear morphology was measured after Hoechst dye staining. Data are expressed as means \pm SD from three independent experiments (n=3). Statistically significant differences versus the control group are expressed as ***P<0.001. Statistically significant differences in comparison with the statins group are indicated by #P<0.05.

3.2.2.8 Total antioxidative capacity of statins and fluvastatin metabolites

The antioxidant activities of M-2 and M-3 are reported in the literature and the protective effect on oxidative events has been demonstrated in various cellular assays (Nakashima *et al.*, 1999, 2001; Imaeda *et al.*, 2001a, b, 2002). The purpose of the present study was to compare the Total antioxidative capacity (TAC) of M-2 and M-3 with Trolox-C and the statin parent compounds in a cell free assay, where a stable green colored ABTS radical is generated and the quenching effect of antioxidants is compared at different time lines at 600 nm.

The ABTS radical follows a linear time-dependency. The analysis after treatment with M-2, M-3 and TPGS like Trolox-C, revealed similar kinetic profiles. All compounds concentration dependently showed a concentration dependent increase of the lag phase, the time until which ABTS signal starts its onset. After starting beyond the lag phases the curves are in parallel to the unquenched ABTS control curve. It is important to mention that M2 and M3 showed the highest quenching, similar to Trolox-C in the micromolar range, whereas TPGS was in the milimolar concentration range, where significant inhibition was achieved. M-3 was more potent than M-2 (fig. 35).

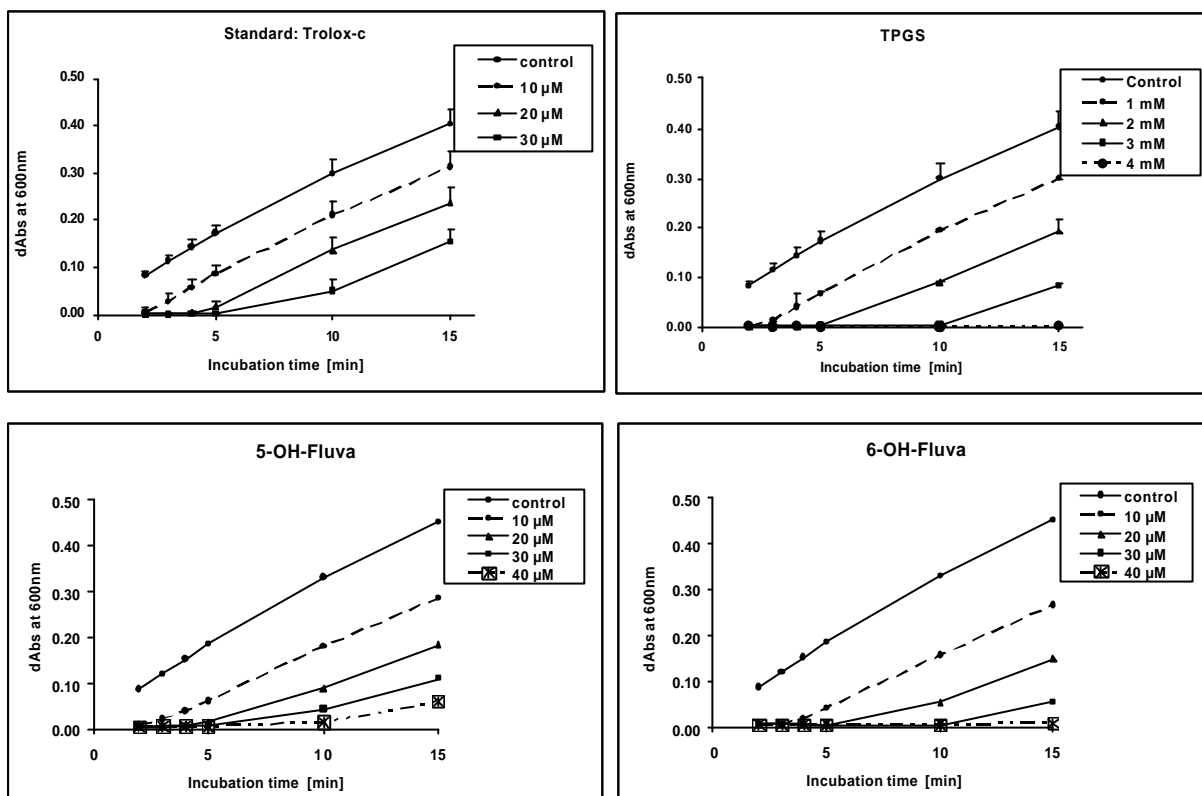


Fig. 35: Radical cation scavenging capacity of M-2, M-3 and TPGS.

The radical cation scavenging capacity of the M-2, M-3 and TPGS was expressed as Trolox-C equivalent. The Trolox-C equivalent was calculated and used to compare the radical cation scavenging activity of each antioxidant. Data are expressed as means \pm SD from three independent experiments for each sample (n=3).

There was no lag phase for the statin parent compounds. Among all statins tested, FV had the greatest activity for quenching ABTS^{•+}, followed by PRA, NKS and LOV. SIM and ATV had no antioxidant effect at the maximum concentration of 2 mM (fig. 35).

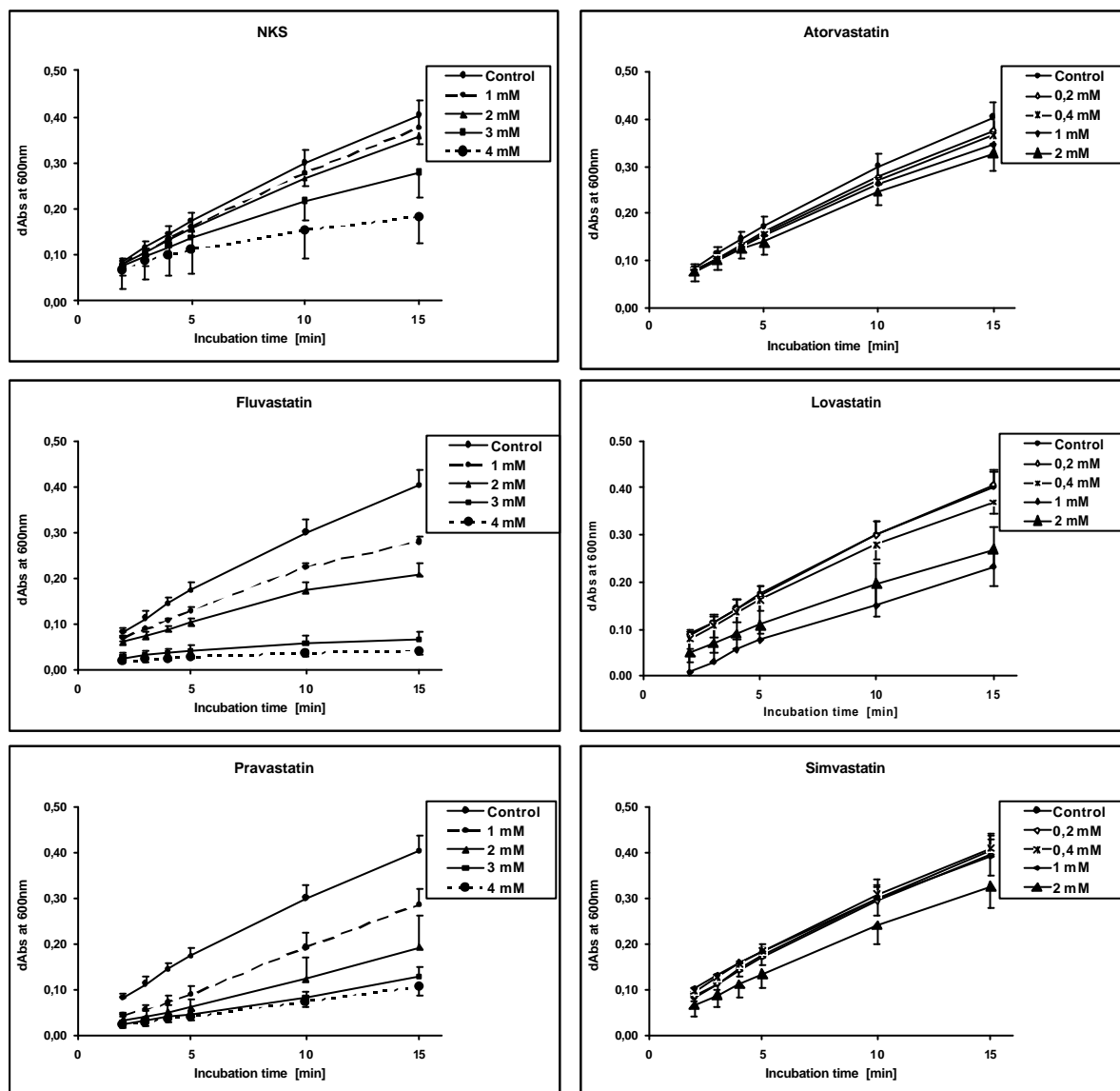


Fig. 36: Radical cation scavenging capacity of statins.

The radical cation scavenging capacity of the six statins was expressed as trolox-C equivalent. The trolox-C equivalent was calculated and used to compare the radical cation scavenging activity of each antioxidant. Data are expressed as means \pm SD from three independent experiments for each sample (n=3).

3.2.2.9 Discussion

Although enhanced ROS formation is an early event of the statin's cellular effects, which in principle could trigger a cascade of subsequent events, the direct link between ROS and impaired cellular functions has not yet been established. In order to show the direct link between oxidative stress and myotoxicity, antioxidants (TPGS, NAC and DTT) and pro-oxidants (BSO) were used in combination experiments as mechanistic tools.

TPGS is water soluble vitamin E derivative, which showed potent protection against lipid peroxidation and toxicity in various experiments with toxic compounds (Witting *et al.*, 1999; Bieri *et al.*, 1983). In cells, TPGS is cleaved and the active lipid peroxy radical reducing tocopherol is formed, which in membranes is a potent protector against lipid peroxidation. In various experiments with other toxic compounds the meaning of lipid peroxidation as the mechanism of toxicity was identified by supplementation with TPGS. If toxicity was inhibited by vitamin E, this suggests a possible relevant involvement of lipid peroxidation in the mechanism of toxic action. In our experiments with LOV and SIM, TPGS supplementation reduced ROS formation, caspase-3 activation, in parallel protected from LDH leakage. TPGS also reduced ATV-induced ROS formation as well as caspase-3 activity. Protective effect of TPGS could not be investigated longer than 4 hours. Thus TPGS in combination with ATV, FV and NKS was not evaluated.

Although TPGS reduced NKS or FV-induced ROS formation after 30 min, it showed no significant protection on caspase-3 activation. The reason for the inability to inhibit caspase-3 activity may be the result of the stronger ROS formation induced by ATV, FV and NKS compared to SIM and LOV. In the case of SIM and LOV the applied TPGS concentrations could be sufficient to protect the cells against the ROS formation. Although TPGS was able to scavenge their ROS formation within 30 min, it may be possible that the amount of TPGS is limiting in order to prevent reasonable caspase-3 activation after 4 hours. In order to confirm this hypothesis, experiments with higher TPGS concentrations should be performed.

BSO is an inhibitor of glutathione synthesis as reported in the literature (Wolf *et al.*, 1997, Maeda *et al.*, 2004). Inhibition of BSO results in GSH depletion. When cells are depleted by GSH, a compound following a prooxidative mechanism of toxicity would become more toxic. In control hSKMCs, BSO could not be used longer than 4 hours

because of its myotoxicity. In combination with statins and BSO, we did not see statistically significant differences in all investigated parameters compared to cells without BSO. However, there was a tendency in all BSO-treated samples towards an increase of ROS formation, caspase-3 activation as well as LDH leakage.

NAC is a precursor for glutathione synthesis and a potent antioxidant, showing protective effects against various toxic compounds. In all experiments, NAC was able to decrease statin-induced ROS formation, caspase-3 activation as well as being protective against LDH-leakages.

DTT is the GSSG-reducing agent (Wolf *et al.*, 1997; Obatomi *et al.*, 2001; Vaknin *et al.*, 2005). Because of myotoxicity, DTT could not be studied longer than 4 hours. Same as for NAC, DTT was able to decrease statin-induced ROS formation, caspase-3 activation as well as being protective against increased LDH-leakages. The protective effects on statin-induced ROS formation were stronger for DTT as compared to NAC.

M-2 and M-3 are fluvastatin metabolites reported in the literature having strong antioxidant properties (Nakashima *et al.*, 1999, 2001; Imaeda *et al.*, 2001a, b, 2002). In our cell-free assay, we could confirm by TAC measurements that the antioxidant effects were even stronger than that of TPGS. M-2 and M-3 inhibited very efficiently ROS formation also in the cellular system. There was also a decrease of caspase-3 and LDH-leakage found for all statins, except for LOV. Although M-2 had an inhibitory effect at 25 μM in combination with LOV, protection was not confirmed at 50 μM . M-3 had clearly no inhibitory effect in combination with LOV, neither on LOV-induced caspase-3 activation nor on the respective LDH leakage.

In conclusion, the results with the pro-oxidant BSO and the various antioxidants (TPGS, NAC, DTT, M-2 and M-3) basically support the hypothesis that statin-induced ROS formation may be involved in the caspase-3 activation and in the induction of LDH release. However, there are few exceptions which do not totally comply with this assumption. There was no total protection achieved with M-2 and M-3 against LOV-induced caspase-3 activation and LDH-release and TPGS did not fully protect against FV and NKS-induced caspase-3 activation. The reasons for this inability may be the higher production of ROS and the inefficiency to protect caspase-3 activation at the applied TPGS concentrations. It may be that M-2 is competing with LOV for its cellular uptake, due to similar structure elements.

Summary of results from experiments with 5 different statins after supplementation with antioxidants/prooxidant. Protection observed			
Antioxidant	ROS	Caspase-3	LDH
TPGS	5/5	3/5***	2/2
NAC	5/5	5/5	2/2
DTT	5/5	5/5	2/2
M-2	5/5	5/5	5/5*
M-3	5/5	4/5**	4/5**
BSO	(5/5)	(5/5)	(2/2)

*) protective effect of 25 μ M M-2 against LOV. **) no protection against LOV. ***) no protection against NKS and FV.

In the present study, we showed that for 5 statins, hSkMCs were rescued against toxicity by co-incubation with different antioxidants. There also seems to be the tendency that co-incubation with the pro-oxidative BSO increased of caspase-3 mediated toxicity of the statins. Positive correlations between ROS formation and caspase-3 activation were shown for most of the investigated statins and the applied antioxidants.

There is also positive correlation between ROS formation and caspase-3 induction reported in the current literature. These investigations raised the hypothesis of redox-sensitivity of caspase-3 (Hampton *et al.*, 1998, Grub *et al.*, 2000). It is assumed that mild oxidative stress has been shown to activate caspases, such as caspase-3 and caspase-8, however mechanisms by which oxidative stimuli activate the caspase cascade is not yet clear. In contrast, excessive oxidative stress can prevent caspase activation. This is probably due to the oxidation of redox-sensitive thiol groups (Cohen 1997; Hampton *et al.*, 1998; Higuchi *et al.*, 1998).

3.2.3 Role of HMG-CoA reductase in statin-induced cellular events

HMG-CoA reductase inhibitors inhibit L-mevalonic acid (MVA) synthesis leading to the reduction of the synthesis of important isoprenoid intermediates such as farnesylpyrophosphate (FPP), geranylgeranylpyrophosphate (GGPP) and ubiquinone (Q₁₀) (see page 16). In order to clarify their role in statin induced skeletal muscle cell toxicity, we supplemented the statin containing incubation media with the different HMG-CoA reductase downstream metabolites and determined then ROS formation, caspase-3 activation, changes on nuclear morphology and cell membrane damage in hSkMCs.

3.2.3.1 Effect of MVA on statin-induced ROS formation, caspase-3 activity and LDH-leakage

MVA (400 μ M) alone had no effect on hSkMCs cultures (Tab.13). The supplementation of the incubation medium with MVA reduced the statin-induced intracellular ROS formation for all statins very similar in the range of 20-30%. MVA reduced the statin-induced caspase-3 activation in a range of 12-80%. The weakest effect was shown in combination with LOV. MVA treatment also inhibited statin-induced cell membrane damage (LDH-leakage) in the range of 40-87%, Here; the strongest effect was shown for LOV (Tab. 13).

	ROS (30 min) (% of control)		Caspase-3 activity (2h) (% of control)		LDH-leakage (4-24-48h) (% of total)	
	w/o MVA	+ MVA	w/o MVA	+ MVA	w/o MVA	+ MVA
w/o statin	100 ± 0.0	96 ± 17	100 ± 0.0	92 ± 33	4.2 ± 1.0	4.3 ± 0.3
NKS	254.1 ± 17 ***	189.7 ± 24 ##	1083 ± 108 ***	303 ± 89 #	30.9 ± 8.2 *** §	16.7 ± 2.8 ## §
FV	199.5 ± 11 ***	147.6 ± 5 #	1902 ± 420 ***	1222 ± 286 #	41.7 ± 6.5 *** §	24.8 ± 7.3 # §
ATV	328.4 ± 46 ***	232.7 ± 33 #	2077 ± 307 ***	1507 ± 474 #	40.6 ± 6.1 *** β	27.7 ± 7.3 #β
LOV	214.2 ± 17 ***	176.8 ± 10 #	752 ± 240 ***	660 ± 256	32.4 ± 5.0 *** a	4.3 ± 2.5 ### a
SIM	208.6 ± 20 ***	152.7 ± 5 #	1214 ± 233 ***	297 ± 119 #	45.1 ± 3.0 *** a	22.2 ± 3.5 ### a

a = 4 hours incubation, β = 24 hours incubation, § = 48 hours incubation

[Control values: ROS formation: 100% = 0.8-1.6 DCF fluorescence/LDH in cells, Caspase-3 activity: 100% = 4.5-9 pmolAMC/min/mg protein, LDH-leakage: % of total = LDH supernatant/ LDH total]

Tab. 13: Effect of MVA on statin-induced ROS formation, caspase-3 activity and LDH-leakage.

Incubation conditions: HSkMCs were pre-incubated 2 hours with 400 μM MVA before adding the statins in combination with MVA. ROS formation: after 30 min incubation with 50 μM statins. Caspase-3 activity: after 2 hours incubation with 100 μM LOV, 50 μM SIM or 400 μM others statins. LDH-leakage: after incubation with 50 μM SIM, 100 μM LOV or 200 μM others statins. Data are expressed as means ± SD from three independent experiments (n=3). Statistically significant differences versus the control group are expressed as ***P<0.001. Statistically significant differences in comparison with the statins group are indicated by #P<0.05, ##P<0.01 and ###P<0.001.

3.2.3.2 Effect of F or FPP on statin-induced ROS formation, caspase-3 activity and LDH-leakage

ROS formation was measured after short incubation times at F and FPP concentrations of 100 μ M. This concentration was toxic after longer incubation times, thus the investigation of the effects on caspase-3 activity and LDH leakage were performed for both compounds at concentrations of 10 μ M.

Supplementation with F or FPP both resulted in the inhibition of statin-induced increases in intracellular ROS formation, caspase-3 activation and LDH-leakage. F totally inhibited statin-induced ROS formation for all statins tested. The inhibition of ROS formation by FPP was in the range of 31- 43%, but was very similar among the different statins. The presence of F reduced statin-induced caspase-3 activity in the range of 50-87% for ATV, SIM, FV and NKS, whereas there was almost no inhibition of LOV induced caspase-3 activation. The inhibition of statin-induced caspase-3 activity with FPP was in the range of 21-55%. The inhibition of ROS formation and caspase-3 activity were stronger with F compared to FPP.

F reduced the statin-induced cell membrane damage (LDH-leakage) in the range of 50-74% for NKS, ATV and FV. There was no inhibitory effect with F on LOV and SIM induced cytotoxicity after 4h treatment. (Tab. 14). FPP supplementation caused reduction of LDH-leakages induced by statins in the range of 12-64%. The inhibition of caspase-3 activity and LDH-leakage was not strong as expected, probably due to the low concentration of F or FPP applied.

	ROS (30 min) (% of control)		Caspase-3 activity (2h) (% of control)		LDH-leakage (4-24-48h) (% of total)	
	w/o F	+ F	w/o F	+ F	w/o F	+ F
w/o statin	100 ± 0.0	93.3 ± 20	100 ± 0.0	87 ± 3.0	4.2 ± 1.0	3.7 ± 0.7
NKS	254.1 ± 17 ***	94.8 ± 10 ###	1083 ± 108 ***	185 ± 68 ##	30.9 ± 8.2 *** §	15.1 ± 2.4 ### §
FV	199.5 ± 11 ***	109.1 ± 5 ###	1902 ± 420 ***	691 ± 87 ##	41.7 ± 6.5 *** §	11.0 ± 0.8 ### §
ATV	328.4 ± 46 ***	98.6 ± 20 ###	2077 ± 307 ***	1026 ± 136 #	40.6 ± 6.1 *** β	21.1 ± 5.8 ### β
LOV	214.2 ± 17 ***	100.8 ± 16 ###	752 ± 240 ***	660 ± 231	32.4 ± 5.0 *** a	30.6 ± 4.2 a
SIM	208.6 ± 20 ***	88 ± 10 ##	1214 ± 233 ***	577 ± 93 ###	45.1 ± 3.0 *** a	39 ± 2.8 a

	ROS (30 min) (% of control)		Caspase-3 activity (2h) (% of control)		LDH-leakage (4-24-48h) (% of total)	
	w/o FPP	+ FPP	w/o FPP	+ FPP	w/o FPP	+ FPP
w/o statin	100 ± 0.0	104.9 ± 2.3	100 ± 0.0	80.1 ± 20	4.2 ± 1.0	4.6 ± 2.0
NKS	254.1 ± 17 ***	155.2 ± 26 ###	1083 ± 108 ***	858 ± 211 ###	30.9 ± 8.2 *** §	17.1 ± 2.4 # §
FV	199.5 ± 11 ***	129.7 ± 27 ##	1902 ± 420 ***	1402 ± 300 ###	41.7 ± 6.5 *** §	22.1 ± 3.1 ## §
ATV	328.4 ± 46 ***	187.6 ± 9 #	2077 ± 307 ***	1084 ± 273 ##	40.6 ± 6.1 *** β	35.6 ± 2.2 β
LOV	214.2 ± 17 ***	147.8 ± 27 ##	752 ± 240 ***	476 ± 150 #	32.4 ± 5.0 *** a	11.7 ± 8.7 ## a
SIM	208.6 ± 20 ***	134.2 ± 18 #	1214 ± 233 ***	553 ± 187 ###	45.1 ± 3.0 *** a	31.7 ± 1.0 # a

a = 4 hours incubation, β = 24 hours incubation, § = 48 hours incubation

[Control values: ROS formation: 100% = 0.8-1.6 DCF fluorescence/LDH in cells, Caspase-3 activity: 100% = 4.5-9 pmolAMC/min/mg protein, LDH-leakage: % of total = LDH supernatant/ LDH total]

Tab. 14: Effect of F or FPP on statin-induced ROS formation, caspase-3 activity and LDH-leakage.

Incubation conditions: HSkMCs were pre-incubated 2 hours with 10 or 100 μM F or FPP before adding the statins in combination with F or FPP. ROS formation: after 30 min incubation with 50 μM statins and 100 μM F or FPP. Caspase-3 activity: after 2 hours incubation with 50 μM SIM, 100 μM LOV or 400 μM others statins and 10 μM F or FPP. LDH-leakage: with 50 μM SIM, 100 μM LOV or 200 μM others statins and 10 μM F or FPP. Data are expressed as means ± SD from three independent experiments (n=3). Statistically significant differences versus the control group are expressed as P*** < 0.001. Statistically significant differences in comparison with the statins group are indicated by #P < 0.05, ##P < 0.01 and ###P < 0.001.

3.2.3.3 Effect of GG or GGPP on statin-induced ROS formation, caspase-3 activity and LDH-leakage

ROS formation was measured after short incubation times at GG or GGPP concentrations of 100 μ M. This concentration was toxic after longer incubation times, thus the investigation of the effects on caspase-3 activity and LDH leakage were performed for both compounds at concentrations of 10 μ M.

The inhibitory effect of GG on statin-induced ROS formation was almost 100 % for all statins applied (Tab.15). The inhibition of ROS formation by GGPP was in the range of 35-55 %. Statins induced caspase-3 activity, which was measured after 2 hours treatment, was also significantly inhibited by GG supplementation in the range of 26-88%. There was almost no inhibitory effect on LOV induced caspase-3 activation. GGPP inhibited the statin-induced caspase-3 activation in the range of 21-46%. There was no inhibition of the FV-induced increase of caspase-3 activity by GGPP. In general, the inhibition of ROS formation and caspase-3 activity were strongest with G compared to GGPP.

GG statistically significantly reduced the cell membrane damage (LDH-leakage) to about 60% of the increases with NKS, FV and ATV. There was no inhibitory effect with GG on LOV and SIM-induced cytotoxicity after 4h treatment. By supplementation with GGPP, the changes in LDH-leakages induced by statins were in the range of 28-48%.

	ROS (30 min) (% of control)		Caspase-3 activity (2h) (% of control)		LDH-leakage (4-24-48h) (% of total)	
	w/o GG	+ GG	w/o GG	+ GG	w/o GG	+ GG
w/o statin	100 ± 0.0	92.9 ± 13	100 ± 0.0	113 ± 29	4.2 ± 1.0	4.9 ± 1.1
NKS	254.1 ± 17 ***	101.6 ± 9 ##	1083 ± 108 ***	194 ± 92 ###	30.9 ± 8.2 *** §	11.3 ± 2.0 ### §
FV	199.5 ± 11 ***	98.6 ± 6 ###	1902 ± 420 ***	218 ± 87 ###	41.7 ± 6.5 *** §	16.1 ± 2.1 ### §
ATV	328.4 ± 46 ***	126.2 ± 24 ###	2077 ± 307 ***	1540 ± 244 ###	40.6 ± 6.1 *** β	15.9 ± 1.9 ### β
LOV	214.2 ± 17 ***	103.1 ± 15 ###	752 ± 240 ***	666 ± 288	32.4 ± 5.0 *** §	35.8 ± 10.6 a
SIM	208.6 ± 20 ***	98.4 ± 26 ##	1214 ± 233 ***	632 ± 86 ###	45.1 ± 3.0 *** §	43.5 ± 4.5 a

	ROS (30 min) (% of control)		Caspase-3 activity (2h) (% of control)		LDH-leakage (4-24-48h) (% of total)	
	w/o GGPP	+ GGPP	w/o GGPP	+ GGPP	w/o GGPP	+ GGPP
w/o statin	100 ± 0.0	93.3 ± 2.2	100 ± 0.0	96.3 ± 8	4.2 ± 1.0	4.5 ± 1.5
NKS	254.1 ± 17 ***	135.9 ± 39 ###	1083 ± 108 ***	588 ± 211 ##	30.9 ± 8.2 *** §	16 ± 4.5 # §
FV	199.5 ± 11 ***	120.4 ± 35 ##	1902 ± 420 ***	1873 ± 411	41.7 ± 6.5 *** §	25.7 ± 4.4 ## §
ATV	328.4 ± 46 ***	149.9 ± 31 ###	2077 ± 307 ***	1422 ± 254 ###	40.6 ± 6.1 *** β	28.6 ± 7.7 # β
LOV	214.2 ± 17 ***	106.6 ± 21 ###	752 ± 240 ***	462 ± 97 #	32.4 ± 5.0 *** a	13.5 ± 10 ## a
SIM	208.6 ± 20 ***	134.8 ± 40 #	1214 ± 233 ***	967 ± 375 ###	45.1 ± 3.0 *** a	32.4 ± 8.3 ## a

a = 4 hours incubation, β = 24 hours incubation, § = 48 hours incubation

[Control values: ROS formation: 100% = 0.8-1.6 DCF fluorescence/LDH in cells, Caspase-3 activity: 100% = 4.5-9 pmolAMC/min/mg protein, LDH-leakage: % of total = LDH supernatant/ LDH total]

Tab. 15: Effect of GG or GGPP on statin-induced ROS formation, caspase-3 activity and LDH-leakage.

Incubation conditions: HSkMCs were pre-incubated 2 hours with 10 or 100 μM GG or GGPP before adding the statins in combination with GG or GGPP. ROS formation: after 30 min incubation with 50 μM statins and 100 μM GG or GGPP. Caspase-3 activity: after 2 hours incubation with 50 μM SIM, 100 μM LOV or 400 μM others statins and 10 μM GG or GGPP. LDH-leakage: with 50 μM SIM, 100 μM LOV or 200 μM others statins and 10 μM GG or GGPP. Data are expressed as means ± SD from three independent experiments (n=3). Statistically significant differences versus the control group are expressed as P***<0.001. Statistically significant differences in comparison with the statins group are indicated by #P<0.05, ##P<0.01 and ###P<0.001.

3.2.3.4 Effects of MVA, F and GG on statin-induced changes of nuclear morphology

Changes in nuclear morphology, characterized in general by shrank nuclei, were determined in hSkMCs cultures pre-incubated with 10 μ M GG or F or 400 μ M MVA for 2 hours and then co-incubated with 10 μ M of the different statins for 72 hours. The medium containing these substances was renewed daily. The addition of F, GG and MVA reduced the changes in nuclear morphology induced by the statins. F had only little protective effects whereas GG completely prevented the cytotoxic effects of 10 μ M NKS, FV, ATV and strongly reduced the effects of 10 μ M LOV and SIM (Fig. 38).

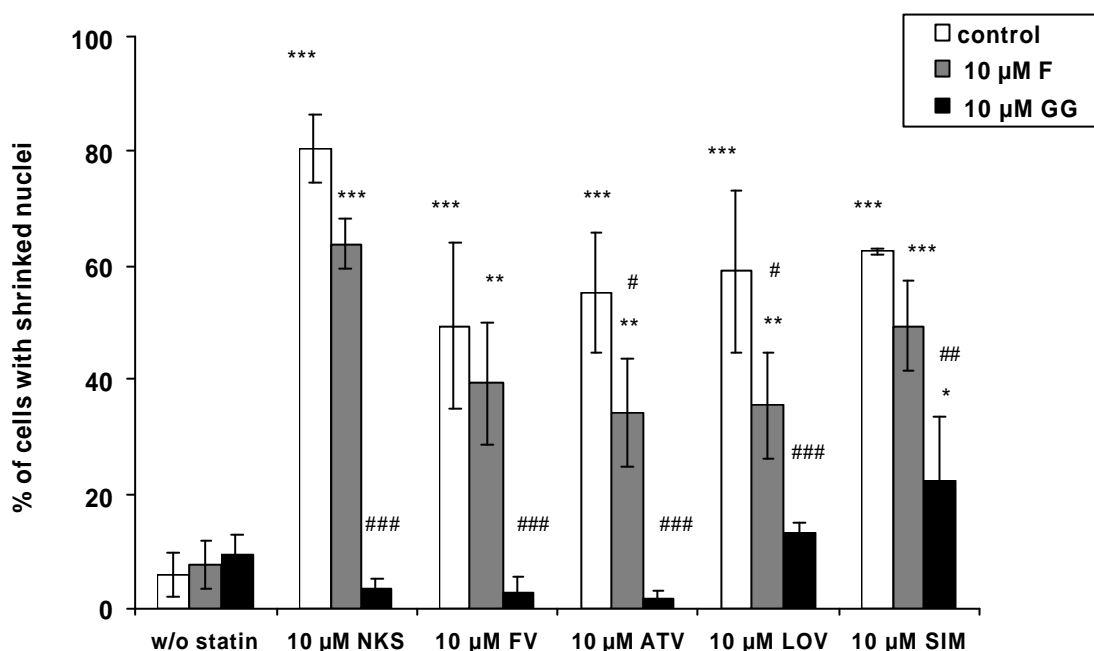


Fig. 38: Effect of F and GG on statin-induced nuclear change on hSkMCs.

hSkMCs were incubated with the different statins with or without 10 μ M GG or F for 72 hours and the change on nuclear diameter was measured after Hoechst dye staining. Data are expressed as means \pm SD from three independent experiments (n=3). Statistically significant differences versus the control group are expressed as *P<0.05, **P<0.01 and ***P<0.001. Statistically significant differences in comparison with the statins group are indicated by #P<0.05, ##P<0.01 and ###P<0.001.

The addition of MVA completely prevented the statins induced late nuclear changes (Fig. 39)

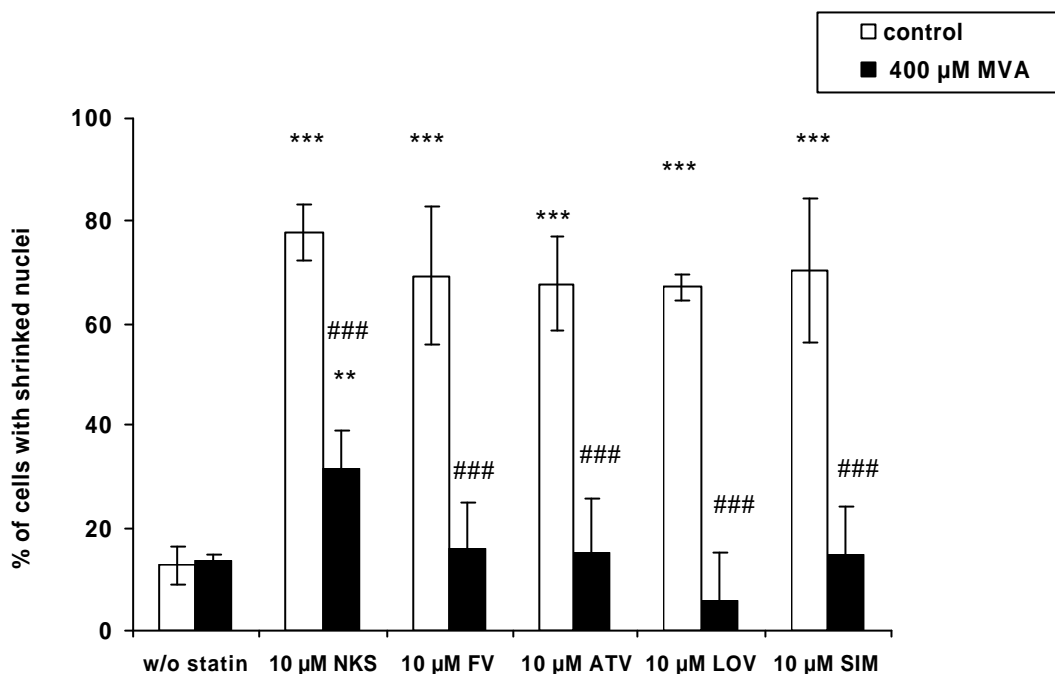


Fig. 39: Effect of MVA in statin-induced nuclear changes on hSkMCs.

HSkMCs were incubated with the different statins with or without 400 µM MVA for 72 hours and the change on nuclear diameter was measured after Hoechst dye staining. Data are expressed as means \pm SD from three independent experiments (n=3). Statistically significant differences versus the control group are expressed as **P<0.01 and ***P<0.001. Statistically significant differences in comparison with the statins group are indicated by ###P<0.001

Pictures of control hSkMCs, statins treated cells and cells co-incubated with statins and MVA are shown in figure 40. Cells treated with 10 µM SIM, ATV or FV show great changes in nuclear morphology as compared to controls. Almost all nuclei appear much smaller, whereas in the presence of MVA, the nuclei of statin treated cells are similar to the controls.

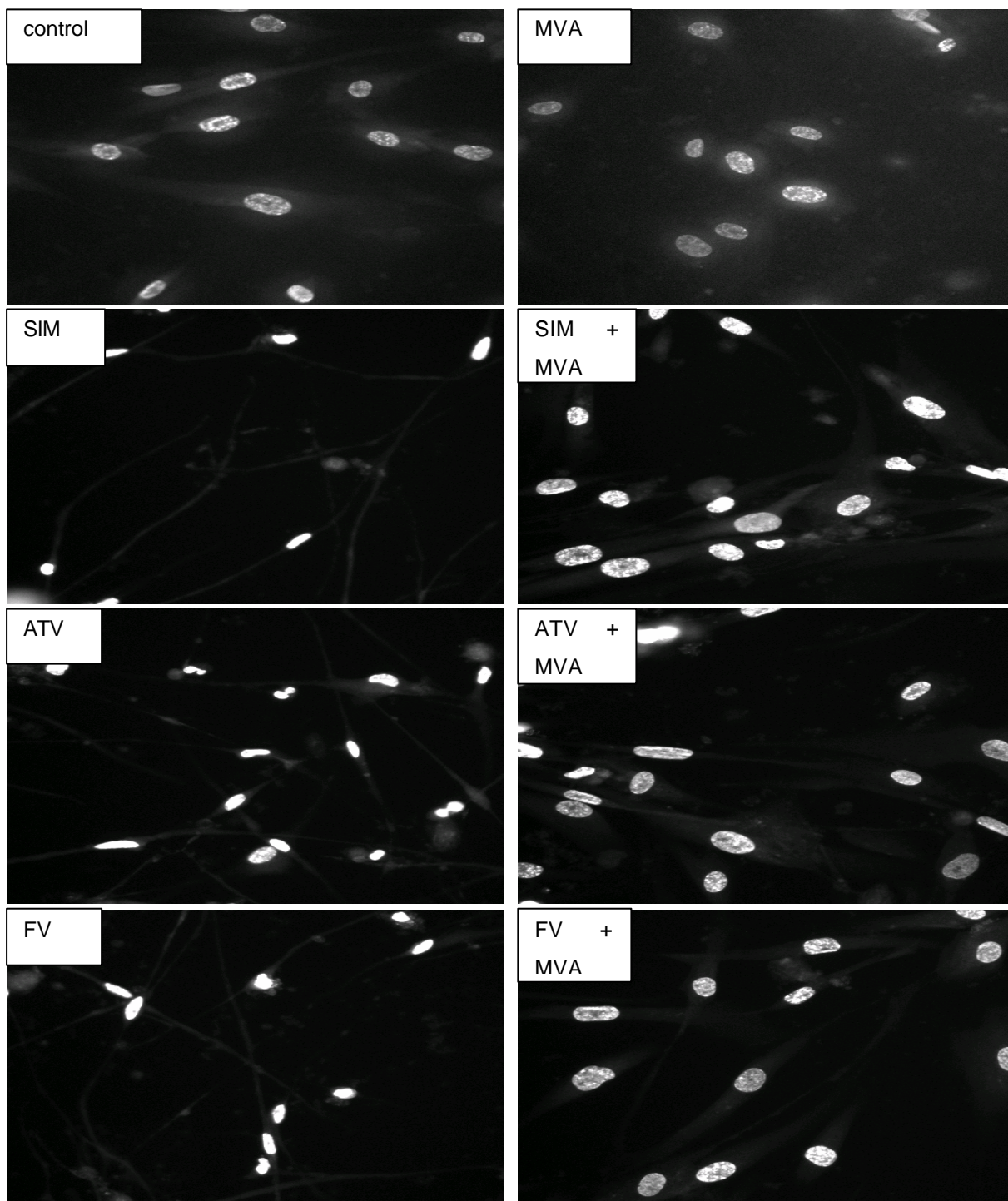
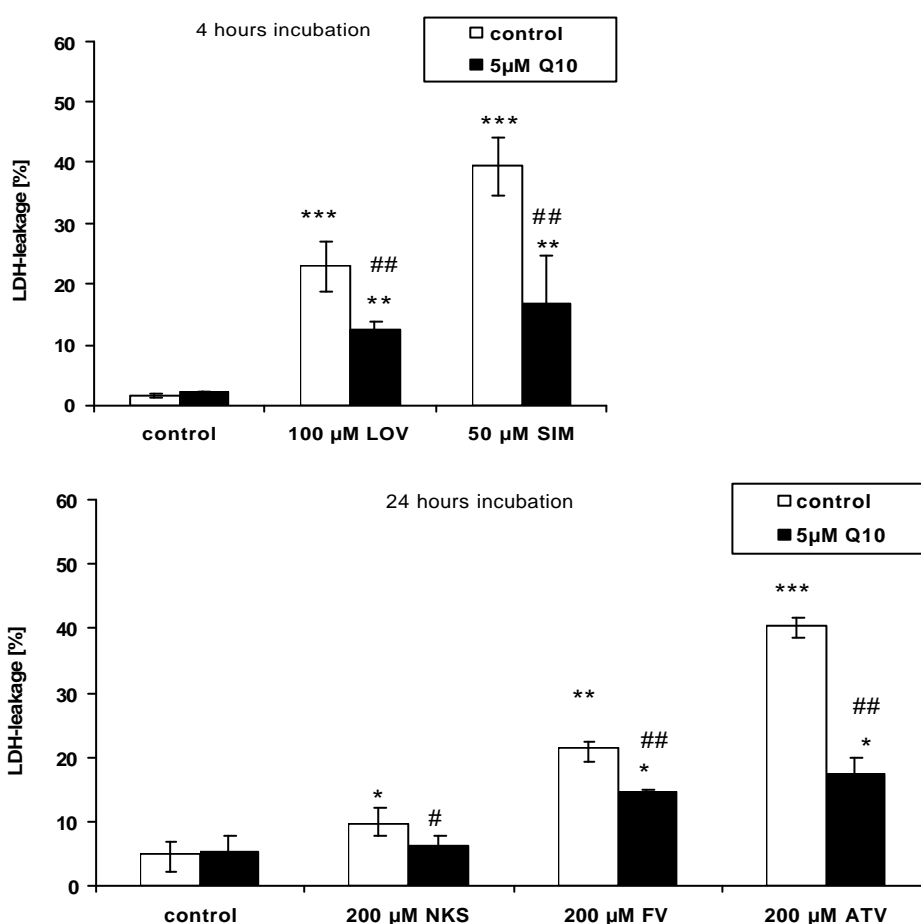


Fig. 40: Micrographs of Hoechst-stained hSkMCs after treatment with FV, ATV, SIM at the concentrations of 10 μ M for 72 hours supplemented with 400 μ M MVA.

The micrographs showed the decrease nuclear size (shrinking). Bright fluorescence in faintly stained cell was nuclear condensation. The presence of MVA abrogated the effect of statins on hSkMCs. Magnification x20.

3.2.3.5 Effect of ubiquinone on statin-induced cytotoxicity

The experiments with ubiquinone (Q₁₀) were very challenging. Q₁₀ supplementation of the medium was difficult to achieve because of the poor solubility. Q₁₀ which was reported being soluble up to a concentration of 5 μ M, may precipitate under certain conditions at the microscopical level. In two independent experiments, out of three, a concentration of 5 μ M Q₁₀ reduced the cell membrane damage (LDH-leakage) in the range of 33-57% (Fig. 41). No significant inhibitory effect was found in the third experiment, where Q₁₀ might have been not dissolved properly. The supplementation with Q₁₀ had no significant effect on intracellular ROS production and on caspase-3 activation (data not shown).



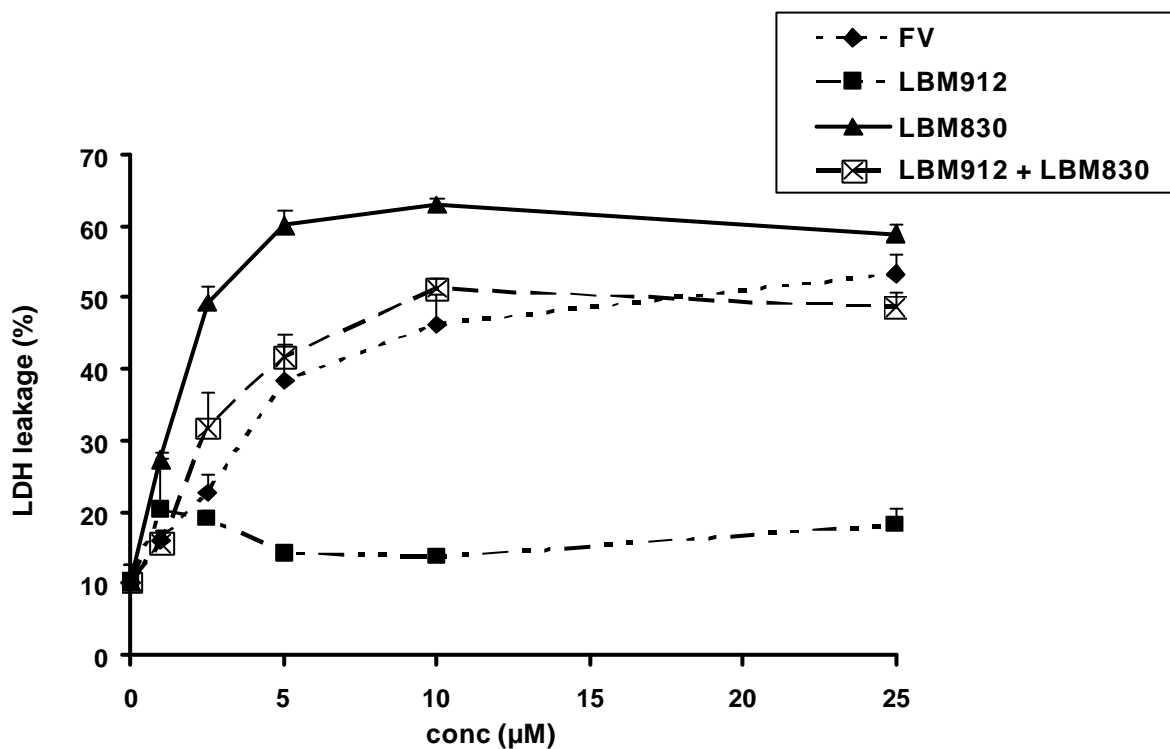
[Control values: LDH-leakage: % of total= LDH supernatant/ LDH total]

Fig. 41: Effect of Q₁₀ in statin-induced cell membrane damage on hSkMCs.

HskMCs cultures were pre-incubated 2 hours with Q₁₀ (5 μ M), before incubated with or without ATV, NKS and FV [24 h] (A), SIM and LOV [4 h] (B) and the LDH-leakage was measured. Data are expressed as means \pm SD from three independent experiments (n=2). Statistically significant differences versus the control group are expressed as *P<0.05, **P<0.01 and ***P<0.001. Statistically significant differences in comparison with the statins group are indicated by #P<0.05 and ##P<0.01.

3.2.3.6 Cytotoxic effect of active and inactive HMG-CoA reductase inhibitors

FV is a 50/50 mixture of two enantiomers, one active and one inactive with regard to their inhibitory effect on HMG-CoA reductase activity. In order to test, whether the toxicity of FV is related to its pharmacological activity, hSkMCs were either treated with FV, its active enantiomers LBM830 or the inactive FV enantiomer LBM912 at the concentrations of 1, 2.5, 5, 10 and 25 μM for 72 hours. The results showed an increase of cytotoxicity with FV and its active enantiomer LBM830. In contrast, the treatment with the inactive enantiomer LBM912 was not cytotoxic. The combination of LBM912 and LBM830 was most potent (Fig. 42).

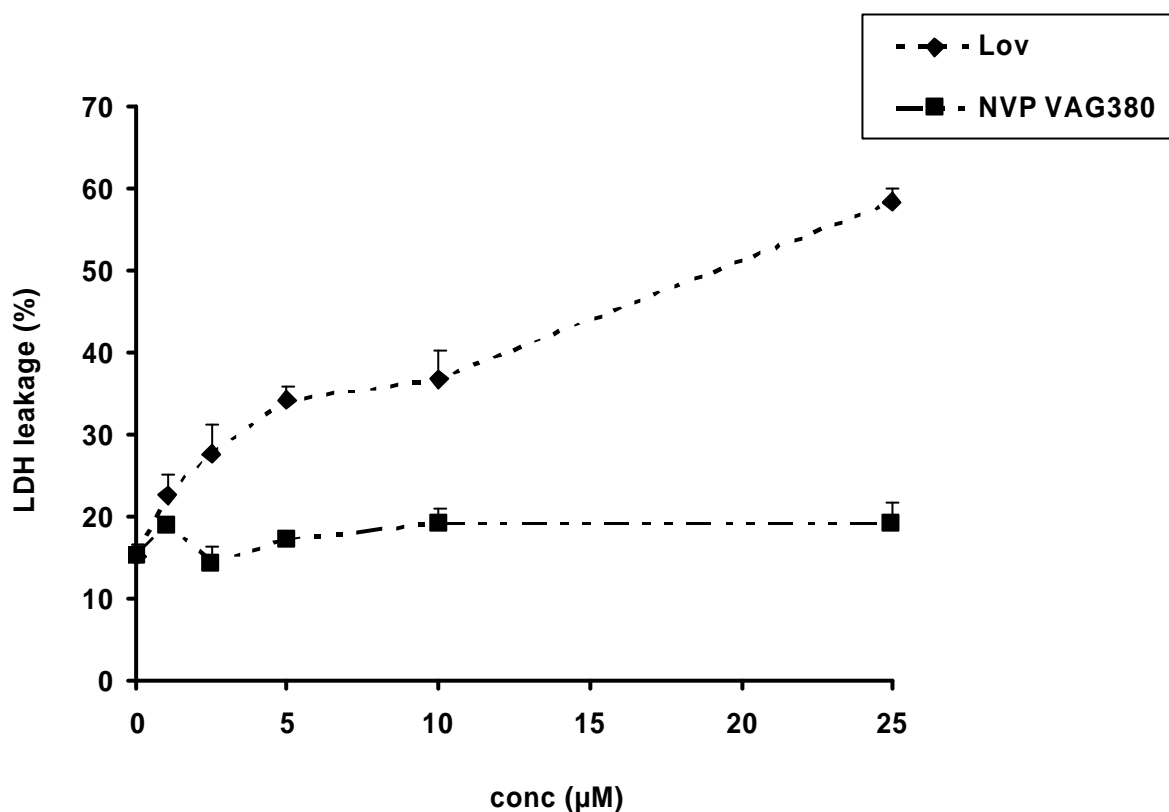


[Control values: LDH-leakage: % of total= LDH supernatant/ LDH total]

Fig. 42: Concentration-dependency cytotoxicity after 72 hours incubation of hSkMCs with FV and its enantiomers LBM830 (active), LBM912 (inactive).

Data are expressed as means \pm SD from two independent experiments (n=2).

HSkMCs were incubated with LOV or deoxy-lovastatin (NVP VAG380), which is an inactive LOV derivative lacking the hydroxyl group at the active part of the molecule, at the concentrations of 1, 2.5, 5, 10 and 25 μM for 72 hours. The results showed a concentration dependent increase of cytotoxicity with LOV, whereas deoxy-lovastatin was not toxic (Fig. 43).



[Control values: LDH-leakage: % of total= LDH supernatant/ LDH total]

Fig. 43: Concentration-dependency of cytotoxicity after 72 hours incubation of hSkMCs with LOV and deoxy-lovastatin (NVP VAG380).

Data are expressed as means \pm SD from two independent experiments (n=2).

3.2.3.7 Total antioxidative capacity of mevalonate and its derivatives F, FPP, GG, and GGPP

The antioxidative capacities of the HMG-CoA reductase downstream metabolites MVA, GG, GGPP, F and FPP were tested by measuring the radical cation ABTS^{•+} scavenging activity in comparison to trolox-C. MVA, G and F showed absolutely no radical cation ABTS^{•+} scavenging activity. The radical cation ABTS^{•+} scavenging activity of GGPP and FPP were low compare to the standard trolox-C.

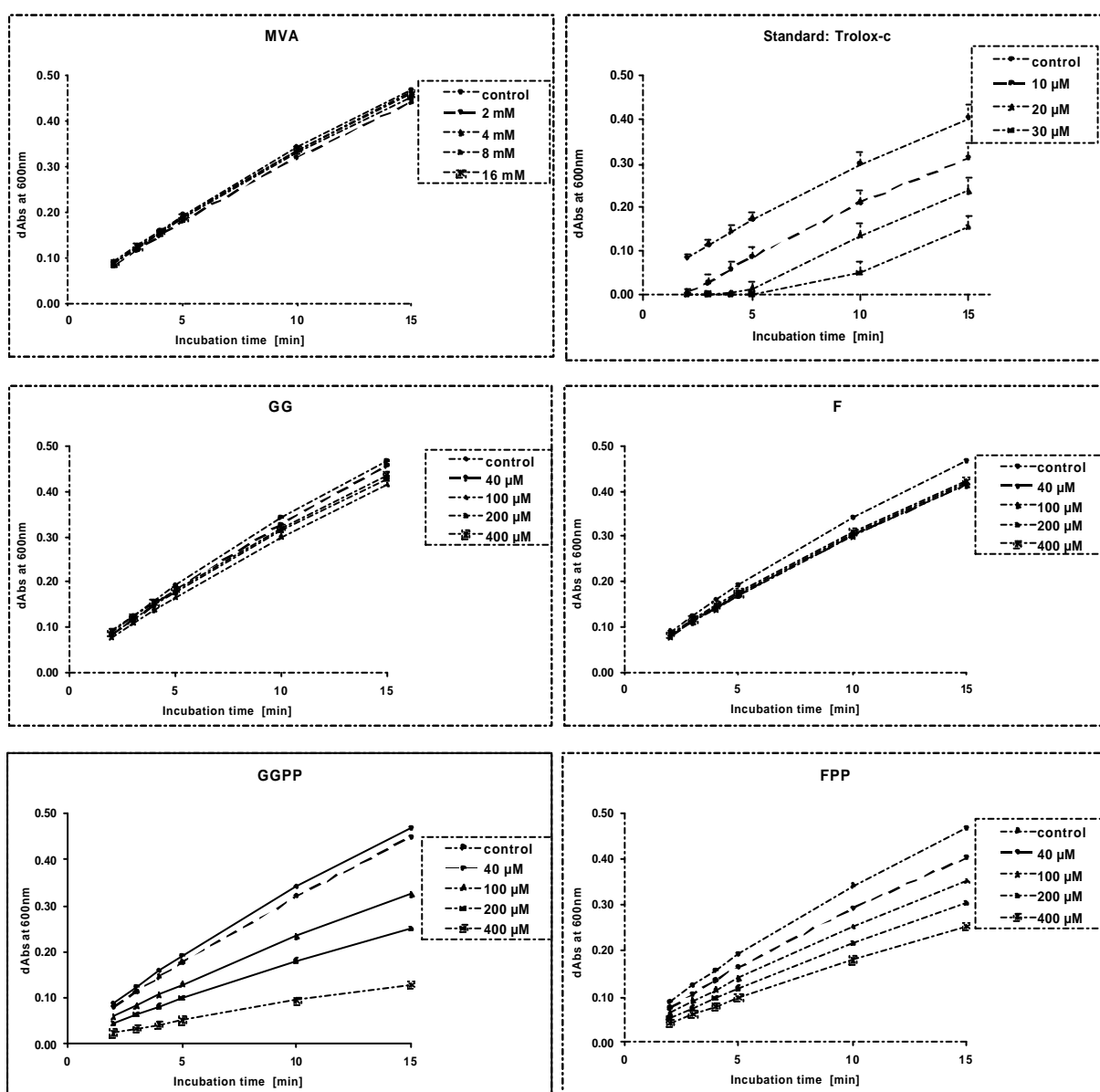


Fig. 44: Radical cation scavenging capacity of MVA and its derivatives (F, FPP, GG, GGPP).

The radical cation scavenging capacity of the MVA and its derivatives (F, FPP, GG, and GGPP) were expressed as trolox-C equivalent. The trolox-C equivalent was calculated and used to compare the radical cation scavenging activity of each antioxidant. Data are expressed as means \pm SD from three independent experiments for each sample (n=3).

3.2.3.8 Discussion

The HMG-CoA reductase, which converts HMG-CoA to mevalonate, is the rate limiting enzyme in the mevalonate pathway. MVA is a precursor not only of cholesterol but also of the isoprenoids F, FPP, GG and GGPP. Farnesylation or geranylgeranylation of cellular molecules is important for signaling functions (Goldstein and Brown, 1990). The inhibition of MVA synthesis reduces isoprenylated metabolite formation, and thus isoprenylation of proteins such as the G proteins Ras, Rab and Rho. Farnesylation of Ras proteins is important for their attachment to the membrane. By this they exert various actions, playing a crucial role in cellular differentiation and proliferation (Maltese and Sheridan, 1987; Laufs *et al.*, 2000). FPP is also involved as an important polyisoprenoid component in the induction of heme A in the electron transport chain.

GG and GGPP are used for the prenylation of Rab proteins, which are necessary for vesicle transportation within the cell. The Rab family is known to play a role in cell replication, platelet activation and the generation of oxygen radicals (Laufs *et al.*, 2000). GGPP is also an inducer of dolichols, required for glycoprotein synthesis and ubiquinone, a polyisoprenylated quinoid cofactor of the electron transport chain (Beyer, 1992; Do TQ *et al.*, 1996; Ernster *et al.*, 1995).

The inhibition of the prenylation of important regulatory proteins could contribute to the mechanisms of statin-induced muscle cell necrosis. This means, that statins would cause myotoxicity by their pharmacological action via inhibition of the HMG-CoA reductase activity (Epstein *et al.*, 1991; Hancock *et al.*, 1991; Cox *et al.*, 1992; Flint *et al.*, 1997a, 1997b; Nishimoto *et al.*, 2003). However, the importance of the reduction of the HMG-CoA reductase downstream metabolites in the statin-induced rhabdomyolysis is still discussed controversially. There are pros and cons arguments for this hypothesis. One argument against this hypothesis is that the intracellular pool of the isoprenoids is too large in order to achieve a decrease, which may be relevant for the induction of myotoxicity by statins (Goldstein and Brown, 1990; Casey and Seabra, 1996). Johnson *et al.* (2004), however, confirmed the hypothesis of HMG-CoA reductase mediated skeletal cell necrosis. They suggested that statins induce apoptosis in rat myotubes by inhibiting the geranylgeranylation of proteins. Their results clearly demonstrated that cerivastatin-induced apoptosis in rat and human myotubes was inhibited by addition of the downstream metabolites GG and MVA. Masters *et al.* (1995) demonstrated that the addition of MVA completely restored

protein synthesis to control values and abrogated morphologic changes induced by LOV in neonatal rat skeletal myocyte primary cultures.

In our experiments we basically confirmed the findings reported in the literature that the pharmacological activity of HMG-CoA reductase inhibitors is involved in the mechanism of muscle toxicity. We investigated this hypothesis by means of LBM830, which is the pharmacologically active enantiomer of FV, and LBM912, which is the pharmacologically inactive enantiomer of FV. While the active enantiomer caused concentration-dependent increase in LDH leakage, its HMG-CoA reductase inactive enantiomer did not. Similar results were obtained with LOV and deoxy-LOV (NVP VAG380), which is lacking the hydroxyl group at the active part of the molecule and thus is inactive. Here we also found cytotoxicity with LOV but not with the inactive deoxy-LOV. Although we did not measure the degree of HMG-CoA reductase inhibition in our experiments, these results supported the hypothesis that the toxicity of the statins is related to the inhibition of HMG-CoA reductase.

In addition, we then showed with 5 different statins in the human relevant cell system that addition of MVA, F, FPP, GG and GGPP to the cells, nearly all inhibited statin-induced toxicity at the level of the induction of apoptosis and induction of membrane damage.

Summary of results from experiments with 5 different statins after co-incubation with HMG-CoA reductase downstream metabolites.			
Protection against ROS formation, caspase-3 activation and LDH-leakage			
HMG-CoA metabolite	ROS formation	Caspase-3 activity	LDH-leakage
MVA	5/5	5/5	5/5
F	5/5	4/5	3/5
FPP	5/5	5/5	5/5
GG	5/5	4/5	5/5
GGPP	5/5	4/5	3/5

It appears in all experiments, that HMG-CoA down-stream metabolite mediated protection against the statin-induced LDH leakages is accompanied by decrease of the statin-induced caspase-3 activation as well as the formation of ROS. The deviations observed from this relation may be the result of the different incubation

conditions, like time of incubations and differences in the applied statin concentrations.

MVA, F, FPP, GG and GGPP were tested for their direct radical scavenging activity by means of the cell free TAC assay. While MVA, F and GG had no direct radical scavenging activity, FPP and GGPP proved to be very weak scavengers in the 100 μ M concentration range. However, in the cellular system all applied isoprenoids showed potent protection against the statin induced ROS formation. F and GG were most effective showing 100 % protection; all other isoprenoids like MVA, FPP and GGPP caused statistically significant reduction of statin-induced ROS formation.

As shown in the previous chapter, that various structurally unrelated antioxidants were very effectively in protecting cells against the statin-induced cytotoxicity and apoptosis, the current result with the HMG-CoA downstream metabolites suggest a possible interaction of ROS formation after HMG-CoA reductase inhibition. It is not yet clear how the HMG-CoA reductase downstream metabolites inhibit against statin-induced ROS formation. Since direct scavenging effect of isoprenoids is not very likely, interference with the ROS generation mechanism may be another possibility. Mobilization of intracellular Ca^{2+} is the mechanism how HMG-CoA reductase inhibitor could increase ROS formation. In various cell types the mobilization of intracellular Ca^{2+} was demonstrated by statins, and MVA was found very effective in blocking this response, suggesting a potential HMG-CoA reductase inhibitor's action (Alvarez de Sotomayor and Andriantsitohaina, 2001). Increase Ca^{2+} uptake into the mitochondrion could trigger ROS formation by uncoupling of the respiratory ETC (see calcium chapter).

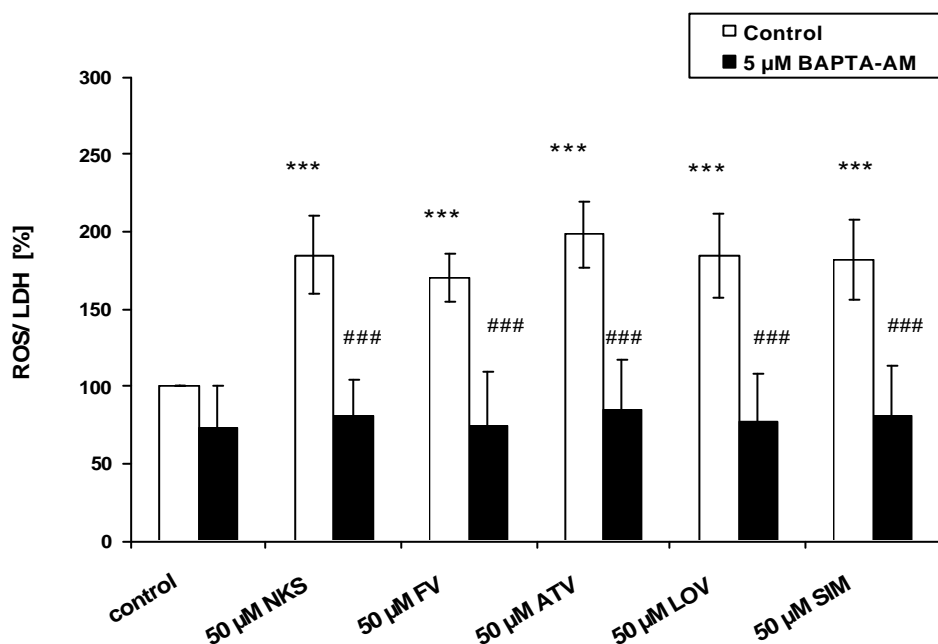
Inhibition of HMG-CoA reductase per se is associated with induction of apoptosis. There is increasing evidence, that products of the mevalonate pathway including MVA, FPP and GGPP can regulate the apoptotic process at different points in the cascade. For example mammalian sterile 20-like kinase, a protein involved in apoptosis, was cleaved in the presence of LOV in osteoclasts and this response was prevented by GG (Reszka *et al.*, 1999). GG and F were also found to prevent the activation of caspases by aminobisphosphonates in 1774 cells (Benford *et al.*, 1999). Depending on the cell type MVA, FPP and GGPP can suppress apoptosis. This may help also to explain the inhibitory effect of the HMG-CoA downstream metabolites on the statin-induced apoptosis observed in hSkMCs.

3.2.4 Role of Calcium on statin-induced cellular events

In order to study the possible role of Ca^{2+} in statins induced hSkMCs toxicity, cells were incubated with statins in the presence or absence of the intracellular Ca^{2+} -chelators BAPTA-AM and ROS formation, caspase-3 activity and cytotoxicity were determined. BAPTA-AM is a membrane-permeable Ca^{2+} chelator. The presence of four AM groups in the molecule allows BAPTA-AM to cross cellular membranes. Esterases located in the cytosol then cleave the AM groups, serving to trap the active chelator inside the cell where it binds Ca^{2+} and effectively decreases the cytosolic free Ca^{2+} concentrations.

3.2.4.1 ROS formation

hSkMCs were pre-incubated with 5 μM BAPTA-AM and then treated for 30 minutes together with the respective statin. The presence of BAPTA-AM completely inhibited statin-mediated ROS formation suggesting that ROS formation is Ca^{2+} -dependent (Fig. 45).



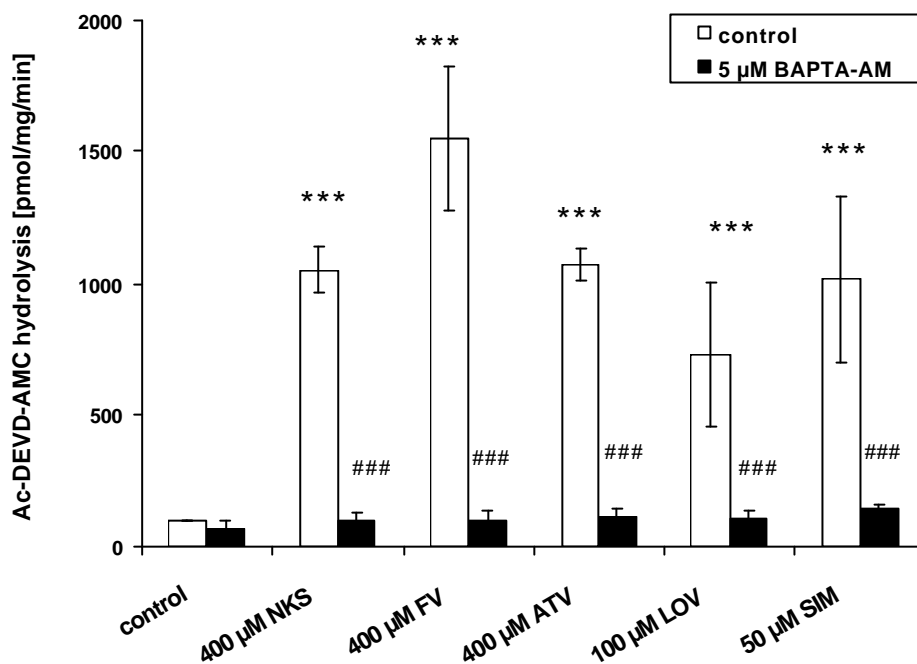
[Control values: ROS formation: 100% = 0.8-1.6 DCF fluorescence/LDH in cells]

Fig. 45: Effect BAPTA-AM on statin-induced ROS formation.

After 2 hours pre-incubation of hSkMCs culture with 5 μM BAPTA-AM, hSkMCs were treated 30 minutes with 50 μM of NKS, FV, ATV, LOV and SIM in combination with 5 μM BAPTA-AM. Data are expressed as means \pm SD from three independent experiments (n=3). Statistically significant differences versus the control group are expressed as ***P<0.05. Statistically significant differences in comparison with the statins group are indicated by ###P<0.001.

3.2.4.2 Caspase-3 activity

BAPTA-AM alone had no effect on caspase-3 activity in hSkMCs culture. The presence of 5 μ M BAPTA-AM completely inhibited statins-induced caspase-3 activation for all statins (Fig. 46).



[Control values: Caspase-3 activity: 100%= 4.5-9 pmolAMC/min/mg protein]

Fig. 46: Effect of BAPTA-AM on statins--induced caspase-3 activity.

HskMCs were pre-incubated 2 hours with calcium intracellular chelator BAPTA-AM (5 μ M), follow by 2 hours co-incubation with the different statins in the presence or absence of BAPTA-AM. Data are expressed as means \pm SD from three independent experiments (n=3). Statistically significant differences versus the control group are expressed as ***P<0.001. Statistically significant differences in comparison with the statins group are indicated by ###P<0.001.

No inhibitory effect on LDH-leakage was found after treatment of human skeletal muscle cells with statins in the presence of BAPTA-AM (data not shown).

3.2.4.3 Discussion

Increase of intracellular Ca^{2+} has been suggested in the literature being involved in the mechanism of the statin-induced myotoxicity. In some studies, increased Ca^{2+} concentrations above the physiological relevant level, were observed in the skeletal muscles after statin treatment (Duncan, 1978; Borgers *et al.*, 1983; Rudge et Duncan, 1984; Gissel and Clausen, 2001; Gommans *et al.*, 2002; Inoue *et al.*, 2003). It was also reported that SIM elevated the cytoplasmic Ca^{2+} concentrations via the release of stored Ca^{2+} in L6 rat myoblasts (Nakahara *et al.*, 1994). In endothelial cells SIM has been shown to increase the intracellular Ca^{2+} level, which was inhibited by the downstream metabolite of HMGCoA, MVA (Alvarez de Sotomayor and Andriantsitohaina, 2001). Cerivastatin had an ability to cause release of Ca^{2+} from sarcoplasmic reticulum (Inoue *et al.*, 2003). It is assumed that the relaxation and contraction of muscle cells is mediated by the modulation of the intracellular Ca^{2+} concentration, a process which is thought to be dependent on the inhibition of the HMG-CoA reductase. Rho prenylation is supposed to play a role into the intracellular uptake mechanisms of Ca^{2+} (Gronroos *et al.*, 1996).

In our studies we did not measure the Ca^{2+} concentrations directly; however there is indirect evidence that calcium is also involved in the mechanism of statin-induced ROS formation and apoptosis. The trapping of Ca^{2+} by the intracellular calcium chelator BAPTA/AM was able to decrease the statin-induced ROS formation as well as apoptosis. Thus, elevation of intracellular Ca^{2+} concentration may be part of the triggering mechanism by which statins produce ROS. The role of Ca^{2+} in generating ROS has been shown in several studies. Extracellular calcium was shown to increase ROS formation in the contracting diaphragm (Supinski *et al.*, 1999). The relation between intracellular Ca^{2+} and ROS was also shown in other cellular models (Bae *et al.*, 1999). Richter demonstrated that isolated mitochondria, when they are exposed to high Ca^{2+} cause uncoupling of the ETC and thus leading to ROS formation (Richter, 1993). Under ischemic conditions the link between mitochondrial Ca^{2+} accumulation and ROS formation has been documented. The early increase of ROS observed in our studies may also be linked to Ca^{2+} mobilization. Comparing the kinetics of intracellular Ca^{2+} level rise, as it is known from the literature and the kinetics of ROS formation from our own experiments, it turns out that both happened relatively rapidly

within 30 min, which are the first cellular events observed after the statin treatment. Taken the literature data together with our own observations, the results of the present study strongly suggest that ROS may be a downstream signal of elevated intracellular Ca^{2+} .

Intracellular calcium plays an important role in the regulation of apoptosis and necrosis (Nicotera *et al.*, 1994). An increase in intracellular free calcium can activate Ca^{2+} dependent enzymes, such as phosphatases, proteases, and endonucleases, which degrade important cellular macromolecules (McCabe *et al.*, 1992; Orrenius *et al.*, 1992; Richter and Kass, 1993). Ca^{2+} is involved in the modification of chromatin conformation by making chromatin regions accessible to enzymes such as DNase I or others endonucleases (McConkey *et al.*, 1989). An increase in intracellular free Ca^{2+} can dissociate the actin filaments from alpha-actin, and activate actin-binding proteins (Mirabelli *et al.*, 1989).

Intracellular Ca^{2+} seems also to play an important role in the apoptotic cell death in statin-treated hSkMCs. In our experiments BAPTA-AM was able to prevent the statin-induced changes very efficiently. The contribution of Ca^{2+} in the mechanism of statin-induced myopathies leading to rhabdomyolysis is not yet fully understood. Further investigation is needed for the better understanding of this event.

In our experiments we did not observe a relevant inhibition of the statin-induced LDH-leakage by means of the intracellular Ca^{2+} chelator BAPTA-AM. This result does not necessarily exclude a link between ROS formation, apoptosis and LDH-leakage. Differences between LDH-leakages compared to ROS formation and apoptosis, might be the result of different concentrations applied under the different incubation conditions. In the long term cytotoxicity experiments it was not possible to further increase the BAPTA-AM concentrations because of toxicity to the hSkMCs.

3.2.5 Gene expression analysis

Independent from our experiments, cynomolgous monkeys were treated with statins for 4 weeks. At the end of the study muscle tissues from untreated control animals was compared with that of treated animals concerning their large scale gene expression profiles at the transcriptional level by means of the Affimetrix technology platform. It is expected that pathways, which are involved in the mechanism of action of a compound are either induced or inhibited at the transcriptional level. This technology has been proven to be a useful tool for the discovery of new mechanism of action of new unknown compounds.

It was the goal of the present study to evaluate the gene expression changes observed *in vivo* in the monkey muscle tissue in the current human skeletal muscle cell model.

3.2.5.1 Gene expression analysis in hSkMCs after treatment with statin

In order to evaluate gene expression changes *in vitro* in hSkMCs at the mRNA level hSkMCs was cultured with 1 μ M NKS, FV, LOV, SIM and 10 μ M ATV for 48 hours. RNA was extracted at the end of the experiment and by means of RT PCR the following genes were analyzed:

PFKFB-2 (6-phosphofructo-2-kinase / fructose-2, 6-bisphosphatase 2)

PFKFB-3 (6-phosphofructo-2-kinase / fructose-2, 6-bisphosphatase 3)

PDK-4 (pyruvate dehydrogenase kinase, isoenzyme 4)

PDP-2 (pyruvate dehydrogenase phosphatase, isoenzyme 2)

PPAR α (peroxisome proliferative activated receptor, alpha)

FOXO3A (forkhead box O3A)

SOD-2 (mitochondrial superoxide dismutase 2)

All the selected genes except PDP-2 were strongly upregulated in the response of nearly all statins. Changes observed on PDK4 mRNA expression were depending on the statin for NKS, FV and LOV more than 1000 fold. Changes on gene expression of FOXO3A, PFKFB-2 and PFKFB-3, were also very potent (Tab. 19).

	Sequence description	Accession number	Gene expression change compare to control				
			NKS	FV	ATV	LOV	SIM
PFKFB-2	6-phosphofructo-2-kinase / fructose-2, 6-bisphosphatase 2	MN_006212	+++	++++	++	+++	+
PFKFB-3	6-phosphofructo-2-kinase / fructose-2, 6-bisphosphatase 3	MN_004566	++	+++	+	++	+
PDK-4	Pyruvate dehydrogenase kinase, isoenzyme 4	MN_002612	++++	++++	++	++++	+
PDP-2	Pyruvate dehydrogenase phosphatase, isoenzyme 2	MN_020786	0	0	0	0	0
PPARα	Peroxisome proliferative activated receptor, alpha	MN_032644	+	+	+	+	+
FOXO3A	Forkhead box O3A	MN_201559	+++	++++	+	++	+
SOD-2	Superoxide dismutase 2, mitochondrial	MN_000636	+	+	+	+	+

(0 no change, + between 2-10 fold change, ++ between 11-100 fold change, +++ between 101-1000 fold change, ++++ >1000 fold change).

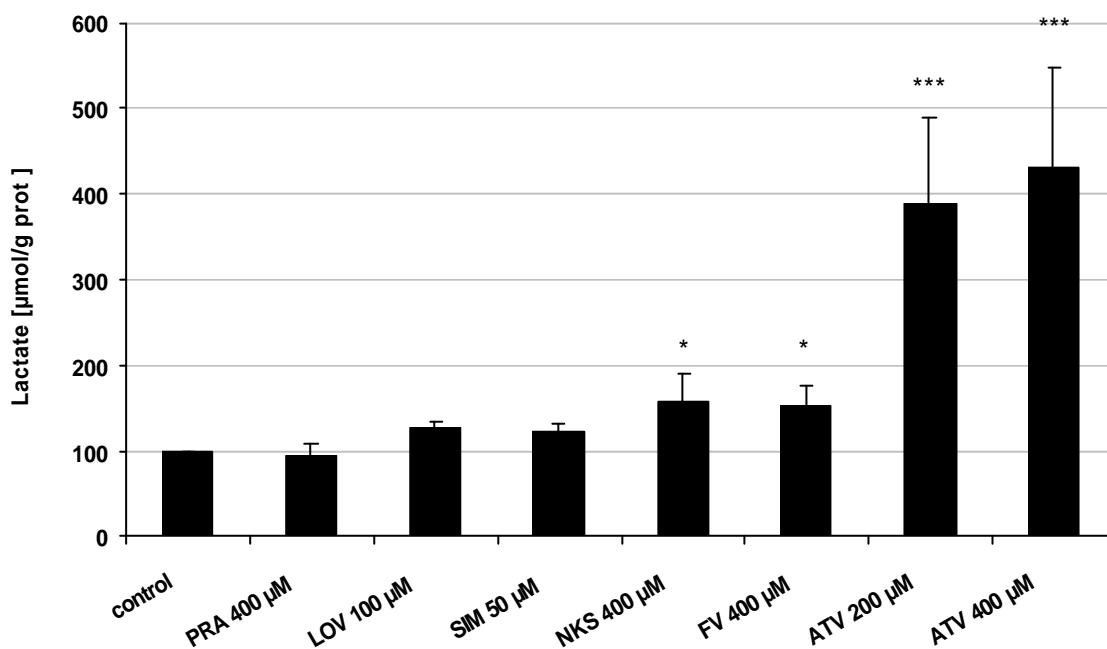
Tab.16: Regulated genes following hSkMCs after 48 hours treatment with statins.

hSkMCs were treated with 1 μ M NKS, FV, LOV, SIM and 10 μ M ATV for 48 hours and the cells lysates were used for DNA extraction and gene expression analysis.

3.2.5.2 Confirmation of glycolytic activity by determination of lactate content in hSkMCs

The results of gene expression analysis strongly suggested the involvement of glycolytic pathway and therefore lactate production on the mechanism of statin-induced cytotoxicity.

After 4 hours treatment of hSkMCs with 400 μM NKS and FV, 100 μM LOV, 50 μM SIM and with 200, 400 μM ATV, the concentration of lactate in the cells increased with NKS, FV and ATV compared to the control. The effect was most pronounced with ATV compared to the other statins used (Fig. 46).



[Control values: Lactate: 100% = 60-110 $\mu\text{mol/g prot}$]

Fig. 47: Effect of statins on the lactate content in the hSkMCs lysates after 4 hours.

The results are means values \pm SD from three independent experiments (n=3). Statistically significant differences compared with the control group are expressed as *P<0.05 and ***P<0.001.

3.2.5.3 Discussion

In order to elucidate the pathways of statin-induced myotoxicity, the *in vitro* expression of some selected genes was investigated. Our results clearly suggest changes of genes involved in oxidative stress and apoptosis. These changes occurred with all the statins tested in the hSkMCs culture.

Among all the genes involved in oxidative stress, the FOXO3A was the mostly upregulated candidate especially with NKS and FV. FOXO3A protects cells from oxidative stress by directly increasing their quantities of manganese superoxide dismutase (MnSOD) messenger RNA and protein (Brunet *et al.*, 1999; Kashii *et al.*, 2000; Tran *et al.*, 2002). FOXO3A itself is under the control of phosphatidylinositol 3-kinase (PI3k/Akt), which blocks FOXO3A expression under normal physiological conditions. PI3k/Akt expression itself can be decreased by reduced availability of active Ras or Rho (Weiss *et al.*, 1999), which may be the direct result of HMG-CoA reductase inhibition (Vidyalakshmi *et al.*, 2004; Brunet *et al.*, 1999)

In the same study we found upregulation of SOD-2, which is a first line antioxidant defence system. FOXO3A activates MnSOD and leads to subsequent reduction of reactive oxygen species. The increase of the expression of MnSOD in the treated hSkMCs provides further evidence that the mitochondrion is the source of the statin-induced ROS formation. The upregulation of SOD-2 in the mitochondrion suggests an increase oxidative stress in this organel, which by upregulation of its enzymatic activity is protecting them against the increased ROS formation.

Our results also indicate a significant change in the genes involved in glycolytic pathway. Our experiments showed the upregulation of PFKFB-2 and PFKFB-3 nearly in the same range. These two bifunctional enzymes who modulate intracellular levels of fructose-2, 6-bisphosphate (F-2, 6-P₂), are potent activator of phosphofructokinase, the key regulatory enzyme of glycolysis. The kinase/bisphosphatase ratio of the bifunctional enzyme is dominated by the kinase activity under physiological conditions. F-2,6-P₂, a key metabolite in the control of glycolysis, is a potent stimulator of PFK-2 and inhibitor of F-2,6-BPase from different tissues. Its synthesis and breakdown are catalyzed by 6-phosphofructo-2-kinase (PFK-2) and fructose-2, 6-bisphosphatase (FBPase-2), respectively (Rousseau and Hue, 1993; Pilkis *et al.*, 1995).

PDK-4 (Pyruvate dehydrogenase kinase, isoenzyme 4) was the highest upregulated among all the genes tested. In contrary, no change had been observed with the PDP-2 gene (Pyruvate dehydrogenase phosphatase, isoenzyme 2). PDP-2 is one of the few mammalian phosphatases residing within the mitochondrial matrix space. It is responsible for dephosphorylation and reactivation of the PDC and, by this means, is involved in the regulation of utilization of carbohydrate fuels in mammals. It supplies the carbon units derived from carbohydrate fuels mainly for complete oxidation by the Krebs cycle. Increased glycolytic activity was demonstrate for some statins by increase lactate formation. The inactivation of PDP-2 by the induction of the PDK-4 is followed by metabolic switching to limit oxidative fuel to fatty acids. However, statins decrease the serum levels of fatty acids and this situation forces the muscle to use amino acids from proteins as an energy source if this special situation persists for long period. It had been suggested that excessive protein degradation will damage the muscle if the situation is rigorous, driving to acute myopathy or rhabdomyolysis (Motojima *et al.*, 1998). It had ben reported that induction of PDK-4 mRNA is involved in the drug (statins, fibrates)-induced acute rhabdomyolysis when the muscle is restricted to use fatty acid as major energy source (Motojima and Seto, 2003).

PPAR α was also upregulated at the same range after treatment with all statins. PPAR α regulates the expression of genes involved in fatty acid beta-oxidation and is a major regulator of energy homeostasis. Activation of PPAR α also stimulates fatty acid oxidation and peroxisome proliferation (PP). Martin *et al.* reported that GGPP pathways is implicated in the activation of PPAR α induced by statins (Martin *et al.*, 2001). Others lipid lowering agents, like fibrates, well-known synthetic agonists of PPAR α , also cause rhabdomyolysis in patients (Poels and Gabreels, 1993; Hodel, 2002).

In summary, the gene expression data obtained after in vitro incubation of hSkMCs with statins were very similar to those obtained after in vivo treatment of monkeys. The results the results help to validate the current in vitro model. Furthermore they showed great usefulness in the interpretation of the mechanisms of toxicity.

4 SUMMARY

The HMG-CoA reductase inhibitors SIM, LOV, ATV, PRA, FV and NKS were investigated for their effects on human SkMCs. We were able to demonstrate that statins can induce oxidative stress (ROS formation, GSH-depletion, TBARS), apoptosis ($\Delta\psi$, caspase-3 activity, nuclear morphology) and necrosis (LDH-leakage) in hSkMCs. After incubation with statins, the sequence of cellular events starts by the increased formation of ROS (30 min) followed by caspase-3 activation (2-4 hours) and necrosis (LDH-leakage) and formation of condensed and fragmented nuclei after 24-72 hours. It was shown that antioxidants (NAC, DTT, TPGS, M-2 and M-3) and the HMG-CoA reductase downstream metabolites (MVA, F, FPP, GG and GGPP) protected against statin-induced ROS formation, caspase-3 activation and partially from necrosis. The caspase-3 inhibitor Ac-DEVD-CHO rescues cells partially from necrosis.

These results suggest that the statin-induced necrosis is HMG-CoA dependent and occurs secondary to apoptosis, which by decrease of ATP is driven into necrosis. The increase of ATP observed at low concentrations and early time points suggest an increased glycolytic activity. This was confirmed by increased PDK-4 gene expression and increased PFK2/F-2,6-BPase expression both activator of glycolysis. Glycolysis was also confirmed for some statins by increased cellular lactate concentrations. The consequence of PDK-4 mediated pyruvate dehydrogenase inactivation is the metabolic switching from fatty acid to amino acid from proteins as energy source.

The oxidative stress hypothesis was further supported by the induction of the FOXO3A transcription factor, which is involved in regulating MnSOD-2 expression in the mitochondrion. The mechanism by which statins produce ROS is still not resolved. There is an indirect evidence from our experiments as well as from the literature, that immediately after the statin treatment, intracellular Ca^{2+} is mobilized due to HMG-CoA reductase inhibition, which after mitochondrial uptake could lead to increased ROS formation.

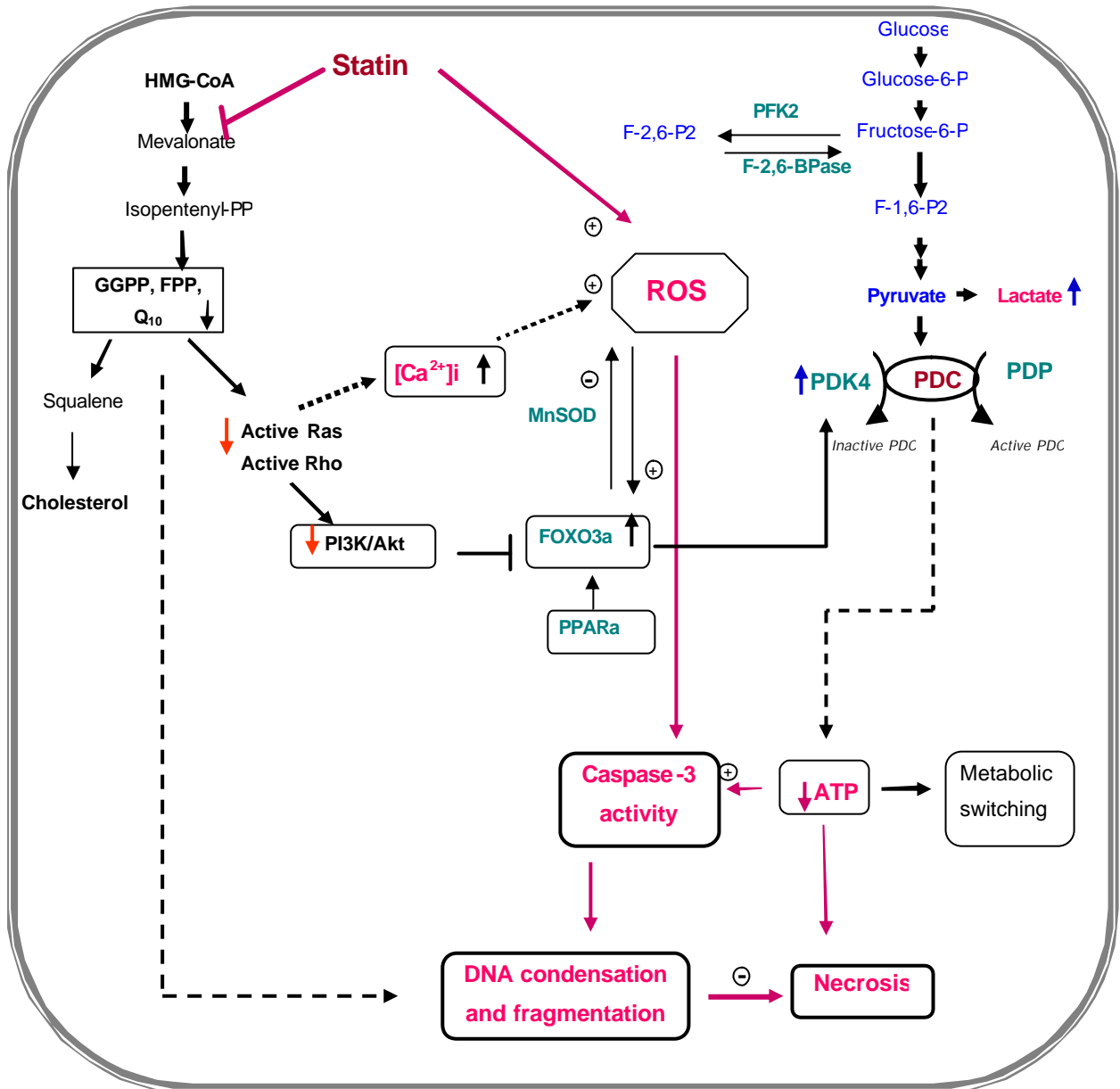


Fig. 48: Molecular hypothesis of statin-induced myopathy.

HMG-CoA reductase pathway: black, glycolysis blue, regulated genes following SkMCs treatment with statin: green cellular events induced by statin: red

5 ZUSAMMENFASSUNG

Die Hydroxymethylglutaryl-CoenzymA-(HMG-CoA)-Reduktaseinhibitoren Simvastatin, Lovastatin, Atorvastatin, Pravastatin, Fluvastatin und Pitavastatin wurden im Hinblick auf ihre Wirkungen auf humane Skelettmuskelzellen untersucht. Wir waren in der Lage zu zeigen, dass Statine oxidativen Stress (Dichlorofluoresceindiacetat, Glutathion-Depletierung, Thiobarbitursäure-reaktive Substanzen), Apoptose (mitochondriales Membranpotential $\Delta\psi_m$, Caspase-3, Kernmorphologie) und Nekrose (Laktatdehydrogenase (LDH)-Verlust) in humanen Skelettmuskelzellen auslösen können. Die Abfolge der zellulären Ereignisse nach Inkubation mit Statinen begann mit erhöhter Bildung reaktiver Sauerstoffspezies (ROS) (30 Min.), gefolgt von Caspase-3-Aktivierung (2-4 Std.) und Nekrose (LDH -Verlust) und kondensierten und fragmentierten Kernen nach 24-72 Std. Es konnte gezeigt werden, dass Antioxidantien (N-Acetylcystein, Dithiothreitol, DL-8-Tocopherol-polyethylenglykol-1000-succinat, die Fluvastatin-Metabolite M1 und M3) und die von im Signalweg der HMG-Co A-Reduktase abwärts gelegenen Enzymen gebildeten Metabolite (Mevalonsäure, Farnesol, Farnesylpyrophosphat, Geranylgeraniol und Geranylgeraniolpyrophosphat) eine Schutzwirkung gegen die statin-induzierte ROS-Bildung, Caspase-3-Aktivierung und teilweise auch gegen die beobachtete Nekrose haben. Der eingesetzte Caspase-3-Inhibitor schützt die Zellen ebenfalls partiell gegen Nekrose.

Diese Ergebnisse legen nahe, dass die statin-induzierte Nekrose ein HMG-Co A-Reduktase abhängiger Sekundärprozess der Apoptose ist, wobei Adenosintriphosphat (ATP)-Depletion das Gleichgewicht in Richtung der Nekrose verschieben kann. Die Erhöhung des ATP-Levels, die bei niedrigen Konzentrationen und frühen Zeitpunkten beobachtet wurde, ist ein Hinweis auf erhöhte glykolytische Aktivität. Dies wurde durch erhöhte Pyruvatdecarboxylase-Kinase-4(PDK-4) Genexpression und erhöhte Phosphofruktokinase2/Fruktose-2,6-bisphosphatase-Expression bestätigt, die beide eine erhöhte glykolytische Aktivität auslösen können. Die Konsequenz der PDK-4-vermittelten Pyruvatdehydrogenase-Inaktivierung ist die metabolische Umstellung der Energierquellen von Fettsäuren hin zu Aminosäuren aus dem Proteinabbau.

Die Hypothese, dass oxidativer Stress beteiligt ist, wurde weiterhin durch die Induktion des Transkriptionsfaktors Forhead box O3A auf mRNA-Ebene untermauert, der an der Regulation der Mangan-Superoxiddismutase-2 beteiligt ist. Der Mechanismus, wie Statine ROS produzieren können, ist noch nicht geklärt. Es gibt indirekte Hinweise- sowohl aus unseren Experimenten als auch aus der Literatur –, dass unmittelbar nach Statin-Behandlung intrazelluläres Calcium mobilisiert wird, wodurch nach einer stattgefundenen mitochondrialer Aufnahme es zu erhöhter ROS-Bildung kommen könnte.

6 REFERENCES

Alvarez de Sotomayor and Andriantsitohaina (2001) Simvastatin and Ca²⁺ signaling in endothelial cells: involvement of rho protein. *Biochem Biophys Res Commun.* 19;280(2):486-90

Anzueto A, Andrade FH, Maxwell LC, Levine SM, Lawrence RA, Gibbons WJ, Jenkinson SG (1992) Resistive breathing activates the glutathione redox cycle and impairs performance of rat diaphragm. *J Appl Physiol.* 72(2):529-34

Arends MJ, Wyllie AH (1991) Apoptosis: mechanisms and roles in pathology. *Int Rev Exp Pathol* 32:223-254

Armstrong RB, Warren GL, Warren JA (1991) Mechanisms of exercise-induced muscle fiber injury. *Sports Med.* 12(3):184-207

Bae GU, Seo DW, Kwon HK, Lee HY, Hong S, Lee ZW, Ha KS, Lee HW, Han JW (1999) Hydrogen peroxide activates p70(S6k) signaling pathway. *J Biol Chem.* 274(46):32596-602

Baker MA, Cerniglia GJ and Zaman A (1990) Microtiter plate assay for the measurement of glutathione and glutathione disulfide in large numbers of biological samples. *Anal. Biochem.* 190: 360-365

Bakker-Arkema RG, Davidson MH, Goldstein RJ, Davignon J, Isaacsohn JL, Weiss SR, Keilson LM, Brown WV, Miller VT, Shurzinske LJ, Black DM (1996) Efficacy and safety of a new HMG-CoA reductase inhibitor, atorvastatin, in patients with hypertriglyceridemia. *JAMA.* 275(2):128-33

Bandoh T, Mitani H, Niihashi M, Kusumi Y, Ishikawa J, Kimura M, Totsuka T, Sakurai I, Hayashi S (1996) Inhibitory effect of fluvastatin at doses insufficient to lower serum lipids on the catheter-induced thickening of intima in rabbit femoral artery. *Eur J Pharmacol.* 315(1):37-42

Baynes JW (1991) Role of oxidative stress in development of complications in diabetes. *Diabetes.* 40(4):405-12

- Benford HL**, Frith JC, Auriola S, Monkkonen J, Rogers MJ (1999) Farnesol and geranylgeraniol prevent activation of caspases by aminobisphosphonates: biochemical evidence for two distinct pharmacological classes of bisphosphonate drugs. *Mol Pharmacol.* 56(1):131-40
- Bermingham RP**, Whitsitt TB, Smart ML, Nowak DP, Scalley RD (2000) Rhabdomyolysis in a patient receiving the combination of cerivastatin and gemfibrozil. *Am J Health Syst Pharm.* 57(5):461-464
- Beyer RE** (1992) An analysis of the role of coenzyme Q in free radical generation and as an antioxidant. *Biochem Cell Biol.* 1992; 70(6):390-403
- Bieri JG**, Corash L, Hubbard VS (1983) Medical uses of vitamin E. *N Engl J Med.* 308(18):1063-71
- Blum CB** (1994) Comparison of properties of four inhibitors of 3-hydroxy-3-methylglutaryl-coenzyme A reductase. *Am J Cardiol.* 1994; 73(14):3D-11D
- Boger RH** (2001) Drug interactions of the statins and consequences for drug selection. *Int J Clin Pharmacol Ther.* 39(9):369-82
- Bolego C**, Baetta R, Bellosta S, Corsini A, Paoletti R (2002) Safety considerations for statins. *Curr Opin Lipidol.* 13(6):637-44
- Bolego C**, Poli A, Cignarella A, Catapano AL, Paoletti R (2002) Novel statins: pharmacological and clinical results. *Cardiovascular Drugs Ther.* 16(3):251-7
- Borgers M**, Thone F, Van Reempts J, Verheyen F (1983) The role of calcium in cellular dysfunction. *Am J Emerg Med.* 1(2):154-61
- Boyde A**, Vesely P, Gray C, Jones SJ (1994) High temporal and spatial resolution studies of bone cells using real-time confocal reflection microscopy. *Scanning.* 16(5):285-94
- Bradford RH**, Shear CL, Chremos AN, Franklin FA, Nash DT, Hurley DP, Dujovne CA, Pool JL, Schnaper H, Hesney M, et al. (1991) Expanded clinical evaluation of lovastatin (EXCEL) study results: III. Efficacy in modifying lipoproteins and implications for managing patients with moderate hypercholesterolemia. *Am J Med.* 91(1B):18S-24S

- Brown AS**, Bakker-Arkema RG, Yellen L, Henley RW Jr, Guthrie R, Campbell CF, Koren M, Woo W, McLain R, Black DM (1998) Treating patients with documented atherosclerosis to National Cholesterol Education Program-recommended low-density-lipoprotein cholesterol goals with atorvastatin, fluvastatin, lovastatin and simvastatin. *J Am Coll Cardiol.* 32(3):665-672
- Brown MS**, Goldstein JL (1986) A receptor-mediated pathway for cholesterol homeostasis. *Science.* 232(4746):34-47
- Brown MS**, Goldstein JL (2004) Lowering plasma cholesterol by raising LDL receptors. 1981. *Atheroscler Suppl.* 5(3):57-9
- Brunet A**, Bonni A, Zigmond MJ, Lin MZ, Juo P, Hu LS, Anderson MJ, Arden KC, Blenis J, Greenberg ME (1999) Akt promotes cell survival by phosphorylating and inhibiting a Forkhead transcription factor. *Cell.* 96(6):857-68
- Casey PJ** and Seabra MC (1996) Protein prenyltransferases. *J Biol Chem.* 271(10):5289-92
- Caye-Vaugien C**, Krempf M, Lamarche P, Charbonnel B, Pieri J (1990) Determination of alpha-tocopherol in plasma, platelets and erythrocytes of type I and type II diabetic patients by high-performance liquid chromatography. *Int J Vitam Nutr Res.* 60(4):324-30
- Chandramohan V**, Jeay S, Pianetti S, Sonenshein G E (2004) Reciprocal control of Forkhead box O 3a and c-Myc via the phosphatidylinositol 3-kinase pathway coordinately regulates p27Kip1 levels. *J Immunol.* 172(9):5522-7
- Chesebro JH**, Zoldhelyi P, Fuster V (1991) Plaque disruption and thrombosis in unstable angina pectoris. *Am J Cardiol.* 68(12):9C-15C
- Cohen GM** (1997) Caspases: the executioners of apoptosis. *Biochem J.* 15;326 (Pt 1):1-16
- Cominacini L**, Garbin U, Pastorino AM, Fratta Pasini A, Campagnola M, De Santis A, Davoli A, Lo Cascio V (1994) Increased susceptibility of LDL to *in vitro* oxidation in patients with insulin-dependent and non-insulin-dependent diabetes mellitus. *Diabetes Res.* 26(4):173-84
- Cominacini L**, Pastorino AM, Garbin U, Campagnola M, de Santis A, Davoli A, Faccini G, Bertozzo L, Pasini F, Pasini AF, et al. (1994) The susceptibility of low-density lipoprotein to *in vitro* oxidation is increased in hypercholesterolemic patients. *Nutrition.* 10(6):527-31

- Cooper AJ**, Pulsinelli WA, Duffy TE. (1980) Glutathione and ascorbate during ischemia and postischemic reperfusion in rat brain. *J Neurochem.* 35(5):1242-5
- Coresh J**, Kwiterovich PO Jr. (1996) Small, dense low-density lipoprotein particles and coronary heart disease risk: A clear association with uncertain implications. *JAMA.* 276(11):914-5
- Corsini A**, Bellosta S, Baetta R, Fumagalli R, Paoletti R, Bernini F (2000) New insights into the pharmacodynamic and pharmacokinetic properties of statins. *Pharmacol Ther.* 1999 Dec;84(3):413-28. Review. Erratum in: *Pharmacol Ther.* 86(2):199
- Cox AD**, Hisaka MM, Buss JE, Der CJ (1992) Specific isoprenoid modification is required for function of normal, but not oncogenic, Ras protein. *Mol Cell Biol.* 12(6):2606-15
- Crouch SP**, Kozlowski R, Slater KJ, Fletcher J (1993) The use of ATP bioluminescence as a measure of cell proliferation and cytotoxicity. *J Immunol Methods.* 160(1):81-8
- Dayer-Berenson L** (1994) Rhabdomyolysis: a comprehensive guide. *ANNA J.* 21(1):15-8; quiz 19-20
- Dayton WR**, Schollmeyer JV, Chan AC, Allen CE (1979) Elevated levels of a calcium-activated muscle protease in rapidly atrophying muscles from vitamin E-deficient rabbits. *Biochim Biophys Acta.* 584(2):216-30
- Dean A** and Voss D (1999) Design and Analysis of Experiments. *Springer-Verlag, New York*
- Do TQ**, Schultz JR, Clarke CF (1996) Enhanced sensitivity of ubiquinone-deficient mutants of *Saccharomyces cerevisiae* to products of autoxidized polyunsaturated fatty acids. *Proc Natl Acad Sci U S A.* 93(15):7534-9
- Downton C**, Clark I (2003) Statins-the heart of the matter. *Nat Rev Drug Discov.* 2(5):343-4
- Draude G**, Hrboticky N, Lorenz RL (1999) The expression of the lectin-like oxidized low-density lipoprotein receptor (LOX-1) on human vascular smooth muscle cells and monocytes and its down-regulation by lovastatin. *Biochem Pharmacol.* 57(4):383-6

- Duncan CJ** (1978) Role of intracellular calcium in promoting muscle damage: a strategy for controlling the dystrophic condition. *Experientia*. 15;34(12):1531-5
- Dunnett CW** (1955) A multiple comparisons procedure for comparing several treatments with a control. *Journal of the American Statistical Association* 50, 1096-1121
- Dusi S**, Donini M, Rossi F (1995) Mechanisms of NADPH oxidase activation in human neutrophils: p67phox is required for the translocation of rac1 but not of rac2 from cytosol to the membranes. *Biochem J*. 308 (Pt 3):991-4
- Endo A**, Kuroda M (1976) Citrinin, an inhibitor of cholesterol synthesis. *J Antibiot (Tokyo)*. 29(8):841-3
- Endo A**, Kuroda M, Tsujita Y (1976) ML-236A, ML-236B, and ML-236C, new inhibitors of cholesterologenesis produced by *Penicillium citrinium*. *J Antibiot (Tokyo)*. 29(12):1346-8
- Endo A**, Tsujita Y, Kuroda M, Tanzawa K (1977) Inhibition of cholesterol synthesis in vitro and in vivo by ML-236A and ML-236B, competitive inhibitors of 3-hydroxy-3-methylglutaryl-coenzyme A reductase. *Eur J Biochem*. 77(1):31-6
- Epstein WW**, Lever D, Leining LM, Bruenger E, Rilling HC (1991) Quantitation of prenylcysteines by a selective cleavage reaction. *Proc Natl Acad Sci U S A*. 88(21):9668-70
- Ernster L**, Dallner G (1995) Biochemical, physiological and medical aspects of ubiquinone function. *Biochim Biophys Acta*. 1271(1):195-204
- Evans M**, Rees A (2002A) Effects of HMG-CoA reductase inhibitors on skeletal muscle: are all statins the same? *Drug Saf*. 25(9):649-63
- Evans M**, Rees A (2002B) The myotoxicity of statins. *Curr Opin Lipidol*. 13(4):415-20
- Evans WJ**, Cannon JG (1991) The metabolic effects of exercise-induced muscle damage. *Exerc Sport Sci Rev*. 19:99-125
- Fariss MW** (1990) Oxygen toxicity: unique cytoprotective properties of vitamin E succinate in hepatocytes. *Free Radic Biol Med*. 9(4):333-43

- Farmer JA** (2001) Learning from the cerivastatin experience. *Lancet*. 358(9291):1383-5
- Fielding PE**, Fielding CJ (1996) Intracellular transport of low density lipoprotein derived free cholesterol begins at clathrin-coated pits and terminates at cell surface caveolae. *Biochemistry*. 35(47):14932-8
- Flint OP**, Masters BA, Gregg RE, Durham SK (1997) HMG CoA reductase inhibitor-induced myotoxicity: pravastatin and lovastatin inhibit the geranylgeranylation of low-molecular-weight proteins in neonatal rat muscle cell culture. *Toxicol Appl Pharmacol*. 145(1):99-110
- Flint OP**, Masters BA, Gregg RE, Durham SK (1997) Inhibition of cholesterol synthesis by squalene synthase inhibitors does not induce myotoxicity *in vitro*. *Toxicol Appl Pharmacol*. 145(1):91-8
- Foulkes WD**, Sewry C, Calam J, Hodgson HJ (1991) Rhabdomyolysis after intramuscular iron-dextran in malabsorption. *Ann Rheum Dis*. 50(3):184-6
- Fuster V** (1995) Elucidation of the role of plaque instability and rupture in acute coronary events. *Am J Cardiol*. 76(9):24C-33C
- Garcia MJ**, Reinoso RF, Sanchez Navarro A, Prous JR (2003) Clinical pharmacokinetics of statins. *Methods Find Exp Clin Pharmacol*. 25(6):457-81
- Garnett WR** (1995) Interactions with hydroxymethylglutaryl-coenzyme A reductase inhibitors. *Am J Health Syst Pharm*. 52(15):1639-45
- Ginsberg HN**, Le NA, Short MP, Ramakrishnan R, Desnick RJ (1987) Suppression of apolipoprotein B production during treatment of cholesteryl ester storage disease with lovastatin. Implications for regulation of apolipoprotein B synthesis. *J Clin Invest*. 80(6):1692-7
- Gissel H**, Clausen T (2001) Excitation-induced Ca²⁺ influx and skeletal muscle cell damage. *Acta Physiol Scand*. 171(3):327-34
- Goldstein JL**, Brown MS (1990) Regulation of the mevalonate pathway. *Nature*. 343(6257):425-30

- Gommans IM**, Vlak MH, de Haan A, van Engelen BG (2002) Calcium regulation and muscle disease. *J Muscle Res Cell Motil.* 2002;23(1):59-63
- Gronroos E**, Andersson T, Schippert A, Zheng L, Sjolander A (1996) Leukotriene D4-induced mobilization of intracellular Ca²⁺ in epithelial cells is critically dependent on activation of the small GTP-binding protein Rho. *Biochem J.* 316 (Pt 1):239-45.
- Grub S**, Persohn E, Trommer WE, Wolf A (2000) Mechanisms of cyclosporine A-induced apoptosis in rat hepatocyte primary cultures. *Toxicol Appl Pharmacol.* 63(3):209-20
- Grundy SM** (1998) Consensus statement: Role of therapy with "statins" in patients with hypertriglyceridemia. *Am J Cardiol.* 81(4A):1B-6B
- Guijarro C**, Blanco-Colio LM, Ortego M, Alonso C, Ortiz A, Plaza JJ, Diaz C, Hernandez G, Egido J (1998) 3-Hydroxy-3-methylglutaryl coenzyme a reductase and isoprenylation inhibitors induce apoptosis of vascular smooth muscle cells in culture. *Circ Res.* 83(5):490-500
- Gutmann I**, Wahlefeld AW (1974) In Bergmeyer HU. *Methods of enzymatic analysis*, Verlag Chemie, Weinheim/Academic Press, Inc., New York and London, 2nd ed., vol3, pp.1464-1468
- Halliwell B**, Gutteridge JM (1986) Oxygen free radicals and iron in relation to biology and medicine: some problems and concepts. *Arch Biochem Biophys.* 246(2):501-14
- Hamer R** (1997) When exercise goes awry: exertional rhabdomyolysis. *South Med J.* 90(5):548-51
- Hampton MB**, Fadeel B, Orrenius S (1998) Redox regulation of the caspases during apoptosis. *Ann N Y Acad Sci.* 20; 854:328-35
- Hancock JF**, Cadwallader K, Paterson H, Marshall CJA (1991) CAAX or a CAAL motif and a second signal are sufficient for plasma membrane targeting of ras proteins. *EMBO J.* 10(13):4033-9
- Higuchi M**, Honda T, Proske RJ, Yeh ET (1998) Regulation of reactive oxygen species-induced apoptosis and necrosis by caspase 3-like proteases. *Oncogene.* 17(21):2753-60

- Hodel C** (2002) Myopathy and rhabdomyolysis with lipid-lowering drugs. *Toxicol Lett.* 128(1-3):159-68
- Holt S**, Reeder B, Wilson M, et al (1999) Increased lipid peroxidation in patients with rhabdomyolysis. *Lancet*, 353: 358-359
- Hsu I**, Spinler SA, Johnson NE (1995) Comparative evaluation of the safety and efficacy of HMG-CoA reductase inhibitor monotherapy in the treatment of primary hypercholesterolemia. *Ann Pharmacother.* 29(7-8):743-759
- Hussein O**, Schlezinger S, Rosenblat M, Keidar S, Aviram M (1997) Reduced susceptibility of low density lipoprotein (LDL) to lipid peroxidation after fluvastatin therapy is associated with the hypocholesterolemic effect of the drug and its binding to the LDL. *Atherosclerosis.* 128(1):11-8
- Iimura O**, Vrtovsnik F, Terzi F, Friedlander G (1997) HMG-CoA reductase inhibitors induce apoptosis in mouse proximal tubular cells in primary culture. *Kidney Int.* 52(4):962-72
- Imaeda A**, Aoki T, Kondo Y, Hori M, Ogata M, Obayashi H, Hasegawa G, Nakamura N, Tokuda K, Nishino H, Yoshikawa T, Kondo M (2001) Protective effects of fluvastatin against reactive oxygen species induced DNA damage and mutagenesis. *Free Radic Res.* 34(1):33-44
- Imaeda A**, Kaneko T, Aoki T, Kondo Y, Nakamura N, Nagase H, Yoshikawa T (2002) Antioxidative effects of fluvastatin and its metabolites against DNA damage in streptozotocin-treated mice. *Food Chem Toxicol.* 40(10):1415-22
- Imaeda A**, Tanigawa T, Aoki T, Kondo Y, Nakamura N, Yoshikawa T (2001) Antioxidative effects of fluvastatin and its metabolites against oxidative DNA damage in mammalian cultured cells. *Free Radic Res.* 35(6):789-801
- Inoue R**, Tanabe M, Kono K, Maruyama K, Ikemoto T, Endo M (2003) Ca²⁺-releasing effect of cerivastatin on the sarcoplasmic reticulum of mouse and rat skeletal muscle fibers. *J Pharmacol Sci.* 93(3):279-88
- Istvan ES**, Deisenhofer J (2000) The structure of the catalytic portion of human HMG-CoA reductase. *Biochim Biophys Acta.* 1529(1-3):9-18

Istvan ES, Palnitkar M, Buchanan SK, Deisenhofer (2000) Crystal structure of the catalytic portion of human HMG-CoA reductase: insights into regulation of activity and catalysis. *EMBO J.* 19(5):819-30

Johnson TE, Zhang X, Bleicher KB, Dysart G, Loughlin AF, Schaefer WH, Umbenhauer DR (2004) Statins induce apoptosis in rat and human myotube cultures by inhibiting protein geranylgeranylation but not ubiquinone. *Toxicol Appl Pharmacol.* 200(3):237-50

Jones BN, Gilligan JP (1983) α -Phthaldialdehyde precolumn derivatization and reversed-phase high-performance liquid chromatography of polypeptide hydrolysates and physiological fluids. *J Chromatogr.* 266:471-82

Jones DP, Kennedy FG (1983) In Larson A *et al.* (eds): Functions of glutathione: Biochemical, physiological, toxicological, and clinical aspects, New York, Raven Press, 109-116, 1983

Jung U, Zheng X, Yoon SO, Chung AS (2001) Se-methylselenocysteine induces apoptosis mediated by reactive oxygen species in HL-60 cells. *Free Radic Biol Med.* 31(4):479-89

Kaneider NC, Reinisch CM, Dunzendorfer S, Meierhofer C, Djanani A, Wiedermann CJ (2001) Induction of apoptosis and inhibition of migration of inflammatory and vascular wall cells by cerivastatin. *Atherosclerosis.* 158(1):23-33

Kashii Y, Uchida M, Kirito K, Tanaka M, Nishijima K, Toshima M, Ando T, Koizumi K, Endoh T, Sawada K, Momoi M, Miura Y, Ozawa K, Komatsu N (2000) A member of Forkhead family transcription factor, FKHL1, is one of the downstream molecules of phosphatidylinositol 3-kinase-Akt activation pathway in erythropoietin signal transduction. *Blood.* 96(3):941-9.

Khosravi-Far R, Cox AD, Kato K, Der CJ (1992) Protein prenylation: key to ras function and cancer intervention? *Cell Growth Differ.* 3(7):461-9

Knopp RH (1999) Drug treatment of lipid disorders. *N Engl J Med.* 341(7):498-511

Knopp RH, Zhu X, Bonet B (1994) Effects of estrogens on lipoprotein metabolism and cardiovascular disease in women. *Atherosclerosis.* 110 Suppl: S83-91

Kondo H, Miura M, Itokawa Y (1993) Antioxidant enzyme systems in skeletal muscle atrophied by immobilization. *Pflugers Arch.* 422(4):404-6

Laufs U, Endres M, Custodis F, Gertz K, Nickenig G, Liao JK, Bohm M (2000) Suppression of endothelial nitric oxide production after withdrawal of statin treatment is mediated by negative feedback regulation of rho GTPase gene transcription. *Circulation*. 102(25):3104-10

Laufs U, Gertz K, Huang P, Nickenig G, Bohm M, Dirnagl U, Endres M (2000) Atorvastatin upregulates type III nitric oxide synthase in thrombocytes, decreases platelet activation, and protects from cerebral ischemia in normocholesterolemic mice. *Stroke*. 31(10):2442-9

Laufs U, La Fata V, Plutzky J, Liao JK (1998) Upregulation of endothelial nitric oxide synthase by HMG CoA reductase inhibitors. *Circulation*. 97(12):1129-35

Lavy A, Brook GJ, Dankner G, Ben Amotz A, Aviram M (1991) Enhanced *in vitro* oxidation of plasma lipoproteins derived from hypercholesterolemic patients. *Metabolism*. (8):794-9

LeBel CP, Ischiropoulos H, Bondy SC (1992) Evaluation of the probe 2',7'-dichlorofluorescein as an indicator of reactive oxygen species formation and oxidative stress. *Chem Res Toxicol*. 5(2):227-31

Leist M, Nicotera P (1997) Breakthroughs and views. The shape of cell death. *Biochem Biophys Res Commun* 236:1-9

Leist M, Single B, Castoldi AF, Kuhnle S, Nicotera P (1997) Intracellular adenosine triphosphate (ATP) concentration: a switch in the decision between apoptosis and necrosis. *J Exp Med* 185:1481-1486

Lemaire C, Andreau K, Souvannavong V, Adam A (1998) Inhibition of caspase activity induces a switch from apoptosis to necrosis. *FEBS Lett*. 425(2):266-70

Leonhardt W, Kurktschiev T, Meissner D, Lattke P, Abletshauser C, Weidinger G, Jaross W, Hanefeld M (1997) Effects of fluvastatin therapy on lipids, antioxidants, oxidation of low density lipoproteins and trace metals. *Eur J Clin Pharmacol*. 53(1):65-9

Levy RI, Troendle AJ, Fattu JM (1993) A quarter century of drug treatment of dyslipoproteinemia, with a focus on the new HMG-CoA reductase inhibitor fluvastatin. *Circulation*. 87(4 Suppl):III45-53

- Levy Y**, Leibowitz R, Aviram M, Brook JG, Cogan U (1992). Reduction of plasma cholesterol by lovastatin normalizes erythrocyte membrane fluidity in patients with severe hypercholesterolaemia. *Br J Clin Pharmacol*. 34(5):427-30
- Libby P** (1995) Molecular bases of the acute coronary syndromes. *Circulation*. 91(11):2844-50
- Libby P**, Geng YJ, Sukhova GK, Simon DI, Lee RT (1997) Molecular determinants of atherosclerotic plaque vulnerability. *Ann N Y Acad Sci*. 811:134-42; discussion 142-5
- Lijnen P**, Celis H, Fagard R, Staessen J, Amery A (1994) Influence of cholesterol lowering on plasma membrane lipids and cationic transport systems. *J Hypertens*. 12(1):59-64
- Maeda H**, Hori S, Ohizumi H, Segawa T, Kakehi Y, Ogawa O, Kakizuka A (2004) Effective treatment of advanced solid tumors by the combination of arsenic trioxide and L-buthionine-sulfoximine. *Cell Death Differ*. 11(7):737-46
- Maltese WA**, Sheridan KM (1987) Isoprenylated proteins in cultured cells: subcellular distribution and changes related to altered morphology and growth arrest induced by mevalonate deprivation. *J Cell Physiol*. 133(3):471-81
- Maltz HC**, Balog DL, Cheigh JS (1999) Rhabdomyolysis associated with concomitant use of atorvastatin and cyclosporine. *Ann Pharmacother*. 33(11):1176-1179
- Marais GE**, Larson KK (1990) Rhabdomyolysis and acute renal failure induced by combination lovastatin and gemfibrozil therapy. *Ann Intern Med*. 112(3):228-230
- Marcelli M**, Cunningham GR, Haidacher SJ, Padayatty SJ, Sturgis L, Kagan C, Denner L (1998) Caspase-7 is activated during lovastatin-induced apoptosis of the prostate cancer cell line LNCaP. *Cancer Res*. 58(1):76-83
- Martin G**, Duez H, Blanquart C, Berezowski V, Poulain P, Fruchart JC, Najib-Fruchart J, Glineur C, Staels B (2001) Statin-induced inhibition of the Rho-signaling pathway activates PPARalpha and induces HDL apoA-I. *J Clin Invest*. 107(11):1423-32
- Martinez-Gonzalez J**, Raposo B, Rodriguez C, Badimon L (2001) 3-hydroxy-3-methylglutaryl coenzyme a reductase inhibition prevents endothelial NO synthase downregulation by atherogenic levels of native LDLs: balance between transcriptional and posttranscriptional regulation. *Arterioscler Thromb Vasc Biol*. 21(5):804-9

- Masters BA**, Palmoski MJ, Flint OP, Gregg RE, Wang-Iverson D, Durham SK (1995) In vitro myotoxicity of the 3-hydroxy-3-methylglutaryl coenzyme A reductase inhibitors, pravastatin, lovastatin, and simvastatin, using neonatal rat skeletal myocytes. *Toxicol Appl Pharmacol.* 131(1):163-74
- Maxa JL**, Melton LB, Ogu CC, Sills MN, Limanni A (2002) Rhabdomyolysis after concomitant use of cyclosporine, simvastatin, gemfibrozil, and itraconazole. *Ann Pharmacother.* 36(5):820-3
- Mayer B**, Oberbauer R (2003) Mitochondrial regulation of apoptosis. *News Physiol Sci.* 18:89-94
- McCabe MJ Jr**, Nicotera P, Orrenius S (1992) Calcium-dependent cell death. Role of the endonuclease, protein kinase C, and chromatin conformation. *Ann N Y Acad Sci.* 663:269-78
- McConkey DJ**, Hartzell P, Nicotera P, Orrenius S (1989) Calcium-activated DNA fragmentation kills immature thymocytes. *FASEB J.* 3(7):1843-9
- McTaggart F**, Buckett L, Davidson R, Holdgate G, McCormick A, Schneck D, Smith G, Warwick M (2001) Preclinical and clinical pharmacology of Rosuvastatin, a new 3-hydroxy-3-methylglutaryl coenzyme A reductase inhibitor. *Am J Cardiol.* 87(5A):28B-32B
- McTavish D**, Sorkin EM (1991) Pravastatin. A review of its pharmacological properties and therapeutic potential in hypercholesterolaemia. *Drugs.* 42(1):65-89
- Mirabelli F**, Salis A, Vairetti M, Bellomo G, Thor H, Orrenius S (1989) Cytoskeletal alterations in human platelets exposed to oxidative stress are mediated by oxidative and Ca²⁺-dependent mechanisms. *Arch Biochem Biophys.* 270(2):478-88
- Mitani H**, Bandoh T, Ishikawa J, Kimura M, Totsuka T, Hayashi S (1996) Inhibitory effects of fluvastatin, a new HMG-CoA reductase inhibitor, on the increase in vascular ACE activity in cholesterol-fed rabbits. *Br J Pharmacol.* 119(6):1269-75
- Morita I**, Sato I, Ma L, Murota S (1997) Enhancement of membrane fluidity in cholesterol-poor endothelial cells pre-treated with simvastatin. *Endothelium.* 5(2):107-13.

Motojima K, Passilly P, Peters JM, Gonzalez FJ, Latruffe N (1998) Expression of putative fatty acid transporter genes are regulated by peroxisome proliferator-activated receptor alpha and gamma activators in a tissue- and inducer-specific manner. *J Biol Chem.* 273(27):16710-4

Motojima K, Seto K (2003) Fibrates and statins rapidly and synergistically induce pyruvate dehydrogenase kinase 4 mRNA in the liver and muscles of mice. *Biol Pharm Bull.* 26(7):954-8

Muller C, Kiehl MG, van de Loo J, Koch OM (1999) Lovastatin induces p21WAF1/Cip1 in human vascular smooth muscle cells: influence on protein phosphorylation, cell cycle, induction of apoptosis, and growth inhibition. *Int J Mol Med.* 3(1):63-8

Nakahara K, Yada T, Kuriyama M, Osame M (1994) Cytosolic Ca²⁺ increase and cell damage in L6 rat myoblasts by HMG-CoA reductase inhibitors. *Biochem Biophys Res Commun.* 202(3):1579-85

Nakashima A, Ohtawa M, Iwasaki K, Wada M, Kuroda N, Nakashima K (2001) Inhibitory effects of fluvastatin and its metabolites on the formation of several reactive oxygen species. *Life Sci.* 69(12):1381-9

Nakashima A, Ohtawa M, Masuda N, Morikawa H, Bando T (1999) Antioxidative effects of fluvastatin, and its major metabolites. *Yakugaku Zasshi.* 119(1):93-9

Negre-Aminou P, van Vliet AK, van Erck M, van Thiel GC, van Leeuwen RE, Cohen LH (1997) Inhibition of proliferation of human smooth muscle cells by various HMG-CoA reductase inhibitors; comparison with other human cell types. *Biochim Biophys Acta.* 1345(3):259-68

Nicholson DW, Thornberry NA (1997) Caspases: killer proteases. *Trends Biochem Sci.* 22(8):299-306

Nicotera P, Zhivotovsky B, Orrenius S (1994) Nuclear calcium transport and the role of calcium in apoptosis. *Cell Calcium.* 16(4):279-88

Nishimoto T, Tozawa R, Amano Y, Wada T, Imura Y, Sugiyama Y (2003) Comparing myotoxic effects of squalene synthase inhibitor, T91485, and 3-hydroxy-3-methylglutaryl

coenzyme A (HMG-CoA) reductase inhibitors in human myocytes. *Biochem Pharmacol.* 66(11):2133-9

Noctor G, Foyer CH (1998) Simultaneous measurement of foliar glutathione, gamma-glutamylcysteine, and amino acids by high-performance liquid chromatography: comparison with two other assay methods for glutathione. *Anal Biochem.* 264(1):98-110

Obatomi DK, Blackburn RO, Bach PH (2001) Effects of the calcium channel blocker verapamil and sulphhydryl reducing agent dithiothreitol on atractyloside toxicity in precision-cut rat renal cortical and liver slices. *Food Chem Toxicol.* 39(10):1013-21

Ogata Y, Takahashi M, Takeuchi K, Ueno S, Mano H, Ookawara S, Kobayashi E, Ikeda U, Shimada K (2002) Fluvastatin induces apoptosis in rat neonatal cardiac myocytes: a possible mechanism of statin-attenuated cardiac hypertrophy. *J Cardiovasc Pharmacol.* 40(6):907-15

Olsson AG (2001) Statin therapy and reductions in low-density lipoprotein cholesterol: initial clinical data on the potent new statin Rosuvastatin. *Am J Cardiol.* 87(5A):33B-36B

Orrenius S, McCabe MJ Jr, Nicotera P (1992) Ca(2+)-dependent mechanisms of cytotoxicity and programmed cell death. *Toxicol Lett.* 64-65 Spec No:357-64

Padayatty SJ, Marcelli M, Shao TC, Cunningham GR (1997) Lovastatin-induced apoptosis in prostate stromal cells. *J Clin Endocrinol Metab.* 82(5):1434-9

Pasternak RC, Smith SC Jr, Bairey-Merz CN, Grundy SM, Cleeman JI, Lenfant C (2002) ACC/AHA/NHLBI clinical advisory on the use and safety of statins. *J Am Coll Cardiol.* 40(3):567-72

Patrono C, FitzGerald GA (1997) Isoprostanes: potential markers of oxidant stress in atherothrombotic disease. *Arterioscler Thromb Vasc Biol.* (11):2309-15

Pattwell D, McArdle A, Griffiths RD, Jackson MJ (2001) Measurement of free radical production by *in vivo* microdialysis during ischemia/reperfusion injury to skeletal muscle. *Free Radic Biol Med.* 30(9):979-85

Pawley JB, Erlandsen SL (1989) The case for low voltage high resolution scanning electron microscopy of biological samples. *Scanning Microsc Suppl.* 3:163-78

- Pietsch A**, Erl W, Lorenz RL (1996) Lovastatin reduces expression of the combined adhesion and scavenger receptor CD36 in human monocytic cells. *Biochem Pharmacol.* 52(3):433-9
- Pilkis SJ**, Claus TH, Kurland IJ and Lange AJ (1995) 6-Phosphofructo-2-kinase/fructose-2, 6-bisphosphatase: a metabolic signaling enzyme. *Annu. Rev. Biochem.* 64: 799–835
- Poels PJ**, Gabreels FJ (1993) Rhabdomyolysis: a review of the literature. *Clin Neurol Neurosurg.* 95(3):175-92
- Ragusa RJ**, Chow CK, Porter JD (1997) Oxidative stress as a potential pathogenic mechanism in an animal model of Duchenne muscular dystrophy. *Neuromuscul Disord.* 7(6-7):379-86
- Reszka AA**, Halasy-Nagy JM, Masarachia PJ, Rodan GA (1999) Bisphosphonates act directly on the osteoclast to induce caspase cleavage of mst1 kinase during apoptosis. A link between inhibition of the mevalonate pathway and regulation of an apoptosis-promoting kinase. *J Biol Chem.* 274(49):34967-73
- Rice-Evans C**, Burdon R (1993) Free radical-lipid interactions and their pathological consequences. *Prog Lipid Res.* 32(1):71-110
- Rice-Evans C**, Green E, Paganga G, Cooper C, Wrigglesworth J (1993) Oxidised low density lipoproteins induce iron release from activated myoglobin. *FEBS Lett.* 326(1-3):177-82
- Rice-Evans C**, McCarthy P, Hallinan T, Green NA, Gor J, Diplock AT (1989) Iron overload and the predisposition of cells to antioxidant consumption and peroxidative damage. *Free Radic Res Commun.* 7(3-6):307-13
- Richter C** (1993) Pro-oxidants and mitochondria Ca^{2+} : their relationship to apoptosis and oncogenesis. *FEBS Lett.* 325:104-107
- Richter C**, Kass GE (1991) Oxidative stress in mitochondria: its relationship to cellular Ca^{2+} homeostasis, cell death, proliferation, and differentiation. *Chem Biol Interact.* 77(1):1-23
- Rinckel LA**, Faris SL, Hitt ND, Kleinberg ME (1999) Rac1 disrupts p67phox/p40phox binding: a novel role for Rac in NADPH oxidase activation. *Biochem Biophys Res Commun.* 263(1):118-22

- Rodriguez I**, Matsuura K, Ody C, Nagata S, Vassalli P (1996) Systemic injection of a tripeptide inhibits the intracellular activation of CPP32-like proteases *in vivo* and fully protects mice against Fas-mediated fulminant liver destruction and death. *J Exp Med* 184:2067-2072
- Romano M**, Mezzetti A, Marulli C, Ciabattini G, Febo F, Di Lenno S, Roccaforte S, Vigneri S, Nubile G, Milani M, Davi G (2000) Fluvastatin reduces soluble P-selectin and ICAM-1 levels in hypercholesterolemic patients: role of nitric oxide. *J Investig Med.* 48(3):183-9
- Roth M** (1971) Fluorescence reaction for amino acids. *Anal Chem.* 43(7):880-2
- Rousseau GG** and Hue L (1993) Mammalian 6-phosphofructo-2-kinase/fructose-2,6-bisphosphatase: a bifunctional enzyme that controls glycolysis. *Prog. Nucleic Acid Res. Mol. Biol.* 45: 99–127
- Rudge MF**, Duncan CJ (1984) Comparative studies on the role of calcium in triggering subcellular damage in cardiac muscle. *Comp Biochem Physiol A.* 1984;77(3):459-68
- Salvesen GS**, Dixit VM (1997) Caspases: intracellular signaling by proteolysis. *Cell* 91(4):443-446
- Sauret JM**, Marinides G, Wang GK (2002) Rhabdomyolysis. *Am Fam Physician.* 65(5):907-12
- Schachter M** (2005) Chemical, pharmacokinetic and pharmacodynamic properties of statins: an update. *Fundamental & Clinical Pharmacology* 19 (1), 117-125
- Schmitz G**, Drobnik W (2003) Pharmacogenomics and Pharmacogenetics of cholesterol-Lowering Therapy *Clin Chem Lab Med* 41(4): 581-589
- Sen CK** (1995) Oxidants and antioxidants in exercise. *J Appl Physiol.* 79(3):675-86.
- Sen CK**, Atalay M, Agren J, Laaksonen DE, Roy S, Hanninen O (1997) Fish oil and vitamin E supplementation in oxidative stress at rest and after physical exercise. *J Appl Physiol.* 83(1):189-95
- Sen CK**, Atalay M, Hanninen O (1994) Exercise-induced oxidative stress: glutathione supplementation and deficiency. *J Appl Physiol.* 77(5):2177-87

- Sen CK**, Rankinen T, Vaisanen S, Rauramaa R (1994) Oxidative stress after human exercise: effect of N-acetylcysteine supplementation. *J Appl Physiol*. 1994 Jun; 76(6):2570-7. Erratum in: *J Appl Physiol* 1994; 77(6): following v. *J Appl Physiol* 77(5)
- Sies H** (1991) Oxidative stress: from basic research to clinical application. *Am J Med*. 91(3C):31S-38S.
- Sinzinger H** (2000) Does vitamin E beneficially affects muscle pains during HMG-Co-enzyme-A-reductase inhibitors without CK-elevation? *Atherosclerosis*, 149:225
- Sinzinger H**, Lupattelli G, Chehne F (2000) Increased lipid peroxidation in a patient with CK-elevation and muscle pain during statin therapy. *Atherosclerosis*, 153:255-256
- Sinzinger H**, Wolfram R, Peskar BA (2002) Muscular side effects of statins. *J Cardiovasc Pharmacol*, 40:163-171
- Staffa JA**, Chang J, Green L (2002) Cerivastatin and reports of fatal rhabdomyolysis. *N Engl J Med*. 346(7):539-40
- Supinski G**, Nethery D, Stofan D, DiMarco A. (1999) Extracellular calcium modulates generation of reactive oxygen species by the contracting diaphragm. *J Appl Physiol*. 87(6):2177-85
- Takemoto M**, Node K, Nakagami H, Liao Y, Grimm M, Takemoto Y, Kitakaze M, Liao JK (2001) Statins as antioxidant therapy for preventing cardiac myocyte hypertrophy. *J Clin Invest*. 108(10):1429-37
- Thompson PD**, Clarkson P, Karas RH (2003) Statin-associated myopathy. *JAMA*. 289(13):1681-90
- Thompson PD**, Gadaleta PA, Yurgalevitch S, Cullinane E, Herbert PN (1991) Effects of exercise and lovastatin on serum creatine kinase activity. *Metabolism*. 40(12):1333-6
- Thompson PD**, Zmuda JM, Domalik LJ, Zimet RJ, Staggars J, Guyton JR (1997) Lovastatin increases exercise-induced skeletal muscle injury. *Metabolism*. 46(10):1206-10

- Tietze T** (1969) Enzymatic method for quantitative determination of nanogram amounts of total and oxidized glutathione: Applications to mammalian blood and other tissues, *Anal. Biochem.* 27: 502-522
- Tobert JA** (1987) New developments in lipid-lowering therapy: the role of inhibitors of hydroxymethylglutaryl-coenzyme A reductase. *Circulation.* 76(3):534-8
- Tobert JA** (2003) Lovastatin and beyond: the history of the HMG-CoA reductase inhibitors. *Nat Rev Drug Discov.* 2(7):517-26
- Tran H**, Brunet A, Grenier JM, Datta SR, Fornace AJ Jr, DiStefano PS, Chiang LW, Greenberg ME (2002) DNA repair pathway stimulated by the forkhead transcription factor FOXO3a through the Gadd45 protein. *Science.*296(5567):530-4
- Tsutsui H**, Ide T, Hayashidani S, Suematsu N, Shiomi T, Wen J, Nakamura Ki, Ichikawa K, Utsumi H, Takeshita A (2001) Enhanced generation of reactive oxygen species in the limb skeletal muscles from a murine infarct model of heart failure. *Circulation.* 104(2):134-6
- Tyson CA**, Green CE (1987) Cytotoxicity measures: Choice and methods. In: Rauckmann EJ, Padilla GM, eds. *The isolated hepatocyte, use in Toxicology and Xenobiotic Biotransformation.* Orlando: Academic Press, 119-158
- Umetani N**, Kanayama Y, Okamura M, Negoro N, Takeda T (1996) Lovastatin inhibits gene expression of type-I scavenger receptor in THP-1 human macrophages. *Biochim Biophys Acta.* 1303(3):199-206
- Vaknin H**, Bar-Akiva A, Ovadia R, Nissim-Levi A, Forer I, Weiss D, Oren-Shamir M (2005) Active anthocyanin degradation in *Brunfelsia calycina* (yesterday-today-tomorrow) flowers. *Planta*
- Van Aelst L**, D'Souza-Schorey C (1997) Rho GTPases and signaling networks. *Genes Dev.* 11(18):2295-322
- Van Dam PS**, Van Asbeck BS, Erkelens DW, Marx JJ, Gispen WH, Bravenboer B (1995) The role of oxidative stress in neuropathy and other diabetic complications. *Diabetes Metab Rev.* 11(3):181-92.

- Van Rij AM**, Thomson CD, McKenzie JM, Robinson MF (1979) Selenium deficiency in total parenteral nutrition. *Am J Clin Nutr.* 32(10):2076-85
- Vandeputte C**, Guizon I., Genestie-Denis, I., Vannier, B. and Lorenzon, G (1994) A microtiter plate assay for total glutathione and glutathione disulfide contents in cultured/isolated cells: Performance study of a new miniaturized protocol. *Cell Biol. Toxicol.* 10:415-421
- Vaughan CJ**, Gotto AM Jr, Basson CT (2000) The evolving role of statins in the management of atherosclerosis. *J Am Coll Cardiol.* 35(1):1-10
- Vega GL** and Grundy SM (1998) Effect of statins on metabolism of apo-B-containing lipoproteins in hypertriglyceridemic men. *Am J Cardiol.* 81(4A):36B-42B
- Wassmann S**, Laufs U, Baumer AT, Muller K, Ahlbory K, Linz W, Itter G, Rosen R, Bohm M, Nickenig G (2001) HMG-CoA reductase inhibitors improve endothelial dysfunction in normocholesterolemic hypertension via reduced production of reactive oxygen species. *Hypertension.* 37(6):1450-7
- Weiss R H**, Ramirez A L and Joo A (1999) Short-term pravastatin mediates growth inhibition and apoptosis, independently of Ras, via the signaling proteins p27Kip1 and P13 kinase. *J Am Soc Nephrol.* 10(9):1880-90
- Welder AA**, Acosta D (1994) Membrane integrity and function. In: Tyson CA, Frazier JM. *Methods in Toxicology.* Vol 1. Part B. San Diego: Academic Press, 46-49
- Werner N**, Nickenig G, Laufs U (2002) Pleiotropic effects of HMG-CoA reductase inhibitors. *Basic Res Cardiol.* 97(2):105-16
- Williams D**, Feely J (2002) Pharmacokinetic-pharmacodynamic drug interactions with HMG-CoA reductase inhibitors. *Clin Pharmacokinet.* 41(5):343-70
- Witting PK**, Willhite CA, Davies MJ, Stocker R (1999) Lipid oxidation in human low-density lipoprotein induced by metmyoglobin/H₂O₂: involvement of alpha-tocopheroxyl and phosphatidylcholine alkoxyl radicals. *Chem Res Toxicol.* 12(12):1173-81
- Wolf A**, Trendelenburg CF, Diez-Fernandez C, Prieto P, Houy S, Trommer WE, Cordier A. (1997) Cyclosporine A-induced oxidative stress in rat hepatocytes. *J Pharmacol Exp Ther.* 280(3):1328-34

Wong WW, Tan MM, Xia Z, Dimitroulakos J, Minden MD, Penn LZ (2001) Cerivastatin triggers tumor-specific apoptosis with higher efficacy than lovastatin. *Clin Cancer Res.* 7(7):2067-75

Wu EY, Smith MT, Bellomo G, Di Monte D (1990) Relationships between the mitochondrial transmembrane potential, ATP concentration, and cytotoxicity in isolated rat hepatocytes. *Arch Biochem Biophys.* 282(2):358-62

Yagi K (1994) Lipid peroxides in hepatic, gastrointestinal, and pancreatic diseases. *Adv Exp Med Biol.* 366:165-9

Yamamoto A Kojima S, Shiba-Harada M, Kawaguchi A, Hatanaka K (1992) Assessment of the biocompatibility and long term effect of LDL-apheresis by dextran sulphate-cellulose column. *Int J Artif Organs.* 16: 177

Zerba E, Komorowski TE, Faulkner JA (1990) Free radical injury to skeletal muscles of young, adult, and old mice. *Am J Physiol.* 258 (3 Pt 1):C429-35

5 APPENDIX

DEDICATION AND ACKNOWLEDGEMENTS

I dedicate this work to my late mother, who instilled in me the spirit to weather all things, good or bad, through dedication and perseverance. To my father, for his support, tolerance and encouragement through the years.

There are many people who through their generosity and knowledge have made important contributions to this dissertation. It would be impossible to list everyone who contributed, or to adequately list the extent of the contributions for those who are mentioned.

I am especially grateful to Dr. U. Schramm for her collaboration, discussion, invaluable advice, patience during this work and for her constructive criticism and useful remarks during the preparation of the manuscript.

My special thanks go to M. Schwald for her patience and her competent technical support in the lab. Her experience and organizing skills are only exceeded by her ability to create a friendly working atmosphere.

My thanks go also to B. Greiner for her brave struggle with the confocal microscope to produce usable results with hSkMCs. I am also very grateful to Dr. F. Staube and T. Da Cuhna for helping me with the Cellomic method. I thank Dr. O. Grenet and M. Gilly for providing me the gene expression data.

I would also want to thank F. Voelker for providing me the pathology images of rhabdomyolysis.

I wish to thank R. Young for the skilful revision of the english language of the manuscript.

I extend many thanks to my colleagues; C. Strupp, A. Nussler, J.M. Grenet, C. Borner for their assistance during this work

Finally, I would like to thank my family and friends for their intellectual and emotional support which helped me during the course of my degree and this dissertation.

CURRICULUM VITAE

Personal data

Leopold Ndountse Tchabda
 Bahnweg 35 (Hintereingang)
 79576 Weil am Rhein

Birthday: 12. April 1971
 Birth-place: Mbanga, KAMERUN
 Nationality: Cameroon

Education background

- 1976-1983 Primary school „St. Andre Mbanga gare“, Cameroon
- 1984-1988 High school „C.E.S“ Mbanga, Cameroon
- 1989-1991 Nkongsamba high school, Cameroon, GCE level (Baccalaureat)
- 1992-1995 Department of biochemistry, University of Yaounde1, Cameroon, B.SC
- 1995-1997 Department of biochemistry, University of Yaounde1, Cameroon
Research Laboratory: Biotechnology Centre/Department of medicine and biomedical sciences, University of Yaoundé 1 (Cameroon)
Master advisors: Prof. Dr. Rose Léké/ Prof. Dr. V. Titandji
- 2002-2005 Department of chemistry/Biochemistry, University of Kaiserslautern, Germany
Research Laboratory: Novartis Pharma AG, BMD/FA, Switzerland
 Dissertation: Mechanisms of 3-hydroxyl-3-methylglutaryl-coenzyme A inhibitor (statin)-induced cytotoxicity in human skeletal muscle cell cultures.
Dissertation Advisors: Prof. Dr. Armin Wolf/Prof. Dr. Wolfgang E.Trommer

Publications and Presentations

Ndountse-Tchapda L, Schramm U, Trommer W E and Wolf A: Partizipation of reactive oxygen formation in the 3-hydroxy-3-methylglutaryl-CoA reductase inhibitor-induced skeletal muscle cell death. Publication, manuscript in preparation.

Ndountse-Tchapda L, Schramm U, Trommer W E and Wolf A: Role of pro- and antioxidants in the 3-hydroxy-3-methylglutaryl-CoA reductase inhibitor-induced myonecrosis in human skeletal muscle cells. Publication, manuscript in preparation.

Ndountse-Tchapda L, Schramm U, Trommer W E and Wolf A: Effect of mevalonate and mevalonate derivatives in the 3-hydroxy-3-methylglutaryl-CoA reductase inhibitor-induced myonecrosis in human skeletal muscle cells. Publication, manuscript in preparation.

Wolf A, **Ndountse-Tchapda L**, Trommer W E and Schramm U: Comparative toxic effects of HMG-coA reductase inhibitors in the human skeletal muscle primary cell culture, 44 Annual Meeting of the Society of Toxicology(SOT), Salt Lake City/USA, Toxicology Sciences, Suppl.72, No. S-1, Abstract 238 (2003)

Ndountse-Tchapda L, Schramm U, Trommer W E and Wolf A: Toxicity of HMG-CoA reductase inhibitors in human skeletal muscle cells, 44. Frühjahrstagung der Deutschen Gesellschaft für experimentelle und klinische Pharmakologie und Toxikologie (DGPT) gemeinsam mit der 20. Tagung der Gesellschaft für Umwelt-Mutationsforschung (GUM), Mainz/Germany; Naunyn-Schmiedeberg's Archives of Pharmacology, Suppl.367 No.1, Abstract 524 (2003)

Wolf A, **Ndountse-Tchapda L**, Schramm U, Trommer W E: Involvement of apoptosis in the HMG-CoA reductase inhibitor-induced myonecrosis in human skeletal muscle cells, 45 Annual Meeting of the Society of Toxicology(SOT), Baltimore/USA, Toxicology Sciences, Abstract (2004)

Ndountse-Tchapda L, Schramm U, Trommer W E and Wolf A: Apoptosis contributes to the generation of statin-induced myonecrosis in human skeletal muscle cells, 7th International ISSX Meeting, Vancouver/Canada, Abstract 468 (2004)

Wolf A, **Ndountse-Tchapda L**, Schramm U, Trommer W E: Involvement of reactive oxygen formation in the 3-hydroxy-3-methylglutaryl-CoA reductase inhibitor-induced skeletal muscle cell death, 46 Annual Meeting of the Society of Toxicology(SOT), New Orleans/USA, Toxicology Sciences, Abstract 1863 (2005)

